The π^0 and η Transition Form Factors: Hadronic Contributions to the Anomalous Magnetic Moment of the Muon

Bastian Kubis

Helmholtz-Institut für Strahlen- und Kernphysik (Theorie)

Bethe Center for Theoretical Physics

Universität Bonn, Germany

Wien, May 19th 2015

Outline

Introduction

- The anomalous magnetic moment of the muon
- Hadronic vacuum polarisation and
  hadronic light-by-light scattering

Dispersion relations for meson transition form factors

- Ingredients for a data-driven analysis of $\pi^0, \eta \to \gamma^*\gamma^{(*)}$

Summary / Outlook

Outline

Introduction

- The anomalous magnetic moment of the muon
- Hadronic vacuum polarisation and
  hadronic light-by-light scattering

Dispersion relations for meson transition form factors

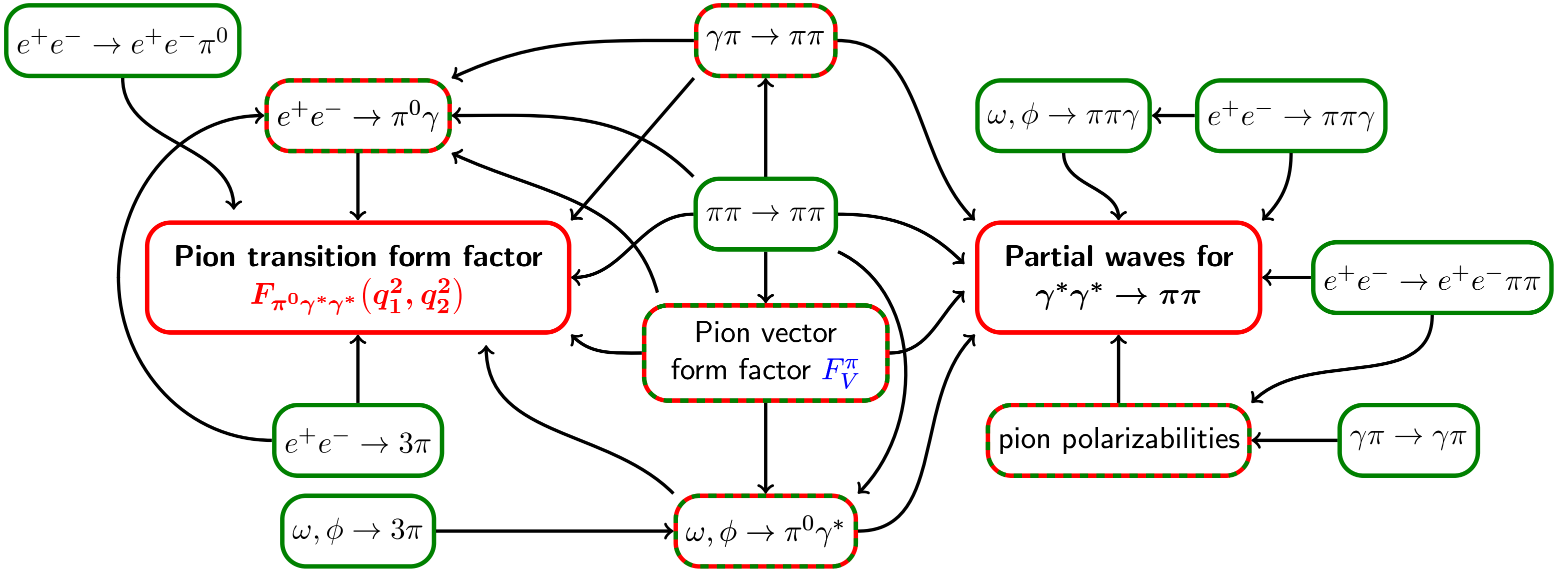

Colangelo, Hoferichter, BK, Procura, Stoffer 2014

Summary / Outlook

The anomalous magnetic moment of the muon

- gyromagnetic ratio: magnetic moment $\leftrightarrow$ spin

$$\vec{\mu} = g \frac{e}{2m} \vec{S}$$

- Dirac theory for spin-1/2 fermions: $g_\mu = 2$
  rad. corr.: $g_\mu = 2(1 + a_\mu)$, a_μ "anomalous magnetic moment"
- one of the most precisely measured quantities in particle physics

$$a_\mu = (116\,592\,089 \pm 63) \times 10^{-11}$$

BNL E821 2006

The anomalous magnetic moment of the muon

- gyromagnetic ratio: magnetic moment $\leftrightarrow$ spin

$$\vec{\mu} = g \frac{e}{2m} \vec{S}$$

- Dirac theory for spin-1/2 fermions: $g_\mu = 2$
  rad. corr.: $g_\mu = 2(1 + a_\mu)$, a_μ "anomalous magnetic moment"

- one of the most precisely measured quantities in particle physics

$$a_\mu = (116\,592\,089 \pm 63) \times 10^{-11} \qquad \text{BNL E821 2006}$$

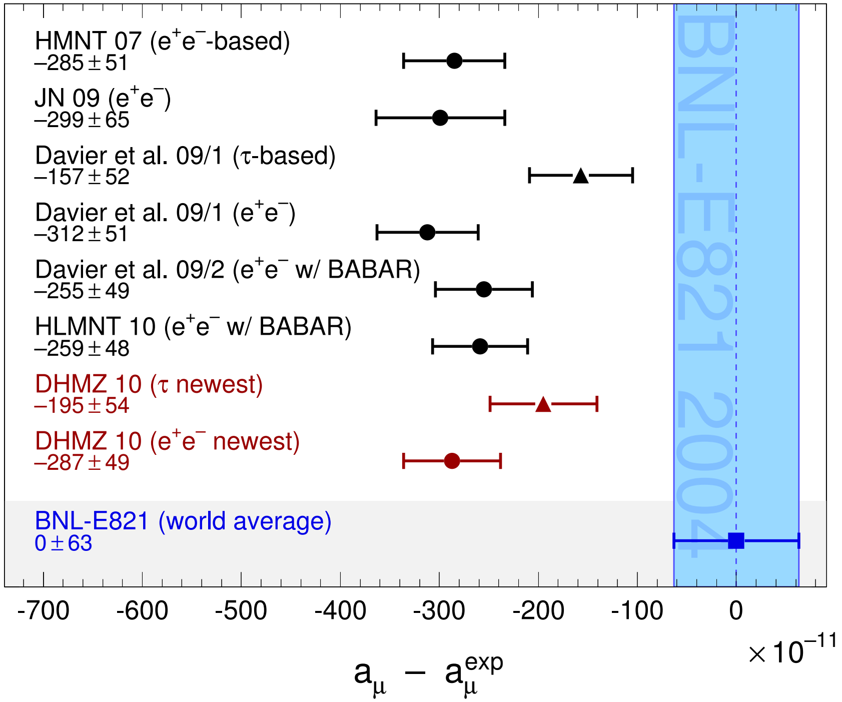

- … and one with a significant (??) deviation from the Standard Model:

$$a_\mu^{\text{exp}} - a_\mu^{\text{SM}} = (27.6 \pm 8.6) \times 10^{-11}$$

Davier et al. 2011

- new $g-2$ experiment at Fermilab: reduce experimental error by factor 4

$(g-2)_\mu$: from Brookhaven to Fermilab

picture: Fermilab

$(g-2)_\mu$: from Brookhaven to Fermilab

photo: BNL

$(g-2)_\mu$: from Brookhaven to Fermilab

photo: Fermilab

$(g-2)_\mu$: from Brookhaven to Fermilab

photo: BNL

$(g-2)_\mu$: from Brookhaven to Fermilab

photo: Fermilab

The Standard Model prediction for a_μ

	a_μ $[10^{-11}]$	Δa_μ $[10^{-11}]$
experiment	116 592 089.	63.
QED $\mathcal{O}(\alpha)$	116 140 973.21	0.03
QED $\mathcal{O}(\alpha^2)$	413 217.63	0.01
QED $\mathcal{O}(\alpha^3)$	30 141.90	0.00
QED $\mathcal{O}(\alpha^4)$	381.01	0.02
QED $\mathcal{O}(\alpha^5)$	5.09	0.01
QED total	116 584 718.85	0.04
electroweak	153.2	1.8
had. VP (LO)	6923.	42.
had. VP (NLO)	–98.	1.
had. LbL	116.	40.
total	116 591 813.	58.

The Standard Model prediction for a_μ

	a_μ $[10^{-11}]$	Δa_μ $[10^{-11}]$
experiment	116 592 089.	63.
QED $\mathcal{O}(\alpha)$	116 140 973.21	0.03
QED $\mathcal{O}(\alpha^2)$	413 217.63	0.01
QED $\mathcal{O}(\alpha^3)$	30 141.90	0.00
QED $\mathcal{O}(\alpha^4)$	381.01	0.02
QED $\mathcal{O}(\alpha^5)$	5.09	0.01
QED total	116 584 718.85	0.04
electroweak	153.2	1.8
had. VP (LO)	6923.	42.
had. VP (NLO)	–98.	1.
had. LbL	116.	40.
total	116 591 813.	58.

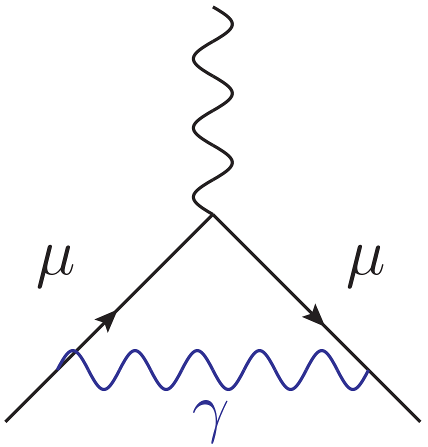

Schwinger 1948

The Standard Model prediction for a_μ

	a_μ $[10^{-11}]$	Δa_μ $[10^{-11}]$
experiment	116 592 089.	63.
QED $\mathcal{O}(\alpha)$	116 140 973.21	0.03
QED $\mathcal{O}(\alpha^2)$	413 217.63	0.01
QED $\mathcal{O}(\alpha^3)$	30 141.90	0.00
QED $\mathcal{O}(\alpha^4)$	381.01	0.02
QED $\mathcal{O}(\alpha^5)$	5.09	0.01
QED total	116 584 718.85	0.04
electroweak	153.2	1.8
had. VP (LO)	6923.	42.
had. VP (NLO)	–98.	1.
had. LbL	116.	40.
total	116 591 813.	58.

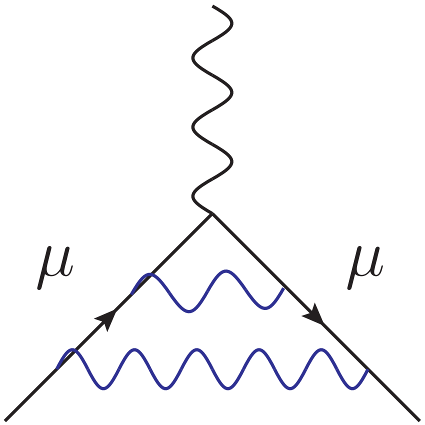

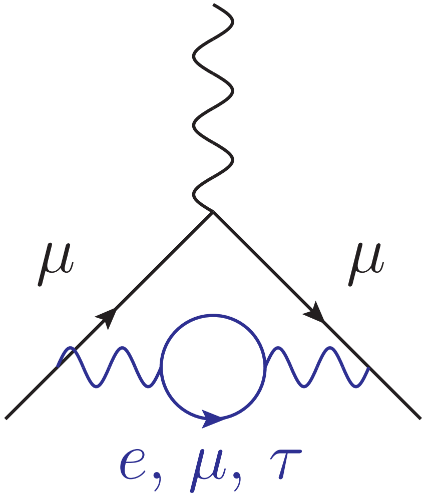

Petermann 1957
Sommerfield 1957

The Standard Model prediction for a_μ

	$a_\mu\ [10^{-11}]$	$\Delta a_\mu\ [10^{-11}]$
experiment	116 592 089.	63.
QED $\mathcal{O}(\alpha)$	116 140 973.21	0.03
QED $\mathcal{O}(\alpha^2)$	413 217.63	0.01
QED $\mathcal{O}(\alpha^3)$	30 141.90	0.00
QED $\mathcal{O}(\alpha^4)$	381.01	0.02
QED $\mathcal{O}(\alpha^5)$	5.09	0.01
QED total	116 584 718.85	0.04
electroweak	153.2	1.8
had. VP (LO)	6923.	42.
had. VP (NLO)	–98.	1.
had. LbL	116.	40.
total	116 591 813.	58.

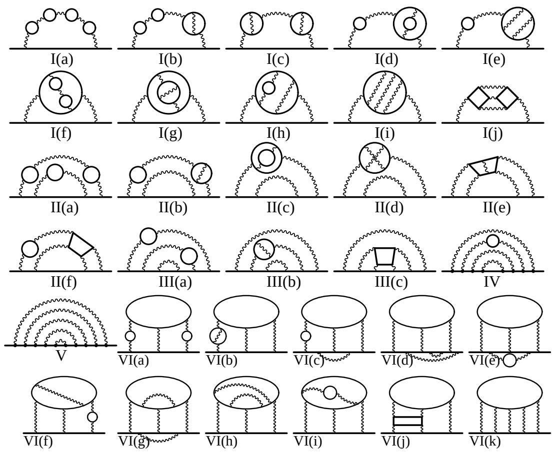

Kinoshita et al. 2012

The Standard Model prediction for a_μ

	a_μ $[10^{-11}]$	Δa_μ $[10^{-11}]$
experiment	116 592 089.	63.
QED $\mathcal{O}(\alpha)$	116 140 973.21	0.03
QED $\mathcal{O}(\alpha^2)$	413 217.63	0.01
QED $\mathcal{O}(\alpha^3)$	30 141.90	0.00
QED $\mathcal{O}(\alpha^4)$	381.01	0.02
QED $\mathcal{O}(\alpha^5)$	5.09	0.01
QED total	116 584 718.85	0.04
electroweak	153.2	1.8
had. VP (LO)	6923.	42.
had. VP (NLO)	–98.	1.
had. LbL	116.	40.
total	116 591 813.	58.

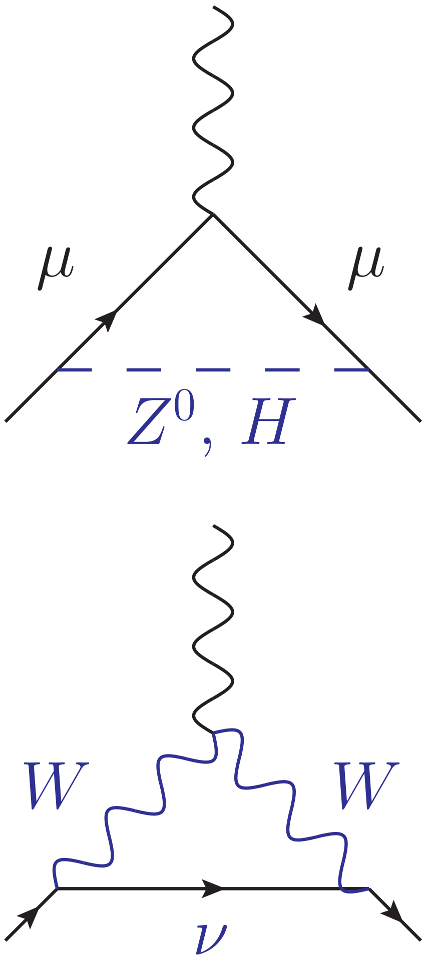

The Standard Model prediction for a_μ

	$a_\mu\ [10^{-11}]$	$\Delta a_\mu\ [10^{-11}]$
experiment	116 592 089.	63.
QED $\mathcal{O}(\alpha)$	116 140 973.21	0.03
QED $\mathcal{O}(\alpha^2)$	413 217.63	0.01
QED $\mathcal{O}(\alpha^3)$	30 141.90	0.00
QED $\mathcal{O}(\alpha^4)$	381.01	0.02
QED $\mathcal{O}(\alpha^5)$	5.09	0.01
QED total	116 584 718.85	0.04
electroweak	153.2	1.8
had. VP (LO)	6923.	42.
had. VP (NLO)	–98.	1.
had. LbL	116.	40.
total	116 591 813.	58.

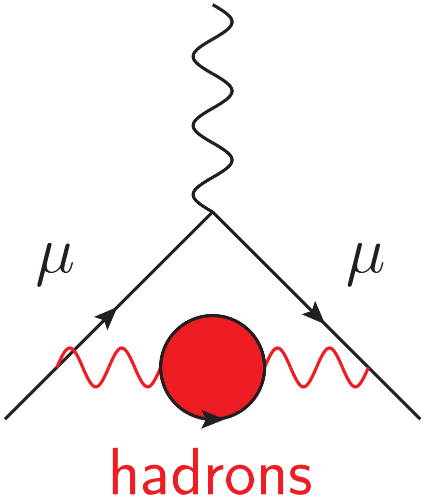

The Standard Model prediction for a_μ

	a_μ $[10^{-11}]$	Δa_μ $[10^{-11}]$
experiment	116 592 089.	63.
QED $\mathcal{O}(\alpha)$	116 140 973.21	0.03
QED $\mathcal{O}(\alpha^2)$	413 217.63	0.01
QED $\mathcal{O}(\alpha^3)$	30 141.90	0.00
QED $\mathcal{O}(\alpha^4)$	381.01	0.02
QED $\mathcal{O}(\alpha^5)$	5.09	0.01
QED total	116 584 718.85	0.04
electroweak	153.2	1.8
had. VP (LO)	6923.	42.
had. VP (NLO)	–98.	1.
had. LbL	116.	40.
total	116 591 813.	58.

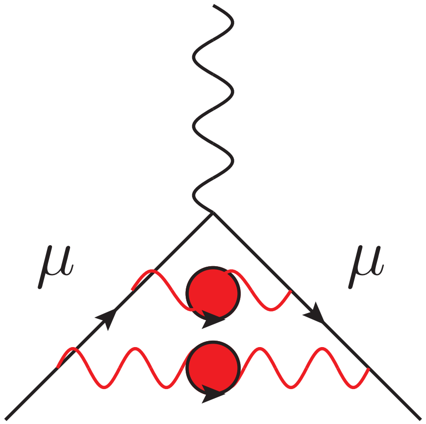

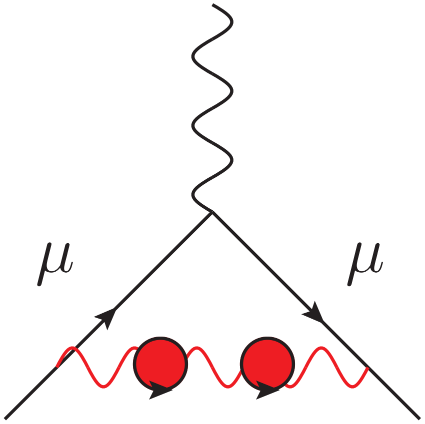

The Standard Model prediction for a_μ

	a_μ $[10^{-11}]$	Δa_μ $[10^{-11}]$
experiment	116 592 089.	63.
QED $\mathcal{O}(\alpha)$	116 140 973.21	0.03
QED $\mathcal{O}(\alpha^2)$	413 217.63	0.01
QED $\mathcal{O}(\alpha^3)$	30 141.90	0.00
QED $\mathcal{O}(\alpha^4)$	381.01	0.02
QED $\mathcal{O}(\alpha^5)$	5.09	0.01
QED total	116 584 718.85	0.04
electroweak	153.2	1.8
had. VP (LO)	6923.	42.
had. VP (NLO)	–98.	1.
had. LbL	116.	40.
total	116 591 813.	58.

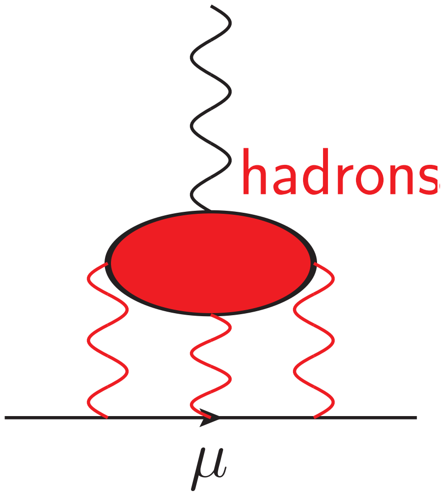

The Standard Model prediction for a_μ

	a_μ $[10^{-11}]$	Δa_μ $[10^{-11}]$
experiment	116 592 089.	63.
QED $\mathcal{O}(\alpha)$	116 140 973.21	0.03
QED $\mathcal{O}(\alpha^2)$	413 217.63	0.01
QED $\mathcal{O}(\alpha^3)$	30 141.90	0.00
QED $\mathcal{O}(\alpha^4)$	381.01	0.02
QED $\mathcal{O}(\alpha^5)$	5.09	0.01
QED total	116 584 718.85	0.04
electroweak	153.2	1.8
had. VP (LO)	6923.	42.
had. VP (NLO)	–98.	1.
had. LbL	116.	40.
total	116 591 813.	58.

$\longrightarrow$ hadronic part dominates the uncertainty by far!

Jegerlehner, Nyffeler 2009
Davier et al. 2011
and references therein

Hadronic vacuum polarization

- how to control hadronic vacuum polarization?
- characteristic scale set by muon mass
  $\longrightarrow$ this is not a perturbative QCD problem!
- dispersion relations to the rescue:
  use the optical theorem!

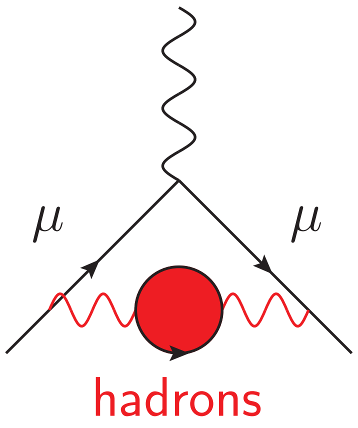

Hadronic vacuum polarization

- how to control hadronic vacuum polarization?
- characteristic scale set by muon mass
  $\longrightarrow$ this is not a perturbative QCD problem!
- dispersion relations to the rescue:
  use the optical theorem!

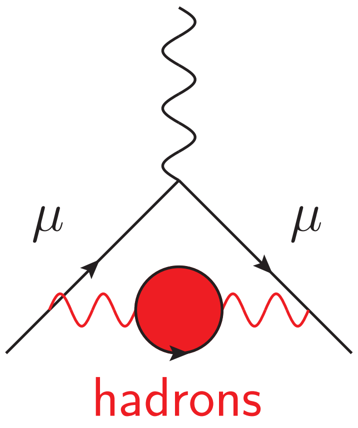

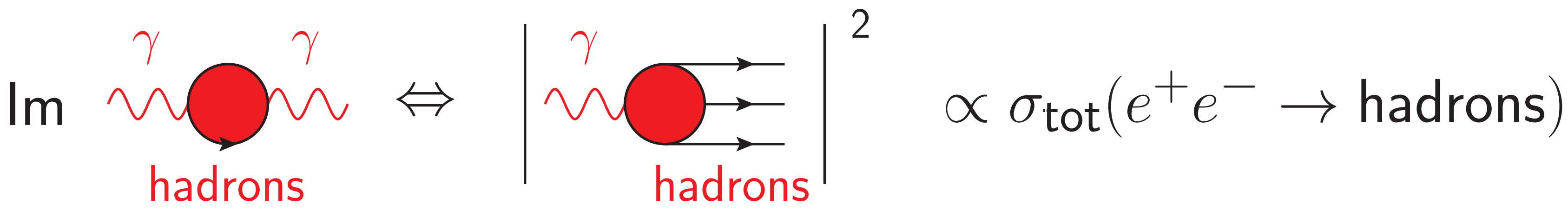

Hadronic vacuum polarization

- how to control hadronic vacuum polarization?
- characteristic scale set by muon mass
  $\longrightarrow$ this is not a perturbative QCD problem!
- dispersion relations to the rescue:
  use the optical theorem!

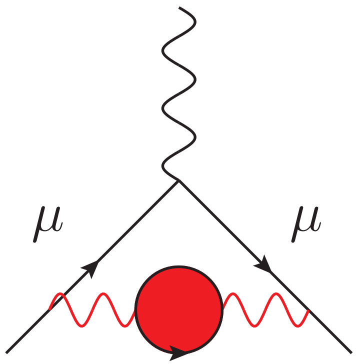

$$a_\mu^{\text{had VP}} \propto \int_{4M_\pi^2}^{\infty} K(s)\sigma_{\text{tot}}(e^+e^- \to \text{hadrons})$$

- $K(s)$: kinematical function, for large s: $\quad K(s) \propto 1/s$,
  $\sigma_{\text{tot}}(e^+e^- \to \text{hadrons}) \propto 1/s$

Hadronic vacuum polarization

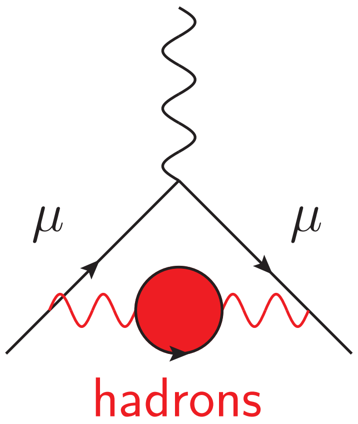

- how to control hadronic vacuum polarization?
- characteristic scale set by muon mass
  $\longrightarrow$ this is not a perturbative QCD problem!
- dispersion relations to the rescue:
  use the optical theorem!

$$a_\mu^{\text{had VP}} \propto \int_{4M_\pi^2}^{\infty} K(s)\sigma_{\text{tot}}(e^+e^- \to \text{hadrons})$$

- $K(s)$: kinematical function, for large s: $K(s) \propto 1/s$,
  $\sigma_{\text{tot}}(e^+e^- \to \text{hadrons}) \propto 1/s$
- more than 75% of $a_\mu^{\text{had VP}}$ given by
  energies $s \leq 1\,\text{GeV}^2$ Jegerlehner, Nyffeler 2009
- dominated by $e^+e^- \to \pi^+\pi^-$
  $\longrightarrow$ pion electromagnetic form factor
- well constrained by data KLOE, BABAR. . .

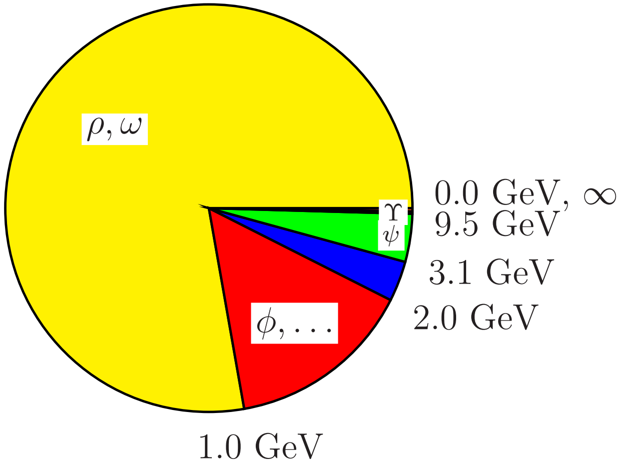

Hadronic light-by-light scattering

- hadronic light-by-light soon to dominate Standard Model uncertainty in $(g-2)_\mu$

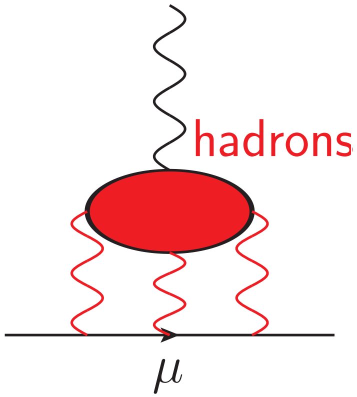

Hadronic light-by-light scattering

- hadronic light-by-light soon to dominate Standard Model uncertainty in $(g-2)_\mu$

- different contributions estimated (in 10^{-11}):

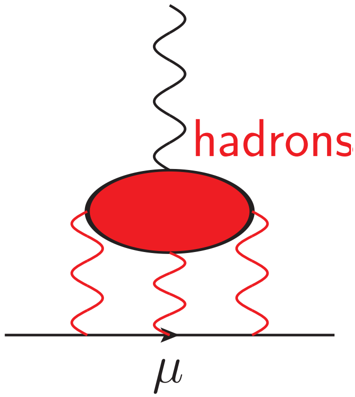

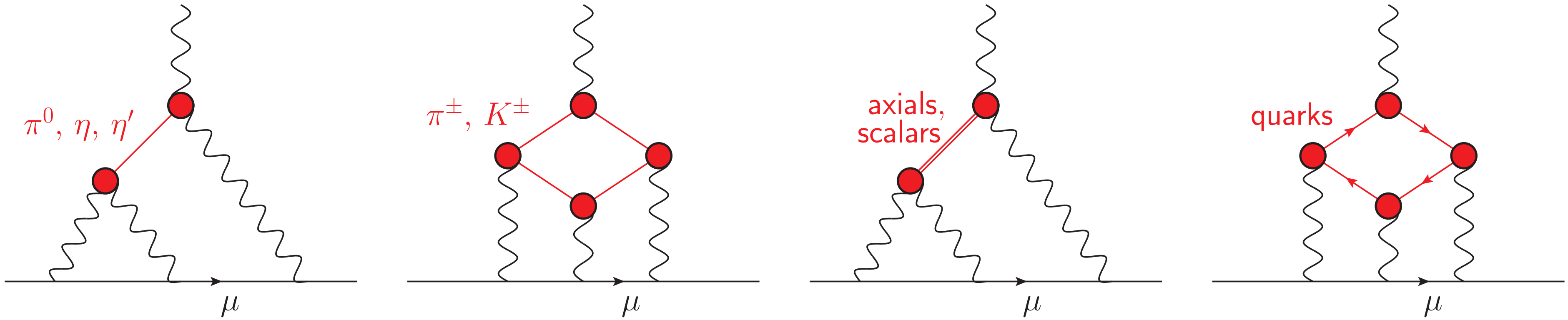

99±16	–19±13	15±7	21±3

$\longrightarrow$ how to control hadronic modelling?

Jegerlehner, Nyffeler 2009

Hadronic light-by-light scattering

- hadronic light-by-light soon to dominate Standard Model uncertainty in $(g-2)_\mu$

- different contributions estimated (in 10^{-11}):

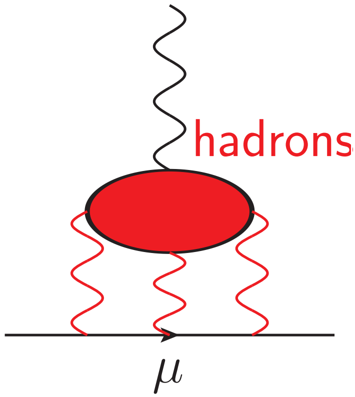

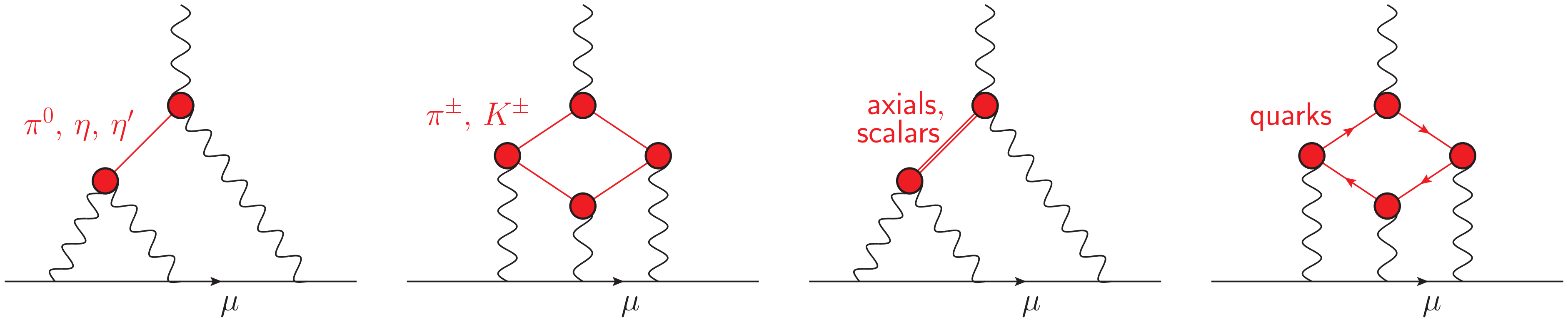

99±16 –19±13 15±7 21±3

$\longrightarrow$ how to control hadronic modelling? Jegerlehner, Nyffeler 2009

- dispersive point of view: analytic structure, cuts and poles
  $\longrightarrow$ (on-shell) form factors and scatt. amplitudes from experiment
  $\longrightarrow$ expansion in masses of intermediate states, partial waves

Dispersion relations for pedestrians

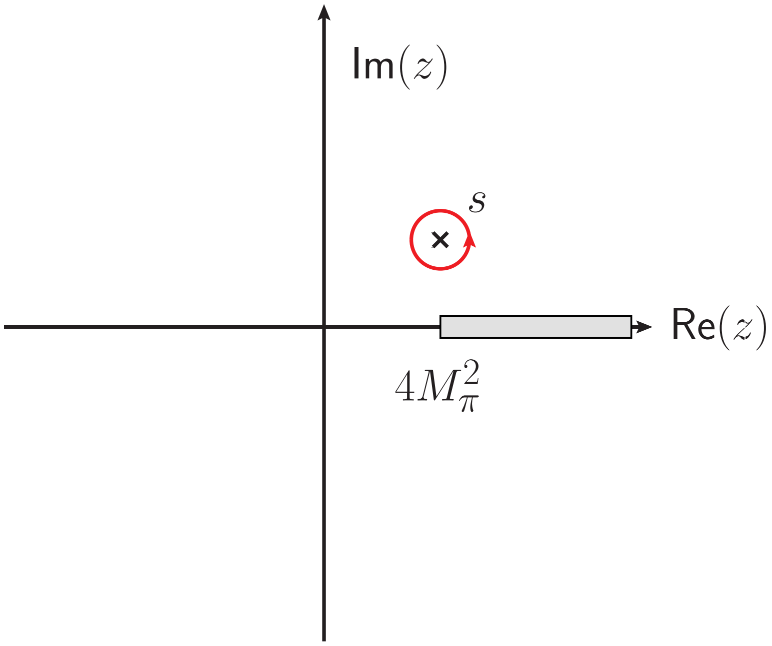

analyticity & Cauchy's theorem:

$$T(s) = \frac{1}{2\pi i} \oint_{\partial\Omega} \frac{T(z)dz}{z-s}$$

Dispersion relations for pedestrians

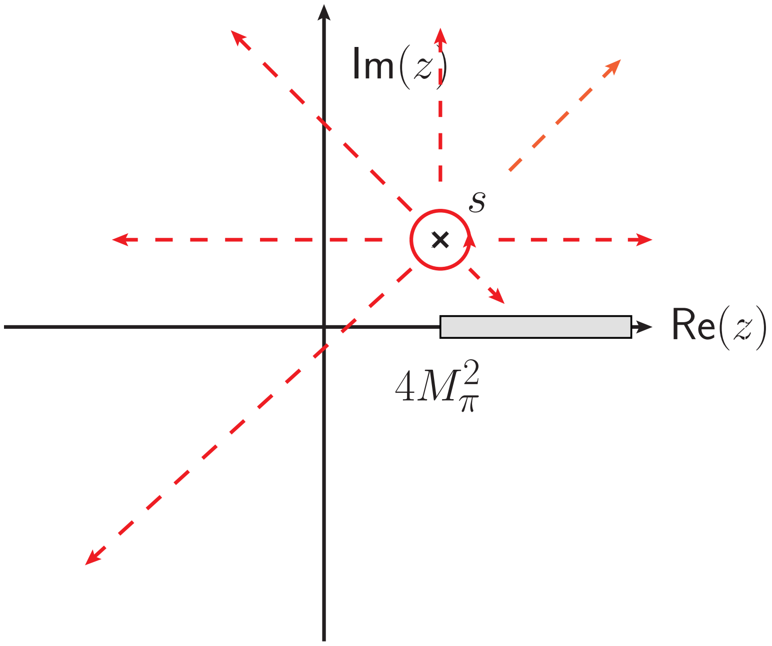

analyticity & Cauchy's theorem:

$$T(s) = \frac{1}{2\pi i} \oint_{\partial\Omega} \frac{T(z)dz}{z-s}$$

Dispersion relations for pedestrians

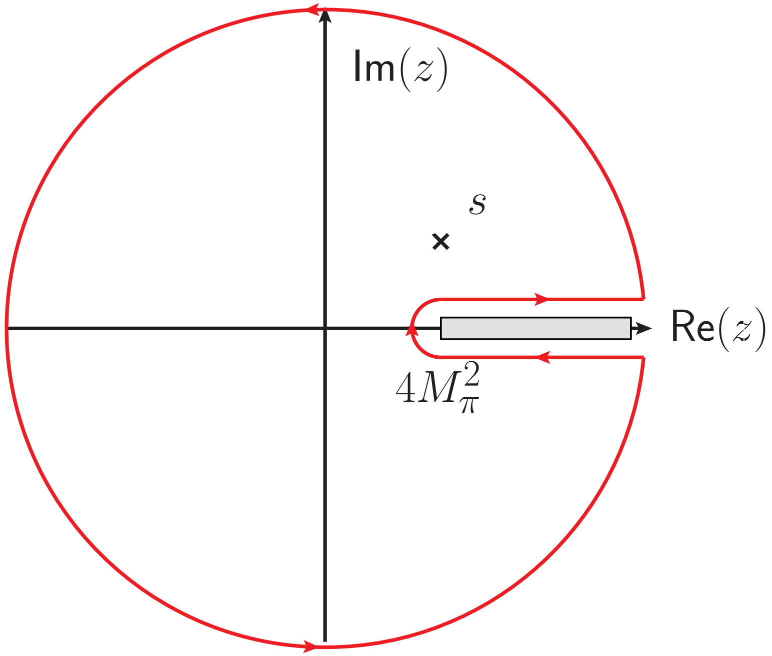

analyticity & Cauchy's theorem:

$$T(s) = \frac{1}{2\pi i} \oint_{\partial\Omega} \frac{T(z)dz}{z-s}$$

Dispersion relations for pedestrians

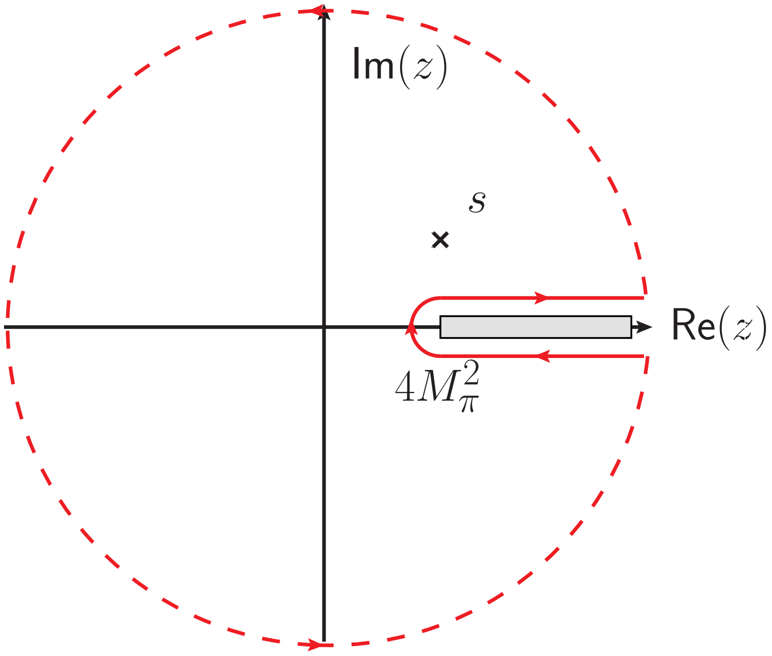

analyticity & Cauchy's theorem:

$$T(s) = \frac{1}{2\pi i} \oint_{\partial\Omega} \frac{T(z)dz}{z-s}$$

Dispersion relations for pedestrians

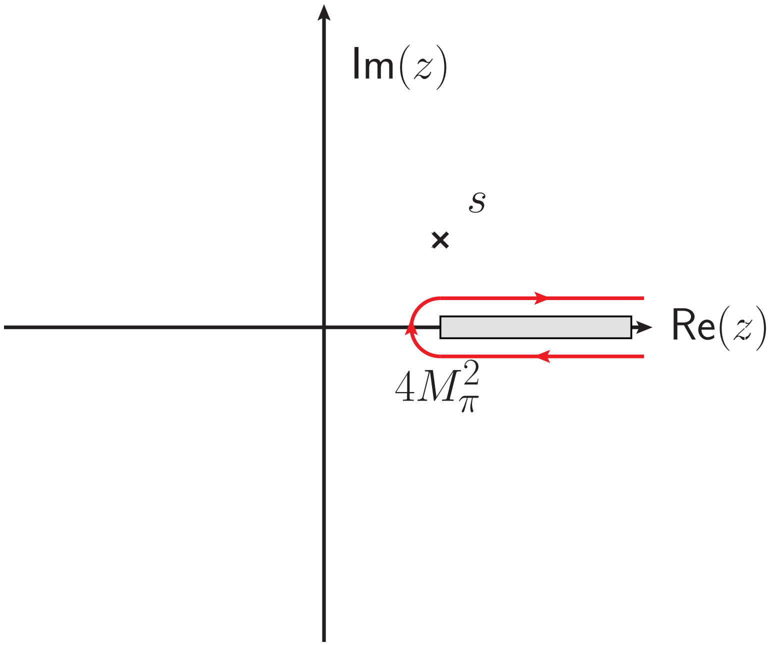

analyticity & Cauchy's theorem:

$$T(s) = \frac{1}{2\pi i} \oint_{\partial\Omega} \frac{T(z)dz}{z-s}$$

$$\longrightarrow \frac{1}{2\pi i} \int_{4M_\pi^2}^{\infty} \frac{\operatorname{disc} T(z)dz}{z-s}$$

$$= \frac{1}{\pi} \int_{4M_\pi^2}^{\infty} \frac{\operatorname{Im} T(z)dz}{z-s}$$

Dispersion relations for pedestrians

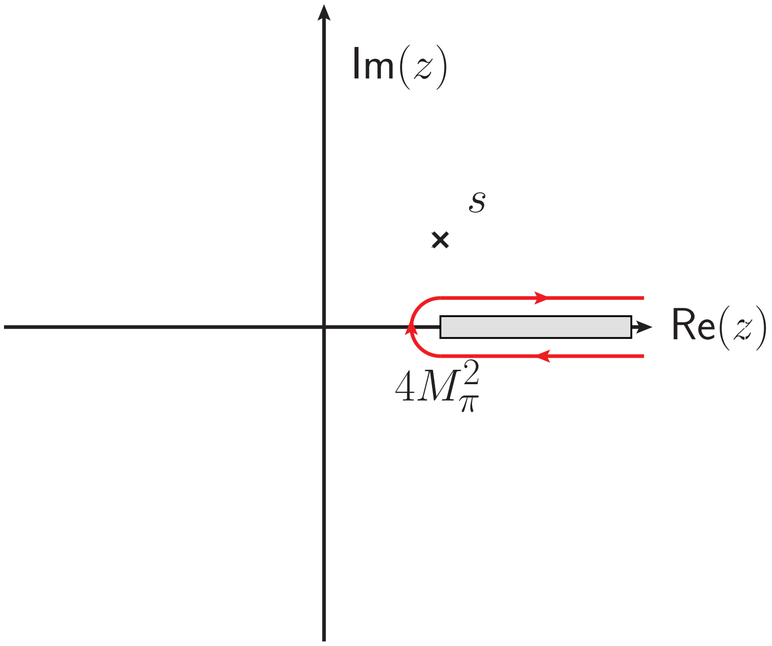

analyticity & Cauchy's theorem:

$$T(s) = \frac{1}{2\pi i}\oint_{\partial\Omega}\frac{T(z)dz}{z-s}$$
$$\longrightarrow \frac{1}{2\pi i}\int_{4M_\pi^2}^{\infty}\frac{\operatorname{disc} T(z)dz}{z-s}$$
$$= \frac{1}{\pi}\int_{4M_\pi^2}^{\infty}\frac{\operatorname{Im} T(z)dz}{z-s}$$

- $\operatorname{disc} T(s) = 2i \operatorname{Im} T(s)$ calculable by "cutting rules":

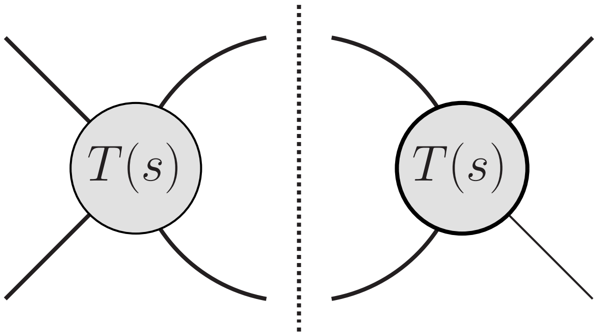

e.g. if $T(s)$ is a $\pi\pi$ partial wave $\longrightarrow$

$$\frac{\operatorname{disc} T(s)}{2i} = \operatorname{Im} T(s) = \frac{2q_\pi}{\sqrt{s}}\theta(s-4M_\pi^2)|T(s)|^2$$

Dispersion relations for pedestrians

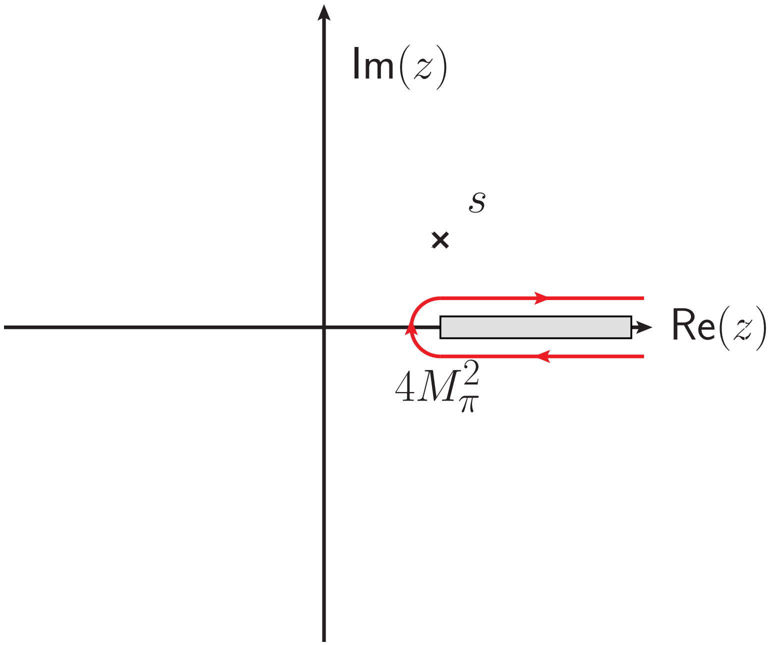

analyticity & Cauchy's theorem:

$$T(s) = \frac{1}{2\pi i} \oint_{\partial\Omega} \frac{T(z)dz}{z-s}$$
$$\longrightarrow \frac{1}{2\pi i} \int_{4M_\pi^2}^{\infty} \frac{\operatorname{disc} T(z)dz}{z-s}$$
$$= \frac{1}{\pi} \int_{4M_\pi^2}^{\infty} \frac{\operatorname{Im} T(z)dz}{z-s}$$

- $\operatorname{disc} T(s) = 2i \operatorname{Im} T(s)$ calculable by "cutting rules":

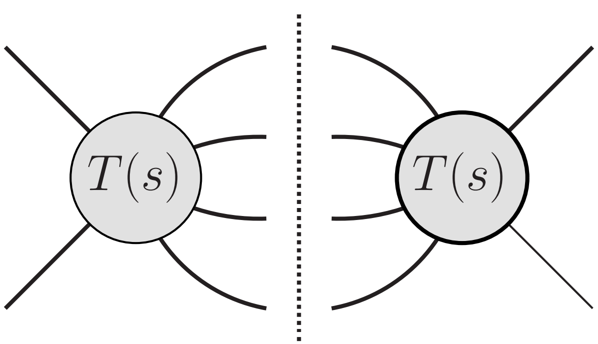

inelastic intermediate states ($K\bar{K}$, 4π) suppressed at low energies
$\longrightarrow$ will be neglected in the following

Dispersive analysis of $\pi^0/\eta \to \gamma^*\gamma^*$

- isospin decomposition:

$$F_{\pi^0\gamma^*\gamma^*}(q_1^2, q_2^2) = F_{vs}(q_1^2, q_2^2) + F_{vs}(q_2^2, q_1^2)$$
$$F_{\eta\gamma^*\gamma^*}(q_1^2, q_2^2) = F_{vv}(q_1^2, q_2^2) + F_{ss}(q_2^2, q_1^2)$$

Dispersive analysis of $\pi^0/\eta \to \gamma^*\gamma^*$

- isospin decomposition:

$$F_{\pi^0\gamma^*\gamma^*}(q_1^2,q_2^2) = F_{vs}(q_1^2,q_2^2) + F_{vs}(q_2^2,q_1^2)$$
$$F_{\eta\gamma^*\gamma^*}(q_1^2,q_2^2) = F_{vv}(q_1^2,q_2^2) + F_{ss}(q_2^2,q_1^2)$$

- analyze the leading hadronic intermediate states:

see also Gorchtein, Guo, Szczepaniak 2012

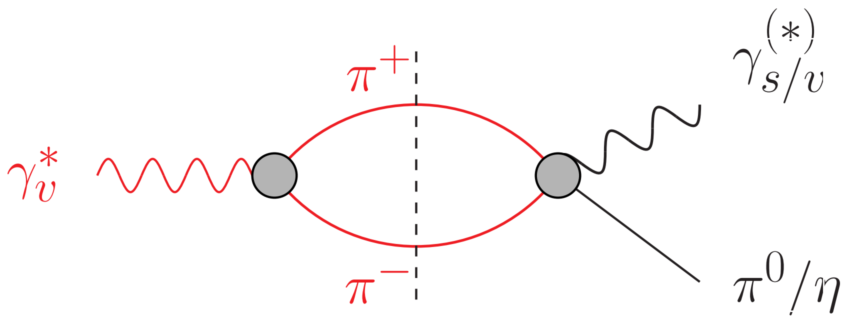

▷ isovector photon: 2 pions

$\propto$ pion vector form factor $\times$ $\gamma\pi \to \pi\pi$ / $\eta \to \pi\pi\gamma$

all determined in terms of pion–pion P-wave phase shift

Dispersive analysis of $\pi^0/\eta \to \gamma^*\gamma^*$

- isospin decomposition:

$$F_{\pi^0\gamma^*\gamma^*}(q_1^2,q_2^2) = F_{vs}(q_1^2,q_2^2) + F_{vs}(q_2^2,q_1^2)$$
$$F_{\eta\gamma^*\gamma^*}(q_1^2,q_2^2) = F_{vv}(q_1^2,q_2^2) + F_{ss}(q_2^2,q_1^2)$$

- analyze the leading hadronic intermediate states:

see also Gorchtein, Guo, Szczepaniak 2012

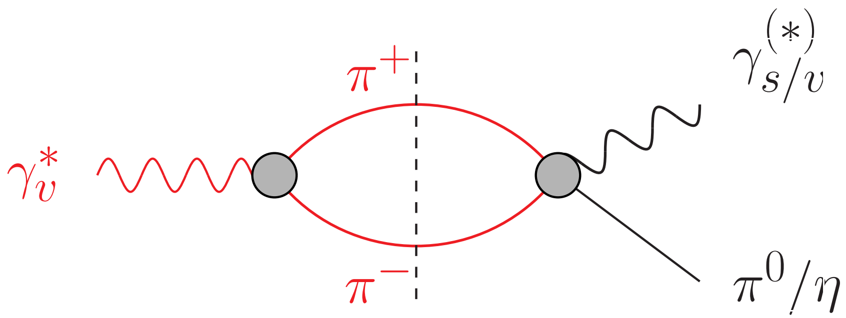

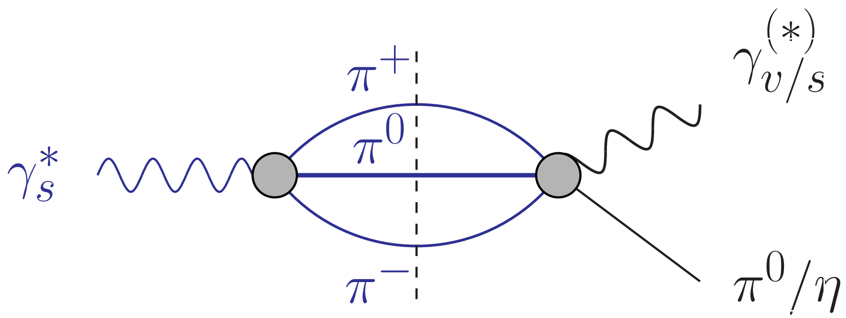

- ▷ isovector photon: 2 pions

  $\propto$ pion vector form factor $\times$ $\gamma\pi \to \pi\pi$ / $\eta \to \pi\pi\gamma$

  all determined in terms of pion–pion P-wave phase shift

- ▷ isoscalar photon: 3 pions

Dispersive analysis of $\pi^0/\eta \to \gamma^*\gamma^*$

- isospin decomposition:

$$F_{\pi^0\gamma^*\gamma^*}(q_1^2,q_2^2) = F_{vs}(q_1^2,q_2^2) + F_{vs}(q_2^2,q_1^2)$$
$$F_{\eta\gamma^*\gamma^*}(q_1^2,q_2^2) = F_{vv}(q_1^2,q_2^2) + F_{ss}(q_2^2,q_1^2)$$

- analyze the leading hadronic intermediate states:

see also Gorchtein, Guo, Szczepaniak 2012

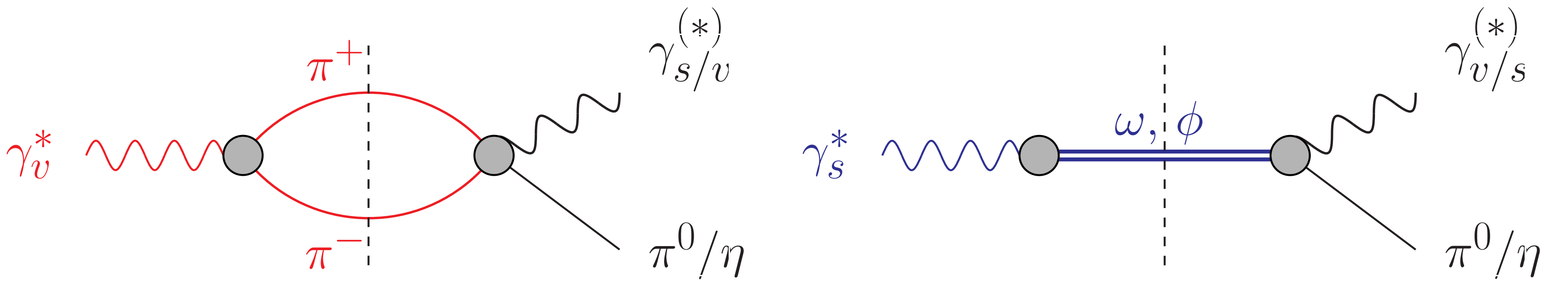

▷ isovector photon: 2 pions

$\propto$ pion vector form factor $\times$ $\gamma\pi \to \pi\pi$ / $\eta \to \pi\pi\gamma$

all determined in terms of pion–pion P-wave phase shift

▷ isoscalar photon: 3 pions $\longrightarrow$ dominated by narrow ω, ϕ

$\leftrightarrow \omega/\phi$ transition form factors; very small for the η

$\pi^0 \to \gamma^*(q_v^2)\gamma^*(q_s^2)$ transition form factor

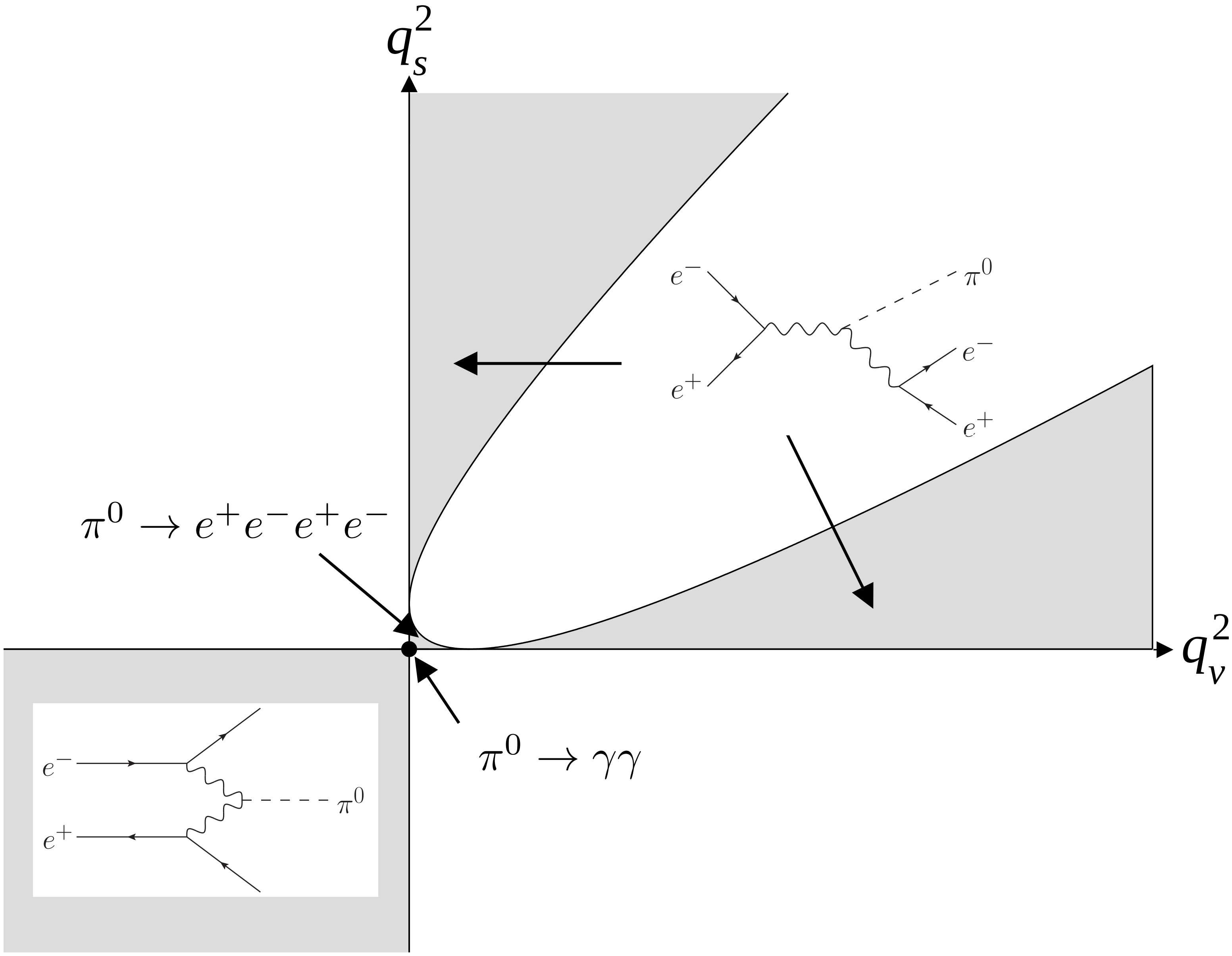

$\pi^0 \to \gamma^*(q_v^2)\gamma^*(q_s^2)$ transition form factor

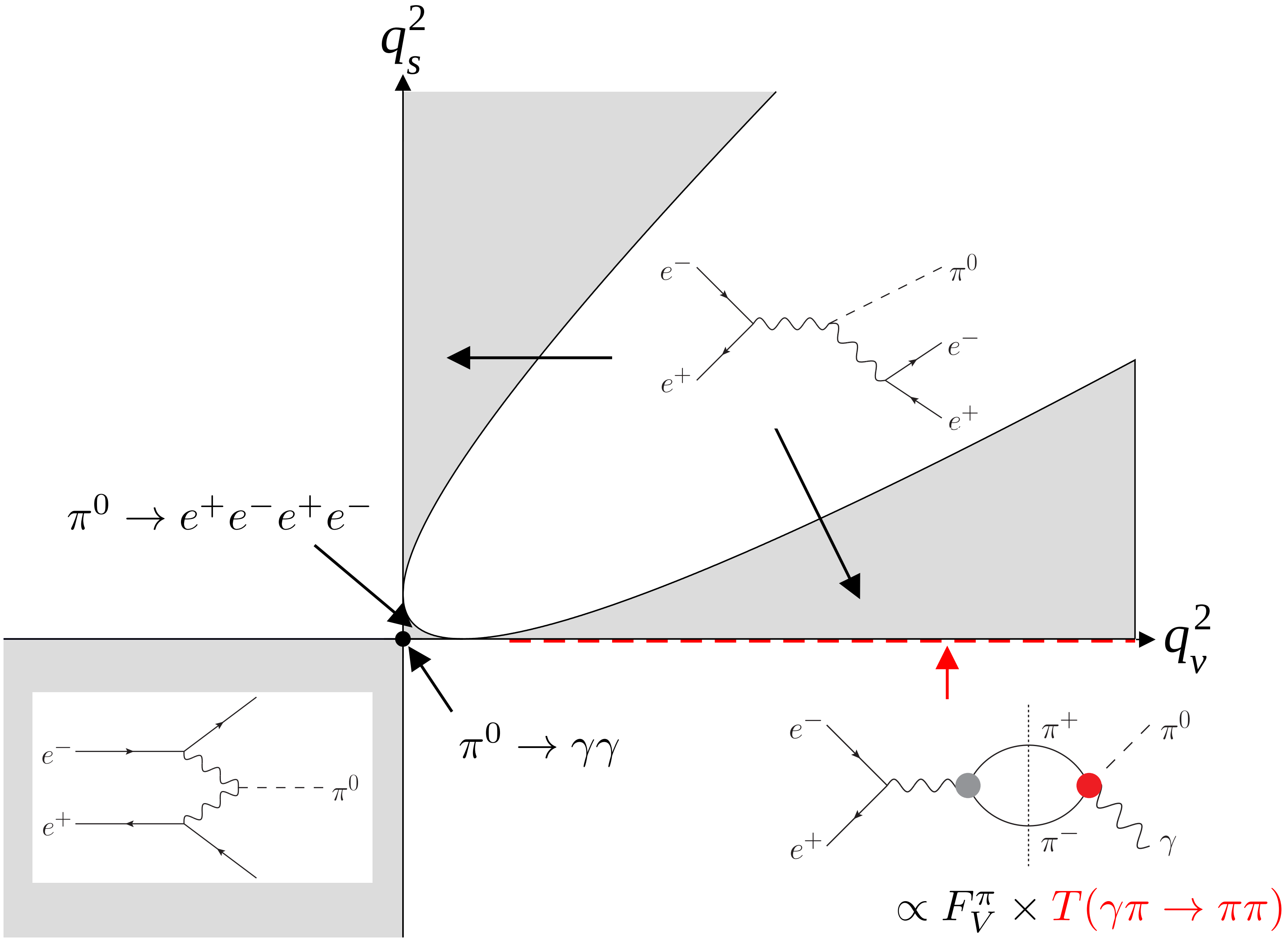

$\pi^0 \to \gamma^*(q_v^2)\gamma^*(q_s^2)$ transition form factor

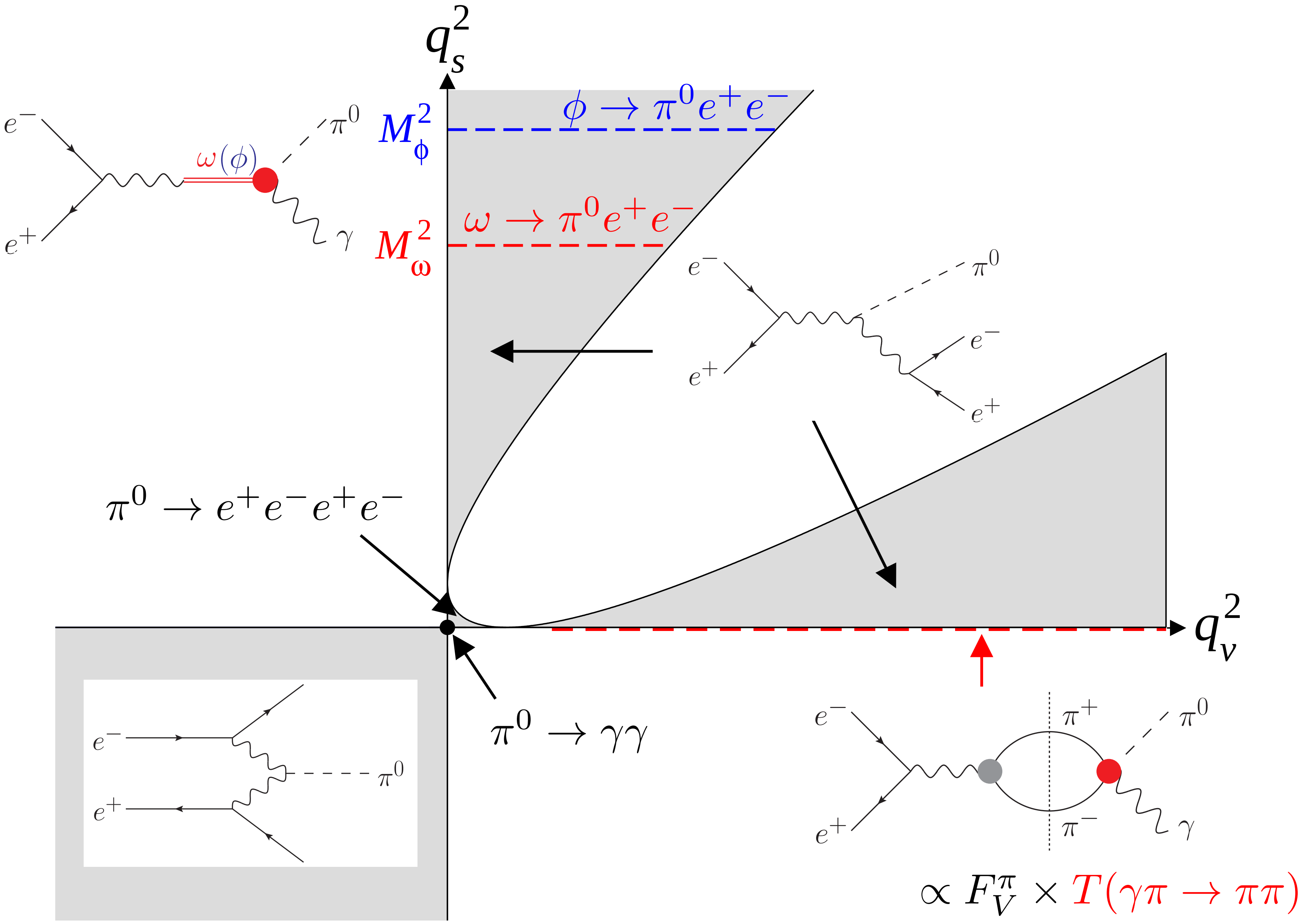

Warm-up: pion form factor from dispersion relations

- just two hadrons: form factor, e.g. $e^+e^- \to \pi^+\pi^-$, $\tau^- \to \pi^-\pi^0\nu_\tau$

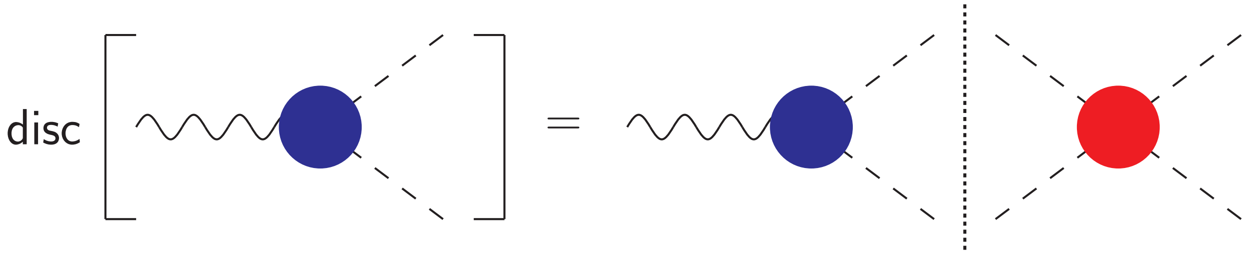

$$\mathrm{Im}\, F(s) \;\propto\; F(s) \times \text{phase space} \times T^*_{\pi\pi}(s)$$

$\longrightarrow$ final-state theorem: phase of $F(s)$ is scattering phase $\delta(s)$

Watson 1954

Warm-up: pion form factor from dispersion relations

- just two hadrons: form factor, e.g. $e^+e^- \to \pi^+\pi^-$, $\tau^- \to \pi^-\pi^0\nu_\tau$

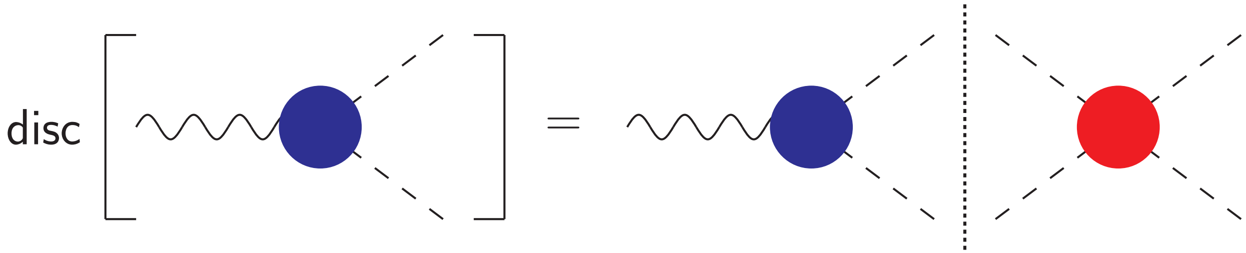

$$\text{Im}\, F(s) \;\propto\; F(s) \times \text{phase space} \times T^*_{\pi\pi}(s)$$

$\longrightarrow$ final-state theorem: phase of $F(s)$ is scattering phase $\delta(s)$

Watson 1954

- dispersion relations allow to reconstruct form factor from imaginary part $\longrightarrow$ elastic scattering phase $\delta(s)$:

$$F(s) = P(s)\Omega(s) \;, \quad \Omega(s) = \exp\left\{ \frac{s}{\pi} \int_{4M_\pi^2}^{\infty} ds' \frac{\delta(s')}{s'(s'-s)} \right\}$$

$P(s)$ polynomial, $\Omega(s)$ Omnès function

Omnès 1958

- today: high-accuracy $\pi\pi$ (and πK) phase shifts available

Ananthanarayan et al. 2001, García-Martín et al. 2011 (Büttiker et al. 2004)

Pion vector form factor from dispersion relations

- pion vector form factor clearly non-perturbative: ρ resonance

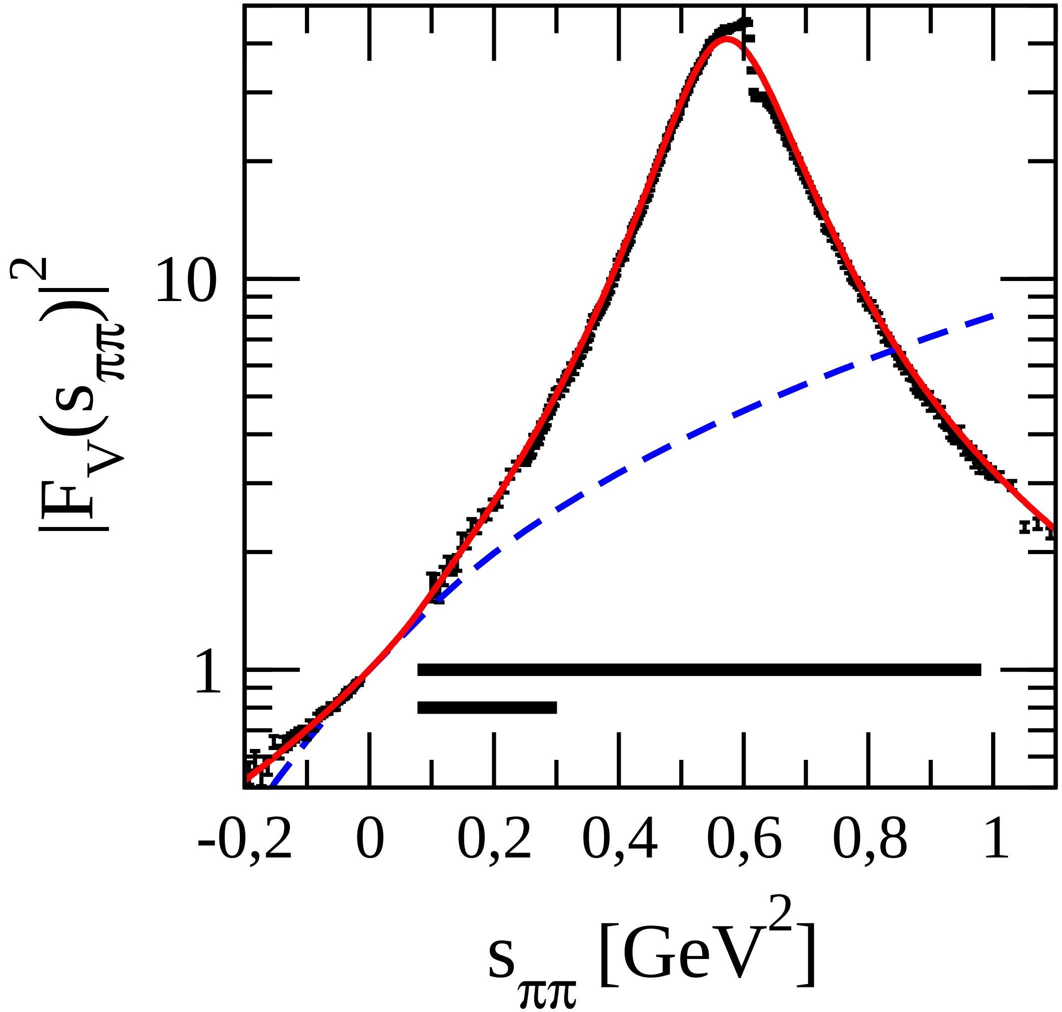

ChPT at one loop

data on $e^+e^- \to \pi^+\pi^-$

(improved)
Omnès representation

Stollenwerk et al. 2012

$\longrightarrow$ Omnès representation vastly extends range of applicability

Pion vector form factor vs. Omnès representation

- divide $\tau^- \to \pi^-\pi^0\nu_\tau$ form factor by Omnès function:

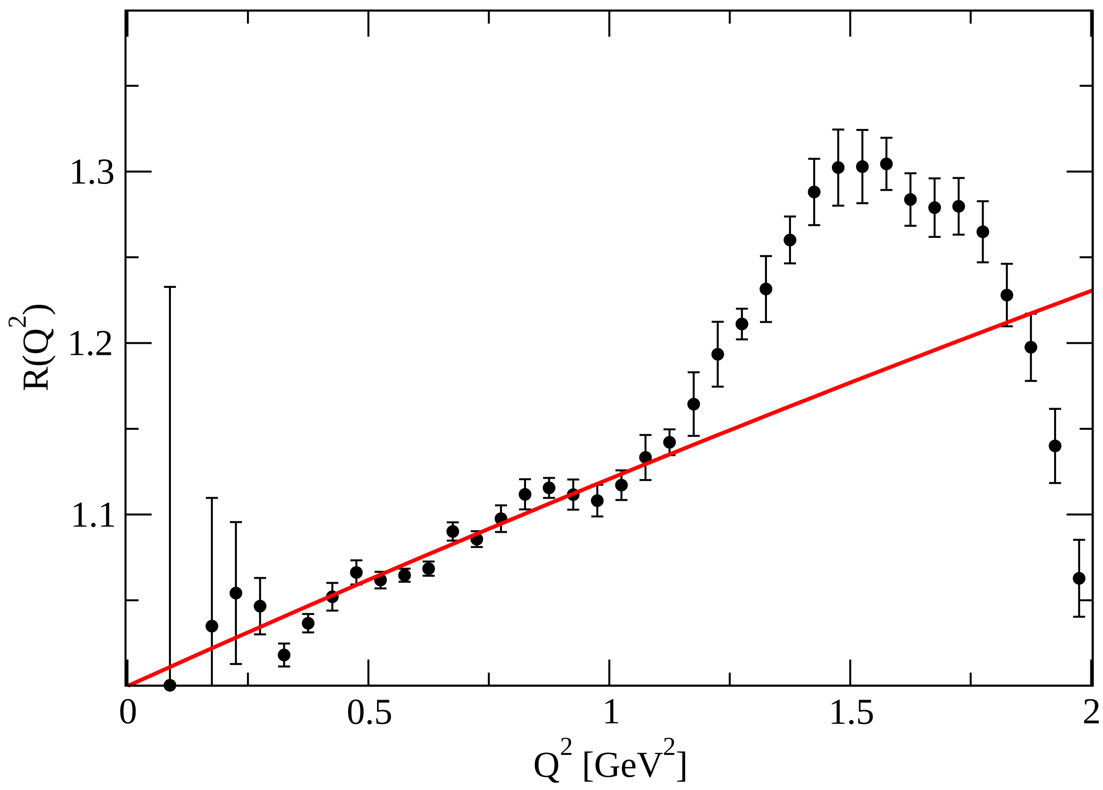

Hanhart et al. 2013

$\longrightarrow$ linear below 1 GeV: $F_\pi^V(s) \approx (1 + 0.1\,\mathrm{GeV}^{-2} s)\Omega(s)$

$\longrightarrow$ above: inelastic resonances ρ', $\rho''\ldots$

Final-state universality: η, $\eta' \to \pi^+\pi^-\gamma$

- $\eta^{(\prime)} \to \pi^+\pi^-\gamma$ driven by the chiral anomaly, $\pi^+\pi^-$ in P-wave $\longrightarrow$ final-state interactions the same as for vector form factor
- ansatz: $\mathcal{F}^{\eta^{(\prime)}}_{\pi\pi\gamma} = A \times P(t) \times \Omega(t)$, $P(t) = 1 + \alpha^{(\prime)} t$, $t = M^2_{\pi\pi}$

Final-state universality: $\eta,\ \eta' \to \pi^+\pi^-\gamma$

- $\eta^{(\prime)} \to \pi^+\pi^-\gamma$ driven by the chiral anomaly, $\pi^+\pi^-$ in P-wave
  $\longrightarrow$ final-state interactions the same as for vector form factor
- ansatz: $\mathcal{F}^{\eta^{(\prime)}}_{\pi\pi\gamma} = A \times P(t) \times \Omega(t)$, $P(t) = 1 + \alpha^{(\prime)} t$, $t = M^2_{\pi\pi}$
- divide data by pion form factor $\longrightarrow P(t)$ Stollenwerk et al. 2012

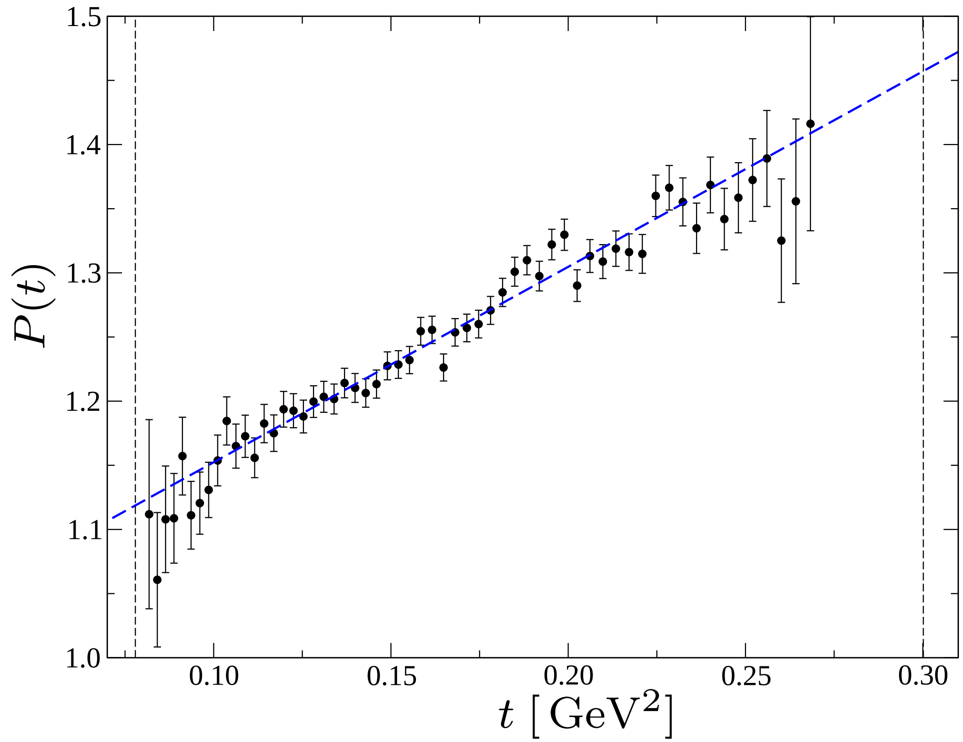

$\longrightarrow$ exp.: $\alpha_{\text{KLOE}} = (1.52 \pm 0.06)$ GeV^{-2} cf. KLOE 2013

Transition form factor $\eta \to \gamma^*\gamma$

Hanhart et al. 2013

$$\bar{F}_{\eta\gamma^*\gamma}(q^2,0) = 1 + \frac{\kappa_\eta q^2}{96\pi^2 F_\pi^2} \int_{4M_\pi^2}^{\infty} ds \sigma(s)^3 P(s) \frac{|F_\pi^V(s)|^2}{s-q^2}$$
$$+ \Delta F_{\eta\gamma^*\gamma}^{I=0}(q^2,0) \; [\longrightarrow \text{VMD}]$$

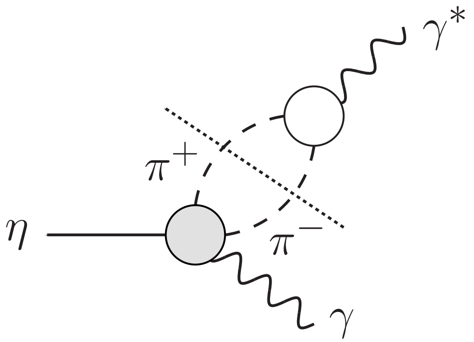

Transition form factor $\eta \to \gamma^*\gamma$

Hanhart et al. 2013

$$\bar{F}_{\eta\gamma^*\gamma}(q^2,0) = 1 + \frac{\kappa_\eta q^2}{96\pi^2 F_\pi^2} \int_{4M_\pi^2}^{\infty} ds \sigma(s)^3 P(s) \frac{|F_\pi^V(s)|^2}{s-q^2} + \Delta F_{\eta\gamma^*\gamma}^{I=0}(q^2,0) \; [\longrightarrow \text{VMD}]$$

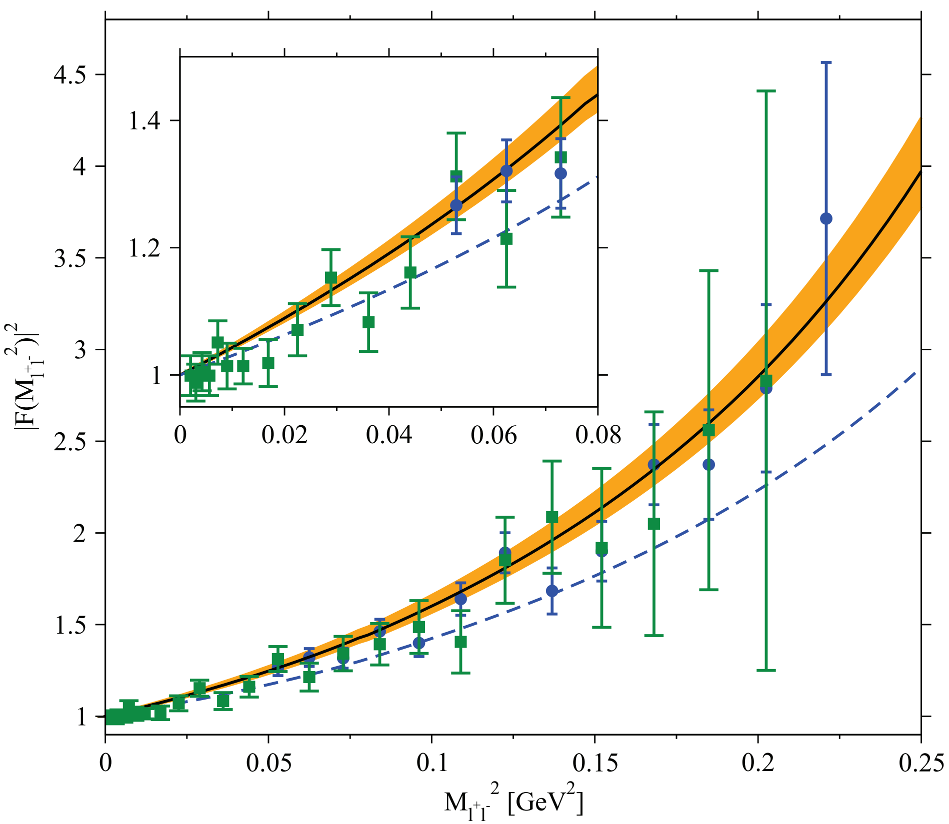

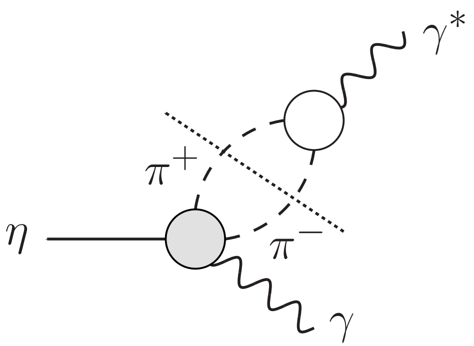

figures courtesy of C. Hanhart

data: NA60 2011, A2 2014

Anomalous decay $\eta \to \pi^+\pi^-\gamma$

- $\alpha_{\text{KLOE}} = (1.52 \pm 0.06)\,\text{GeV}^{-2}$ large
  $\longrightarrow$ implausible to explain through ρ', ρ''...
- for large t, expect $P(t) \to$ const. rather
- $\eta \to \gamma^*\gamma$ transition form factor:
  $\longrightarrow$ dispersion integral covers
  larger energy range

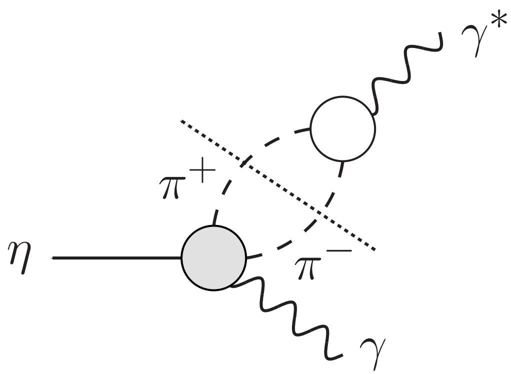

Anomalous decay $\eta \to \pi^+\pi^-\gamma$

- $\alpha_{\text{KLOE}} = (1.52 \pm 0.06)$ GeV^{-2} large
  $\longrightarrow$ implausible to explain through ρ', $\rho''\ldots$
- for large t, expect $P(t) \to$ const. rather
- $\eta \to \gamma^*\gamma$ transition form factor:
  $\longrightarrow$ dispersion integral covers
  larger energy range

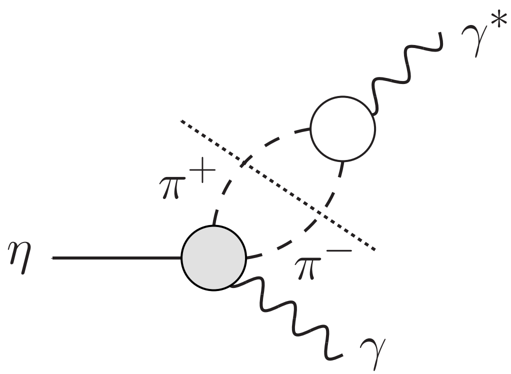

Intriguing observation:

- naive continuation of $\mathcal{F}^{\eta}_{\pi\pi\gamma} = A(1+\alpha t)\Omega(t)$ has zero at $t = -1/\alpha \approx -0.66\,\text{GeV}^2$
  $\longrightarrow$ test this in crossed process $\gamma\pi^- \to \pi^-\eta$
  $\longrightarrow$ "left-hand cuts" in $\pi\eta$ system?

BK, Plenter 2015

What are left-hand cuts?

Example: pion–pion scattering

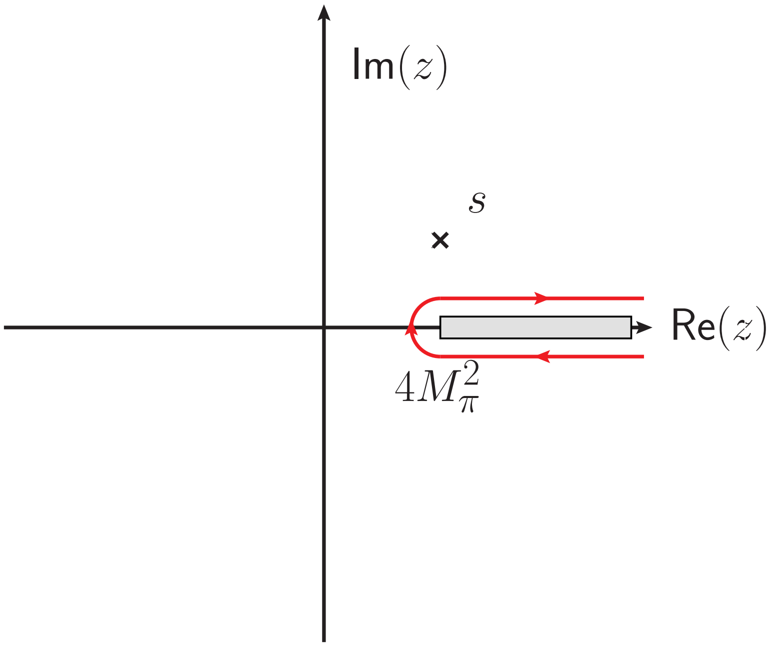

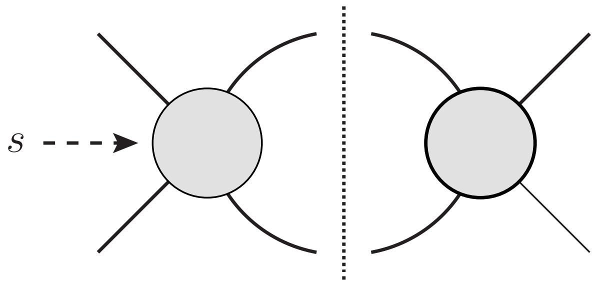

- right-hand cut due to unitarity: $s \geq 4M_\pi^2$

What are left-hand cuts?

Example: pion–pion scattering

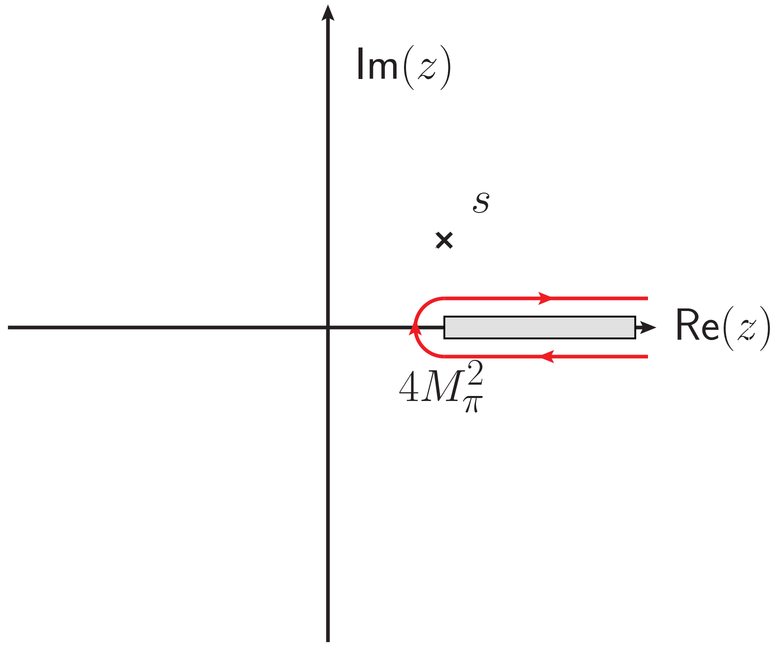

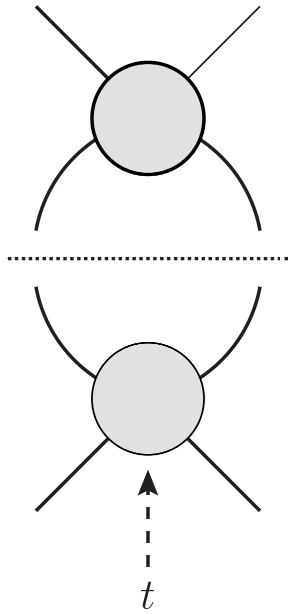

- right-hand cut due to unitarity: $s \geq 4M_\pi^2$
- crossing symmetry: cuts also for $t,\ u \geq 4M_\pi^2$

What are left-hand cuts?

Example: pion–pion scattering

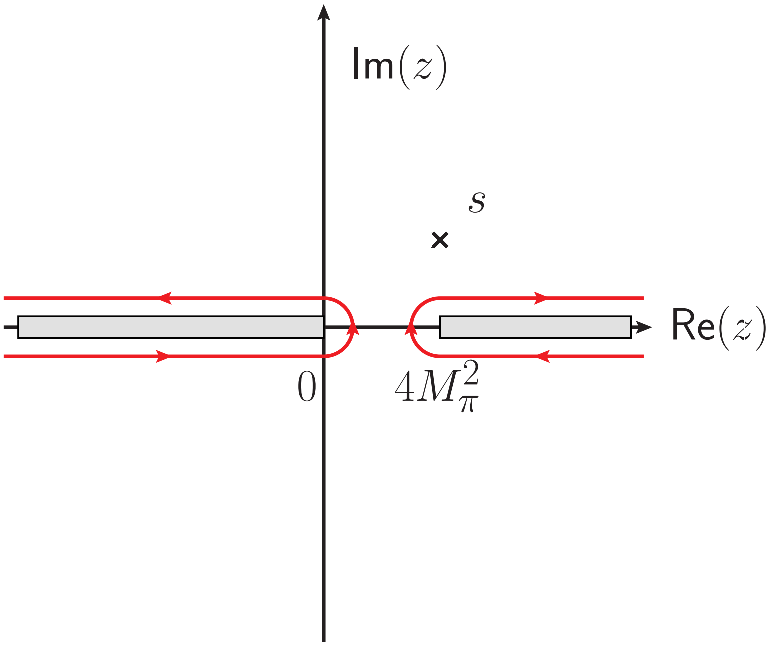

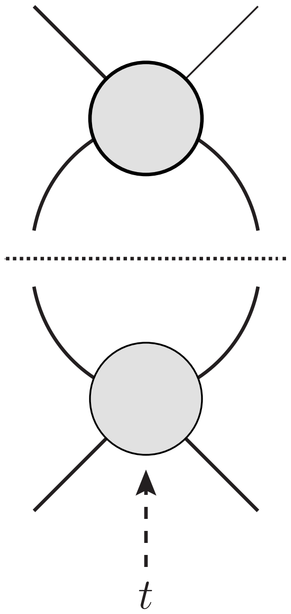

- right-hand cut due to unitarity: $s \geq 4M_\pi^2$
- crossing symmetry: cuts also for $t,\ u \geq 4M_\pi^2$
- partial-wave projection: $T(s,t) = 32\pi \sum_i T_i(s) P_i(\cos\theta)$

$$t(s,\cos\theta) = \tfrac{1-\cos\theta}{2}(4M_\pi^2 - s)$$

$\longrightarrow$ cut for $t \geq 4M_\pi^2$ becomes cut for $s \leq 0$ in partial wave

Primakoff reaction $\gamma\pi \to \pi\eta$

- can be measured in Primakoff reaction

COMPASS

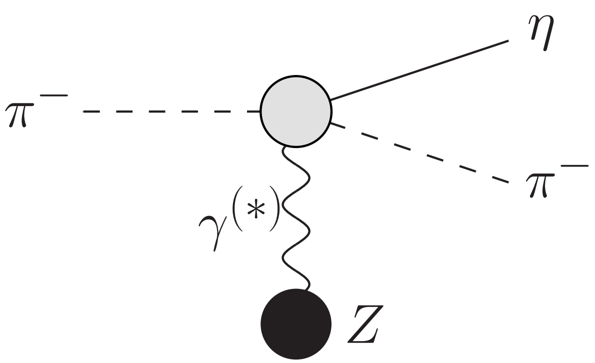

- S-wave forbidden

  P-wave exotic: $J^{PC} = 1^{-+}$

  D-wave $a_2(1320)$ first resonance

Primakoff reaction $\gamma\pi \to \pi\eta$

- can be measured in Primakoff reaction

COMPASS

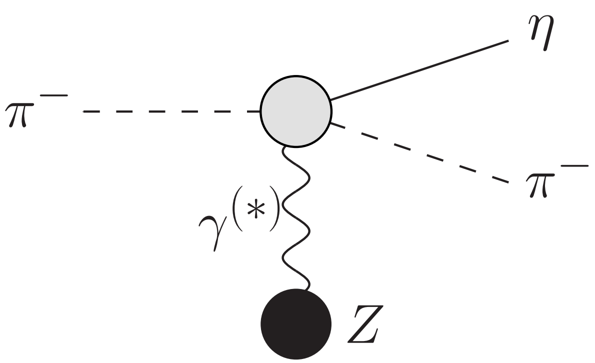

- S-wave forbidden

  P-wave exotic: $J^{PC} = 1^{-+}$

  D-wave $a_2(1320)$ first resonance

- include a_2 as left-hand cut in decay
  couplings fixed from $a_2 \to \pi\eta,\ \pi\gamma$

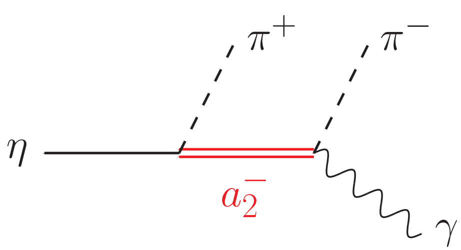

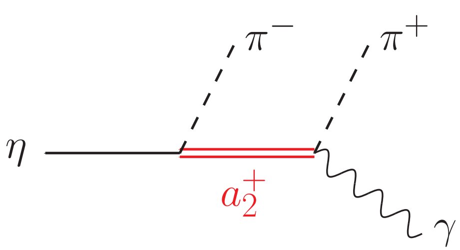

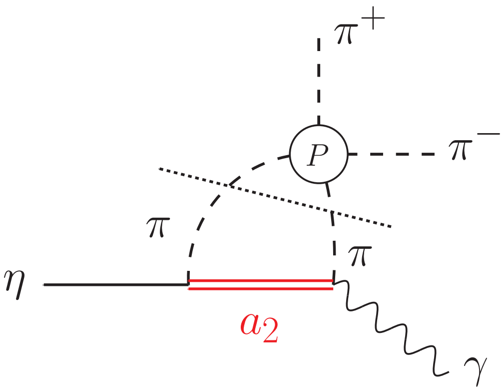

  ▷ compatible with decay data?

  ▷ predictions for $\gamma\pi \to \pi\eta$ cross sections and asymmetries
  [$\longrightarrow$ spares]

Formalism including left-hand cuts

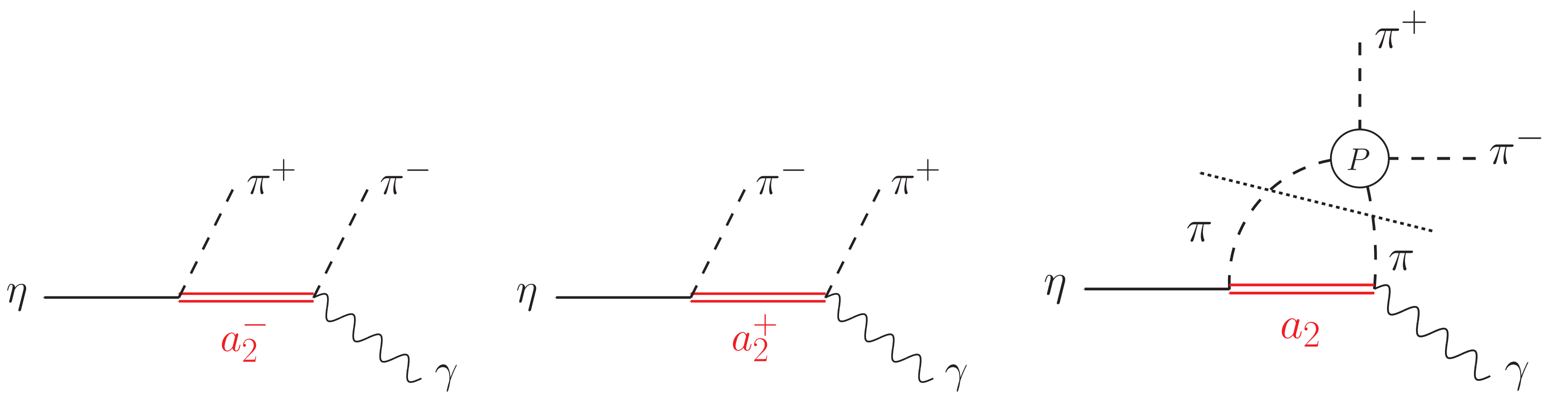

- a_2 + rescattering essential to preserve Watson's theorem
- formally:

$$\mathcal{F}^{\eta}_{\pi\pi\gamma}(s,t,u) = \mathcal{F}(t) + \mathcal{G}_{a_2}(s,t,u) + \mathcal{G}_{a_2}(u,t,s)$$

$$\mathcal{F}(t) = \Omega(t)\left\{ A(1+\alpha t) + \frac{t^2}{\pi}\int_{4M_\pi^2}^{\infty}\frac{dx}{x^2}\frac{\sin\delta(x)\hat{\mathcal{G}}(x)}{|\Omega(x)|(x-t)}\right\}$$

$\hat{\mathcal{G}}$: t-channel P-wave projection of a_2 exchange graphs

- re-fit subtraction constants A, α

$\eta,\, \eta' \to \pi^+\pi^-\gamma$ with a_2

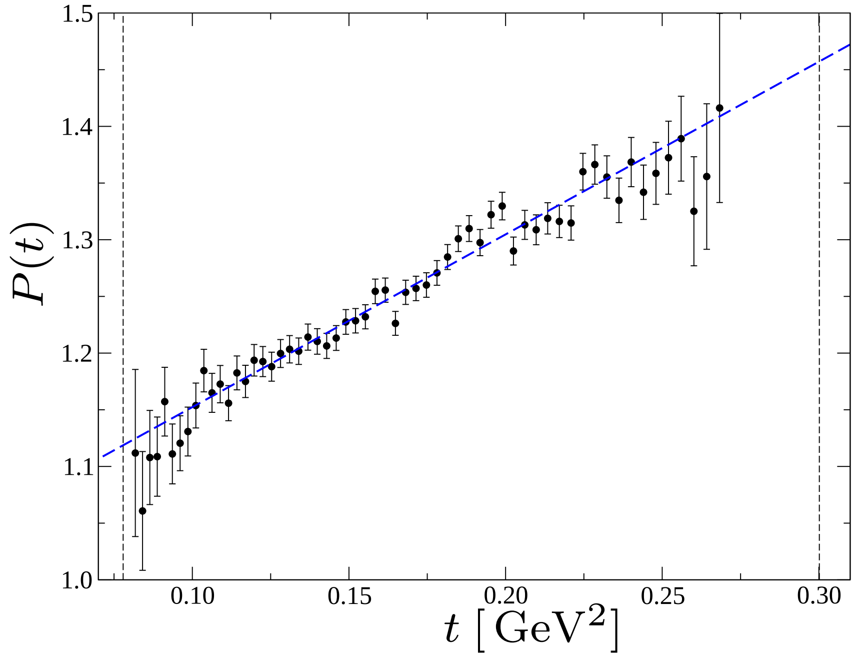

KLOE 2013

$\alpha = 1.52 \pm 0.06$, $\chi^2/\text{ndof} = 0.94$

$\eta,\ \eta' \to \pi^+\pi^-\gamma$ with a_2

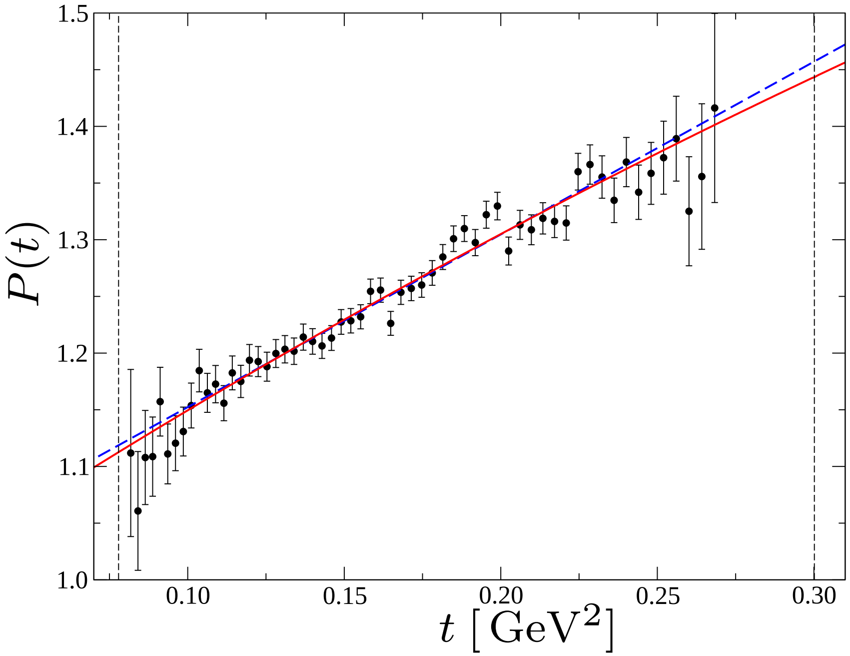

KLOE 2013

$\alpha = 1.52 \pm 0.06$, χ^2/ndof $= 0.94$

$\longrightarrow$ $\alpha = 1.42 \pm 0.06$, χ^2/ndof $= 0.90$

$\eta,\ \eta' \to \pi^+\pi^-\gamma$ with a_2

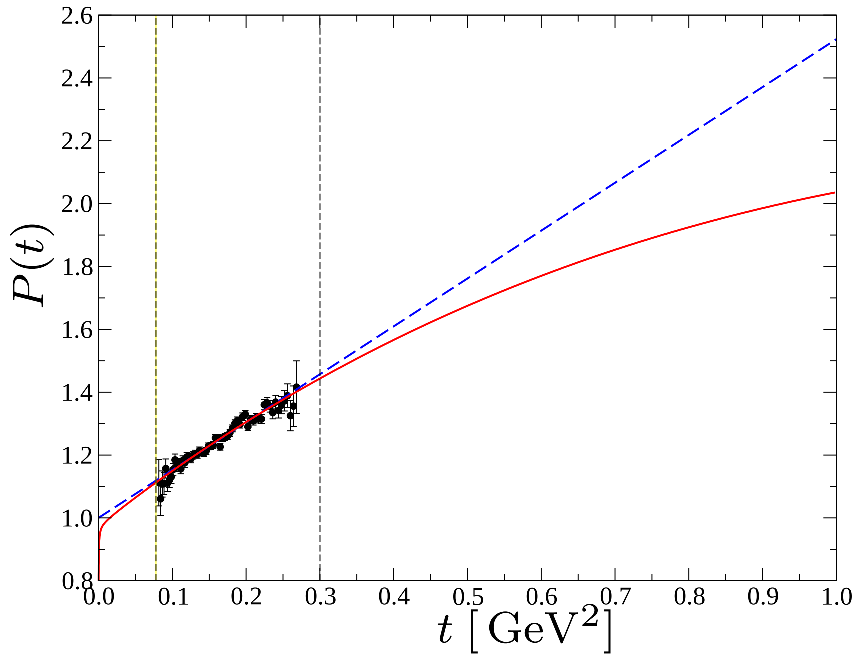

KLOE 2013

$\alpha = 1.52 \pm 0.06$, χ^2/ndof $= 0.94$

$\longrightarrow$ $\alpha = 1.42 \pm 0.06$, χ^2/ndof $= 0.90$

- equally good—why care? sum rule for $\eta \to \gamma^*\gamma$ transition form factor slope reduced by $7-8\%$ cf. Hanhart et al. 2013

$\eta,\ \eta' \to \pi^+\pi^-\gamma$ with a_2

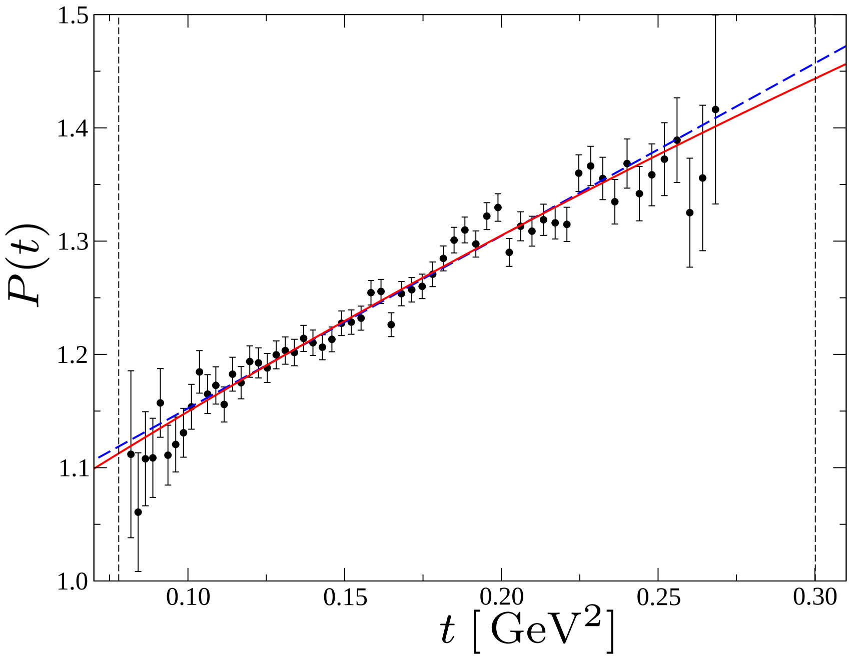

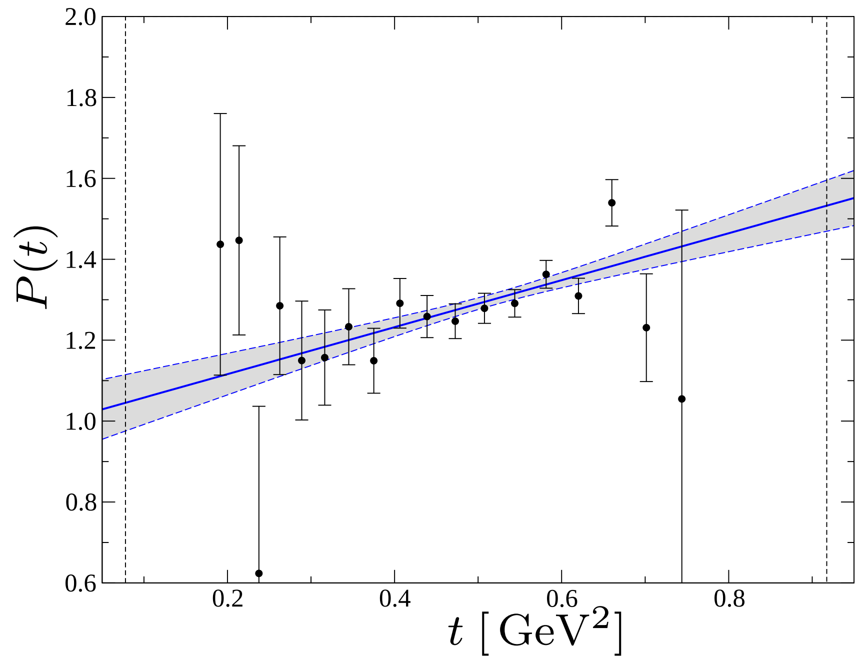

KLOE 2013

$\alpha = 1.52 \pm 0.06$, $\chi^2/$ndof $= 0.94$

$\longrightarrow \alpha = 1.42 \pm 0.06$, $\chi^2/$ndof $= 0.90$

Crystal Barrel 1997

$\alpha' = 0.6 \pm 0.2$, $\chi^2/$ndof $= 1.2$

- equally good—why care? sum rule for $\eta \to \gamma^*\gamma$ transition form factor slope reduced by $7-8\%$

cf. Hanhart et al. 2013

$\eta,\ \eta' \to \pi^+\pi^-\gamma$ with a_2

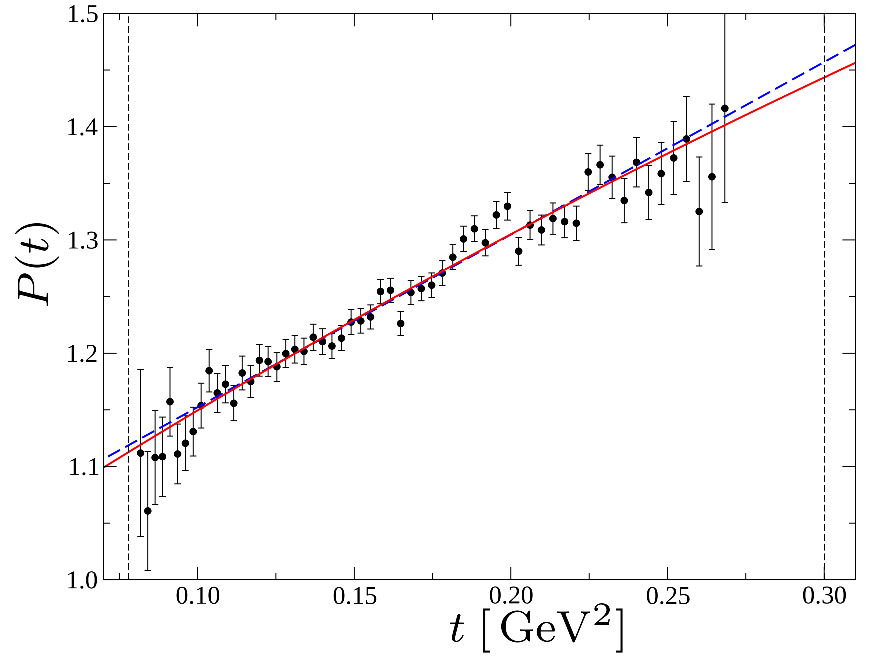

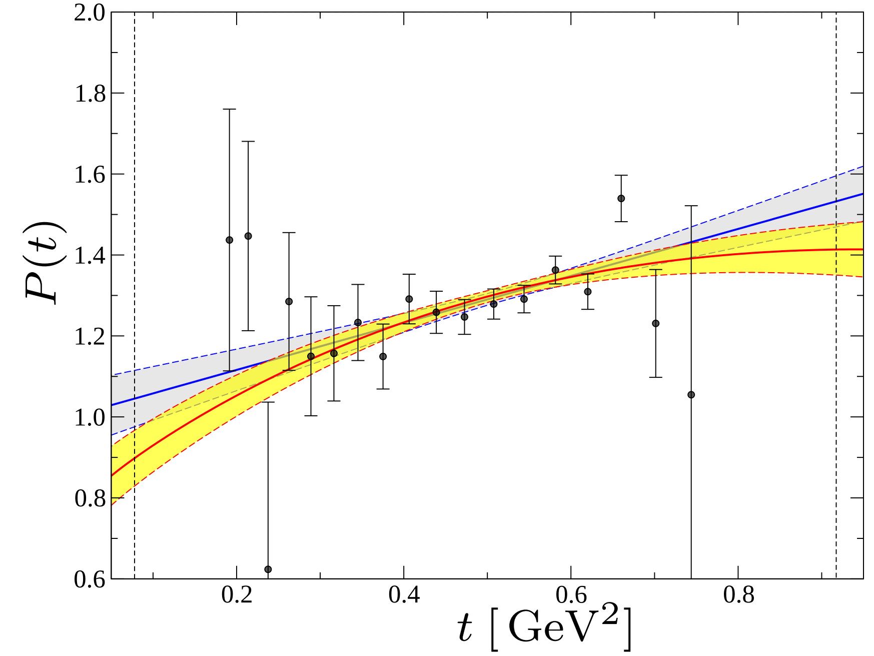

KLOE 2013

$\alpha = 1.52 \pm 0.06$, χ^2/ndof $= 0.94$

$\longrightarrow \alpha = 1.42 \pm 0.06$, χ^2/ndof $= 0.90$

Crystal Barrel 1997

$\alpha' = 0.6 \pm 0.2$, χ^2/ndof $= 1.2$

$\longrightarrow \alpha' = 1.4 \pm 0.4$, χ^2/ndof $= 1.4$

- equally good—why care? sum rule for $\eta \to \gamma^*\gamma$ transition form factor slope reduced by $7 - 8\%$ cf. Hanhart et al. 2013
- $\alpha \approx \alpha'$ (large-N_c) better fulfilled including a_2 BK, Plenter 2015

$\gamma\pi \to \pi\pi$ and the Wess–Zumino–Witten anomaly

- controls low-energy processes of odd intrinsic parity
- π^0 decay $\pi^0 \to \gamma\gamma$: $F_{\pi^0\gamma\gamma} = \dfrac{e^2}{4\pi^2 F_\pi}$

  F_π: pion decay constant $\longrightarrow$ measured at 1.5% level PrimEx 2011

$\gamma\pi \to \pi\pi$ and the Wess–Zumino–Witten anomaly

- controls low-energy processes of odd intrinsic parity
- π^0 decay $\pi^0 \to \gamma\gamma$: $F_{\pi^0\gamma\gamma} = \dfrac{e^2}{4\pi^2 F_\pi}$
  F_π: pion decay constant $\longrightarrow$ measured at 1.5% level   PrimEx 2011
- $\gamma\pi \to \pi\pi$ at zero energy: $F_{3\pi} = \dfrac{e}{4\pi^2 F_\pi^3} = (9.78 \pm 0.05)\,\text{GeV}^{-3}$
  how well can we test this low-energy theorem?

$\gamma\pi \to \pi\pi$ and the Wess–Zumino–Witten anomaly

- controls low-energy processes of odd intrinsic parity
- π^0 decay $\pi^0 \to \gamma\gamma$: $F_{\pi^0\gamma\gamma} = \dfrac{e^2}{4\pi^2 F_\pi}$

  F_π: pion decay constant $\longrightarrow$ measured at 1.5% level   PrimEx 2011
- $\gamma\pi \to \pi\pi$ at zero energy: $F_{3\pi} = \dfrac{e}{4\pi^2 F_\pi^3} = (9.78 \pm 0.05)$ GeV^{-3}

  how well can we test this low-energy theorem?

Primakoff reaction

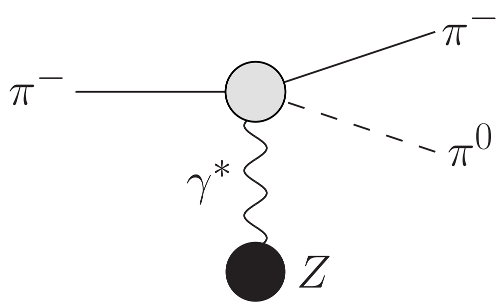

$F_{3\pi} = (10.7 \pm 1.2)$ GeV^{-3}

Serpukhov 1987, Ametller et al. 2001

$\pi^- e^- \to \pi^- e^- \pi^0$

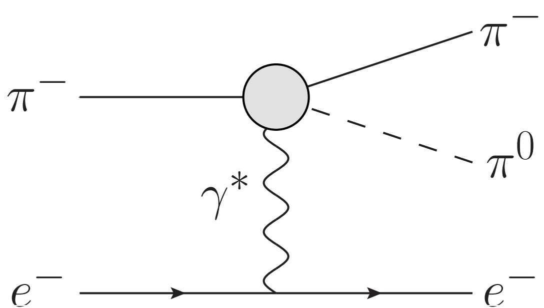

$F_{3\pi} = (9.6 \pm 1.1)$ GeV^{-3}

Giller et al. 2005

$\longrightarrow$ $F_{3\pi}$ tested only at 10% level

Chiral anomaly: Primakoff measurement

- previous analyses based on
  - data in threshold region only — Serpukhov 1987
  - chiral perturbation theory for extraction

Chiral anomaly: Primakoff measurement

- previous analyses based on
  - ▷ data in threshold region only — Serpukhov 1987
  - ▷ chiral perturbation theory for extraction

- Primakoff measurement of whole spectrum
  COMPASS, work in progress
- idea: use dispersion relations to exploit all data below 1 GeV for anomaly extraction
- effect of ρ resonance included model-independently via $\pi\pi$ P-wave phase shift

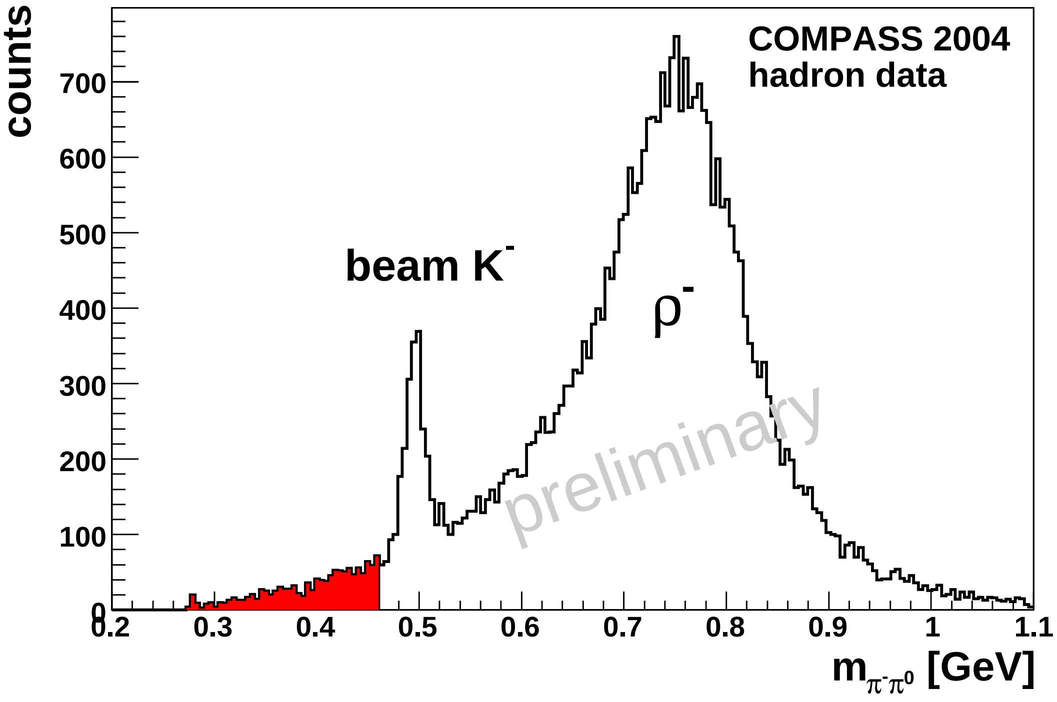

figure courtesy of T. Nagel 2009

Dispersion relations for 3 pions

- $\gamma\pi \to \pi\pi$ fully crossing symmetric: odd partial waves
  $\longrightarrow$ P-waves only (neglecting F- and higher)
- amplitude decomposed into single-variable functions

$$\mathcal{F}(s,t,u) = \mathcal{F}(s) + \mathcal{F}(t) + \mathcal{F}(u)$$

Dispersion relations for 3 pions

- $\gamma\pi \to \pi\pi$ fully crossing symmetric: odd partial waves
  $\longrightarrow$ P-waves only (neglecting F- and higher)
- amplitude decomposed into single-variable functions

$$\mathcal{F}(s,t,u) = \mathcal{F}(s) + \mathcal{F}(t) + \mathcal{F}(u)$$

- left-hand cut $\hat{\mathcal{F}}(s)$ and right-hand cut $\mathcal{F}(s)$ self-consistent:

$$\mathcal{F}(s) = \Omega(s)\left\{\frac{C_1}{3} + \frac{s}{\pi}\int_{4M_\pi^2}^{\infty}\frac{ds'}{s'}\frac{\sin\delta_1^1(s')\hat{\mathcal{F}}(s')}{|\Omega(s')|(s'-s)}\right\}$$

$$\hat{\mathcal{F}}(s) = \frac{3}{2}\int_{-1}^{1} dz\,(1-z^2)\mathcal{F}\big(t(s,z)\big)$$

$\mathcal{F}(s) =$ 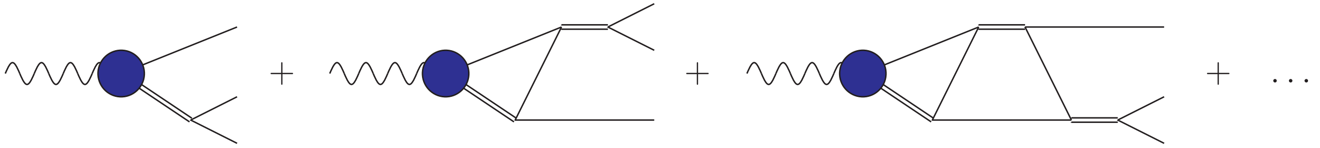

Omnès solution for $\gamma\pi \rightarrow \pi\pi$

$$\mathcal{F}(s) = \Omega(s)\left\{\frac{C_1}{3} + \frac{s}{\pi}\int_{4M_\pi^2}^{\infty}\frac{ds'}{s'}\frac{\sin\delta_1^1(s')\hat{\mathcal{F}}(s')}{|\Omega(s')|(s'-s)}\right\}$$

- important observation: $\mathcal{F}(s)$ linear in C_1

$$\mathcal{F}(s) = C_1 \times \mathcal{F}_{C_1=1}(s)$$

$\longrightarrow$ basis function $\mathcal{F}_{C_1=1}(s)$ calculated independently of C_1

Omnès solution for $\gamma\pi \to \pi\pi$

$$\mathcal{F}(s) = \Omega(s)\left\{\frac{C_1}{3} + \frac{s}{\pi}\int_{4M_\pi^2}^{\infty}\frac{ds'}{s'}\frac{\sin\delta_1^1(s')\hat{\mathcal{F}}(s')}{|\Omega(s')|(s'-s)}\right\}$$

- important observation: $\mathcal{F}(s)$ linear in C_1

$$\mathcal{F}(s) = C_1 \times \mathcal{F}_{C_1=1}(s)$$

$\longrightarrow$ basis function $\mathcal{F}_{C_1=1}(s)$ calculated independently of C_1

- oversubtract $\longrightarrow$ increase precision $\longrightarrow$ representation of cross section in terms of two parameters

  $\longrightarrow$ fit to data, extract

$$F_{3\pi} \simeq C_2 = C_2^{(1)} + C_2^{(2)} M_\pi^2$$

$\longrightarrow \sigma \propto (C_2)^2$ also in ρ region

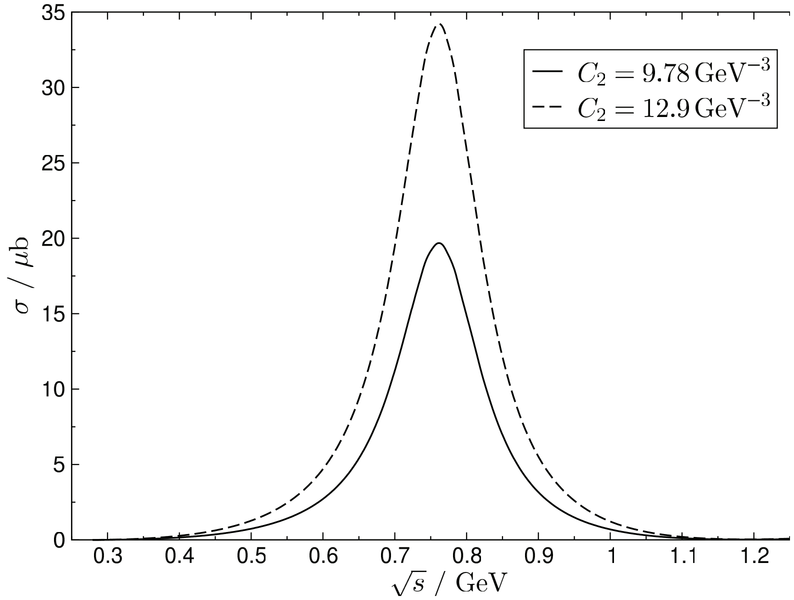

Hoferichter, BK, Sakkas 2012

Extension to vector-meson decays: $\omega/\phi \to 3\pi$

- identical quantum numbers to $\gamma\pi \to \pi\pi$
- beyond ChPT: copious efforts to develop EFT for vector mesons

  Bijnens et al.; Bruns, Meißner; Lutz, Leupold; Gegelia et al.; Kampf et al.. . .
- vector mesons highly important for (virtual) photon processes

Extension to vector-meson decays: $\omega/\phi \to 3\pi$

- identical quantum numbers to $\gamma\pi \to \pi\pi$
- beyond ChPT: copious efforts to develop EFT for vector mesons
  Bijnens et al.; Bruns, Meißner; Lutz, Leupold; Gegelia et al.; Kampf et al. . . .
- vector mesons highly important for (virtual) photon processes
- $\omega/\phi \to 3\pi$ analyzed in terms of KLOE 2003, CMD-2 2006

  sum of 3 Breit–Wigners (ρ^+, ρ^-, ρ^0)

  + constant background term

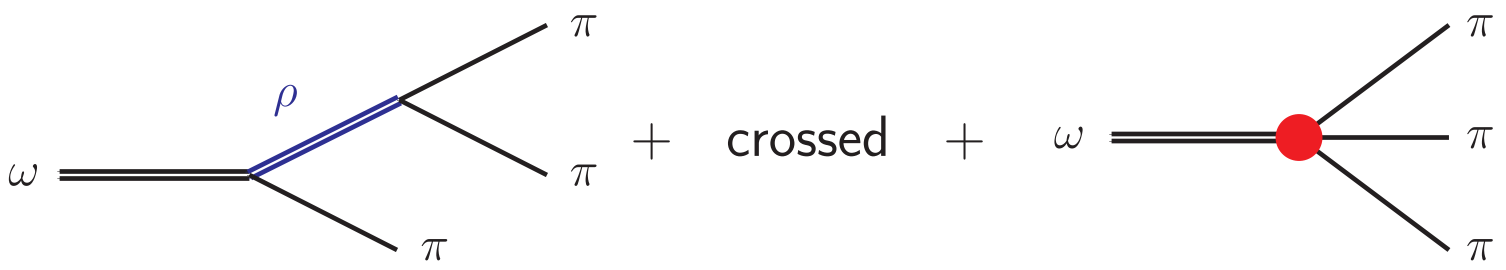

Extension to vector-meson decays: $\omega/\phi \to 3\pi$

- identical quantum numbers to $\gamma\pi \to \pi\pi$
- beyond ChPT: copious efforts to develop EFT for vector mesons
  Bijnens et al.; Bruns, Meißner; Lutz, Leupold; Gegelia et al.; Kampf et al.. . .
- vector mesons highly important for (virtual) photon processes
- $\omega/\phi \to 3\pi$ analyzed in terms of KLOE 2003, CMD-2 2006
  sum of 3 Breit–Wigners (ρ^+, ρ^-, ρ^0)
  \+ constant background term

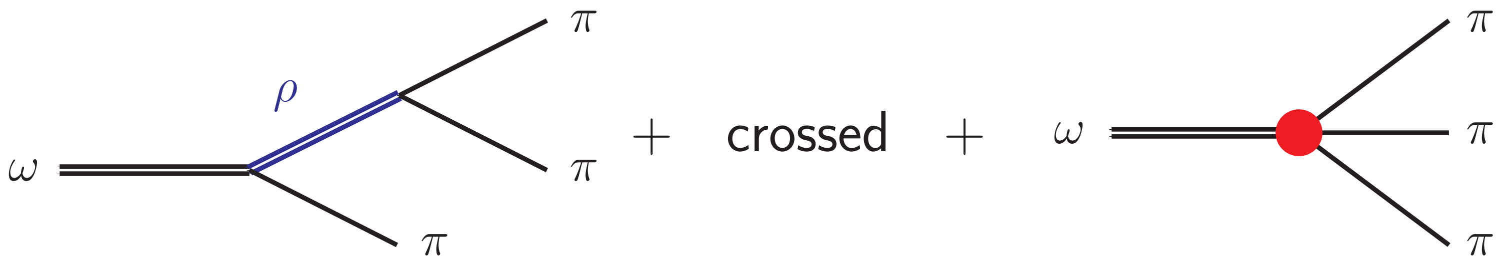

Problem:

$\longrightarrow$ unitarity fixes Im/Re parts

$\longrightarrow$ adding a contact term destroys this relation

$\longrightarrow$ reconcile data with dispersion relations?

$\omega/\phi \to 3\pi$: dispersive solution

- identical quantum numbers to $\gamma\pi \to \pi\pi$

$$\mathcal{F}(s) = a\,\Omega(s)\left\{1 + \frac{s}{\pi}\int_{4M_\pi^2}^{\infty}\frac{ds'}{s'}\frac{\sin\delta_1^1(s')\hat{\mathcal{F}}(s')}{|\Omega(s')|(s'-s-i\epsilon)}\right\}$$

$$\hat{\mathcal{F}}(s) = \frac{3}{2}\int_{-1}^{1} dz\,(1-z^2)\mathcal{F}\big(t(s,z)\big)$$

$\longrightarrow$ fix subtraction constant a to partial width(s) $\omega/\phi \to 3\pi$

$\omega/\phi \to 3\pi$: dispersive solution

- identical quantum numbers to $\gamma\pi \to \pi\pi$

$$\mathcal{F}(s) = a\,\Omega(s)\left\{1 + \frac{s}{\pi}\int_{4M_\pi^2}^{\infty}\frac{ds'}{s'}\frac{\sin\delta_1^1(s')\hat{\mathcal{F}}(s')}{|\Omega(s')|(s'-s-i\epsilon)}\right\}$$

$$\hat{\mathcal{F}}(s) = \frac{3}{2}\int_{t_-(s)}^{t_+(s)} dt\,\left(\tfrac{dz}{dt}\right)\left(1-z(t)^2\right)\mathcal{F}(t)$$

$\longrightarrow$ fix subtraction constant a to partial width(s) $\omega/\phi \to 3\pi$

- complication:
  analytic continuation in
  decay mass M_V required
- $M_V < 3M_\pi$:
  okay

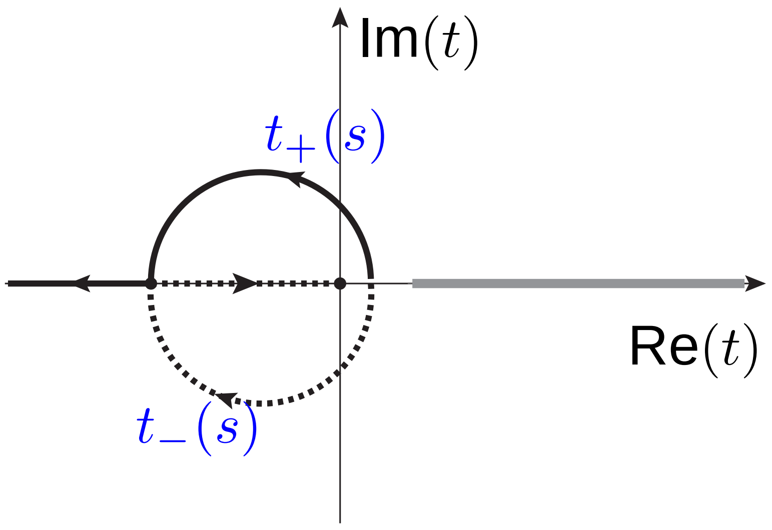

$\omega/\phi \to 3\pi$: dispersive solution

- identical quantum numbers to $\gamma\pi \to \pi\pi$

$$\mathcal{F}(s) = a\,\Omega(s)\bigg\{1 + \frac{s}{\pi}\int_{4M_\pi^2}^{\infty}\frac{ds'}{s'}\frac{\sin\delta_1^1(s')\hat{\mathcal{F}}(s')}{|\Omega(s')|(s'-s-i\epsilon)}\bigg\}$$

$$\hat{\mathcal{F}}(s) = \frac{3}{2}\int_{t_-(s)}^{t_+(s)} dt\,\left(\tfrac{dz}{dt}\right)\left(1-z(t)^2\right)\mathcal{F}(t)$$

$\longrightarrow$ fix subtraction constant a to partial width(s) $\omega/\phi \to 3\pi$

- complication: analytic continuation in decay mass M_V required
- $M_V > 3M_\pi$: path deformation required

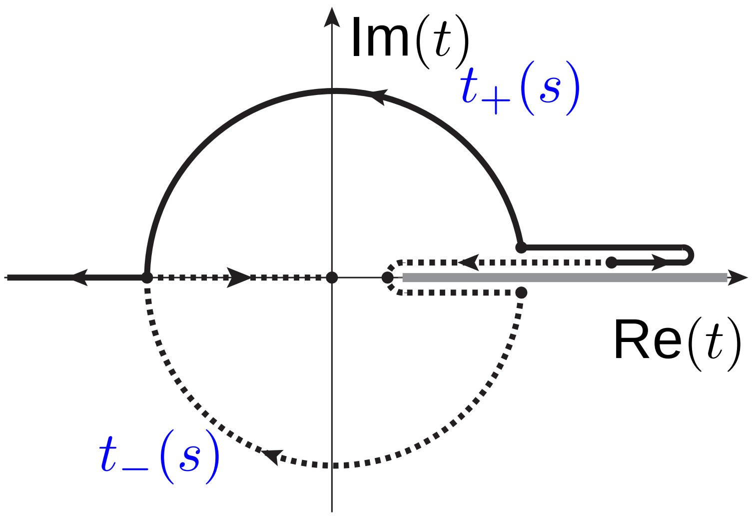

$\omega/\phi \to 3\pi$: dispersive solution

- identical quantum numbers to $\gamma\pi \to \pi\pi$

$$\mathcal{F}(s) = a\,\Omega(s)\left\{1 + \frac{s}{\pi}\int_{4M_\pi^2}^{\infty}\frac{ds'}{s'}\frac{\sin\delta_1^1(s')\hat{\mathcal{F}}(s')}{|\Omega(s')|(s'-s-i\epsilon)}\right\}$$

$$\hat{\mathcal{F}}(s) = \frac{3}{2}\int_{t_-(s)}^{t_+(s)} dt\,\left(\tfrac{dz}{dt}\right)\left(1-z(t)^2\right)\mathcal{F}(t)$$

$\longrightarrow$ fix subtraction constant a to partial width(s) $\omega/\phi \to 3\pi$

- complication:
  analytic continuation in
  decay mass M_V required
- $M_V > 3M_\pi$:
  path deformation required
  $\longrightarrow$ generates 3-particle cuts

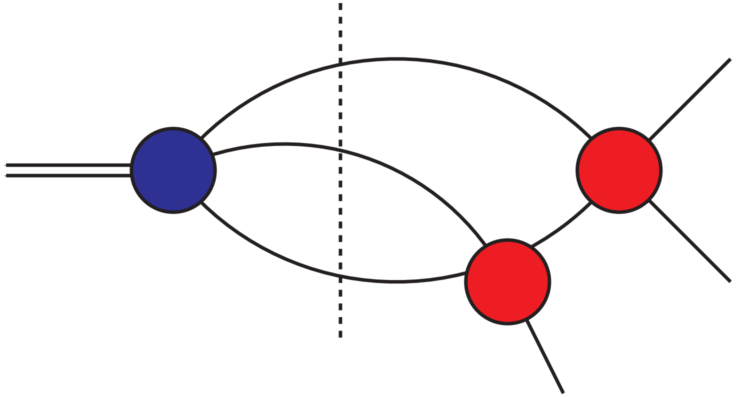

$\omega/\phi \to 3\pi$ Dalitz plots

- subtraction constant a fixed to partial width
  $\longrightarrow$ normalised Dalitz plot a prediction

$\omega \to 3\pi$: $\phi \to 3\pi$:

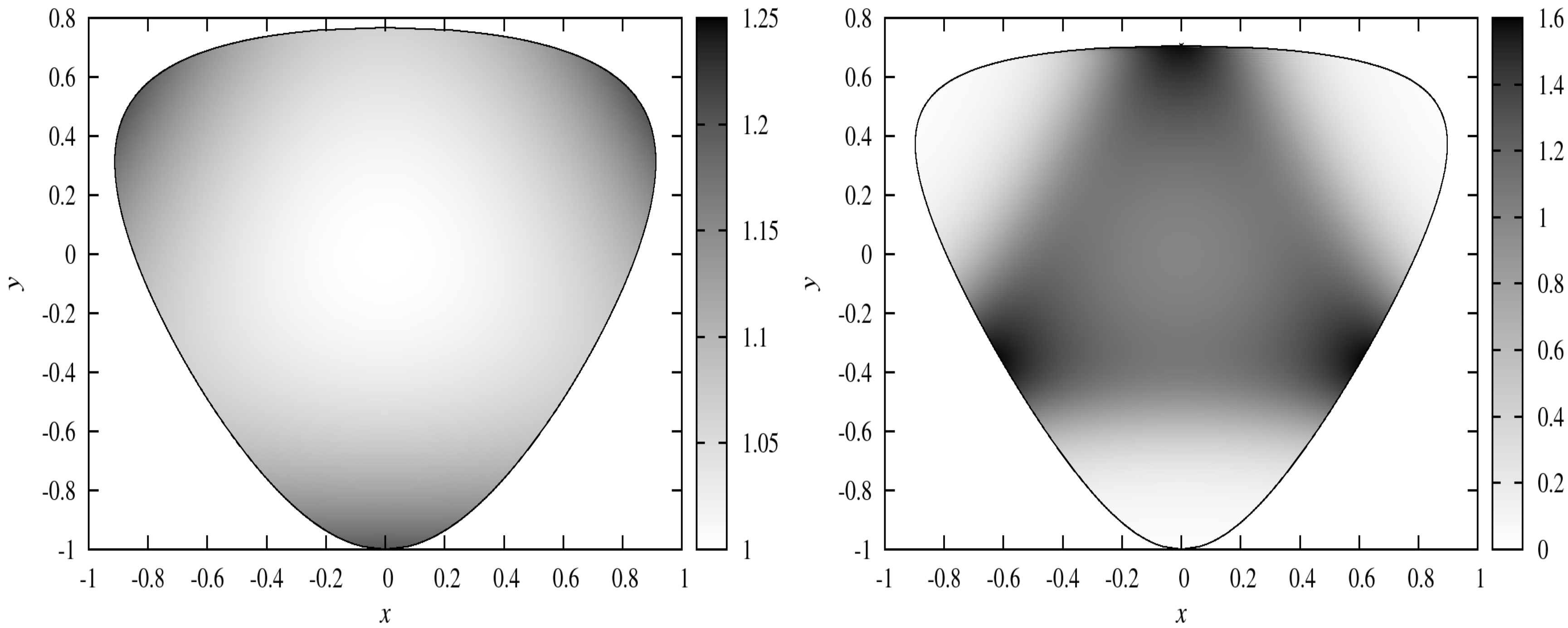

- ω Dalitz plot is relatively smooth
- ϕ Dalitz plot clearly shows ρ resonance bands

Niecknig, BK, Schneider 2012

$\omega/\phi \to 3\pi$ Dalitz plots

- subtraction constant a fixed to partial width
  $\longrightarrow$ normalised Dalitz plot a prediction

$\omega \to 3\pi$:

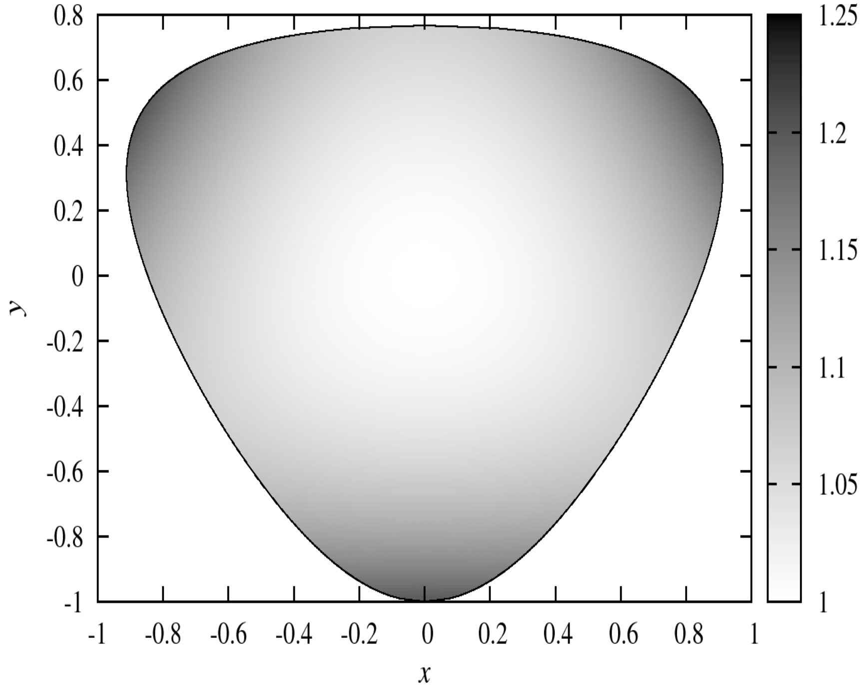

$\phi \to 3\pi$:

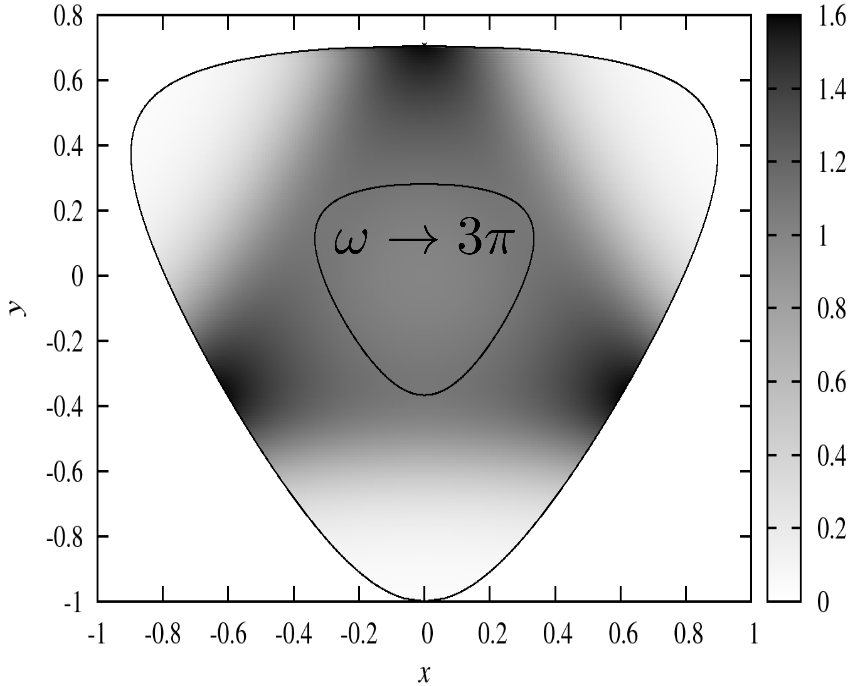

- ω Dalitz plot is relatively smooth
- ϕ Dalitz plot clearly shows ρ resonance bands

Niecknig, BK, Schneider 2012

Experimental comparison to $\phi \to 3\pi$

KLOE Dalitz plot: $2 \cdot 10^6$ events, 1834 bins   Niecknig, BK, Schneider 2012

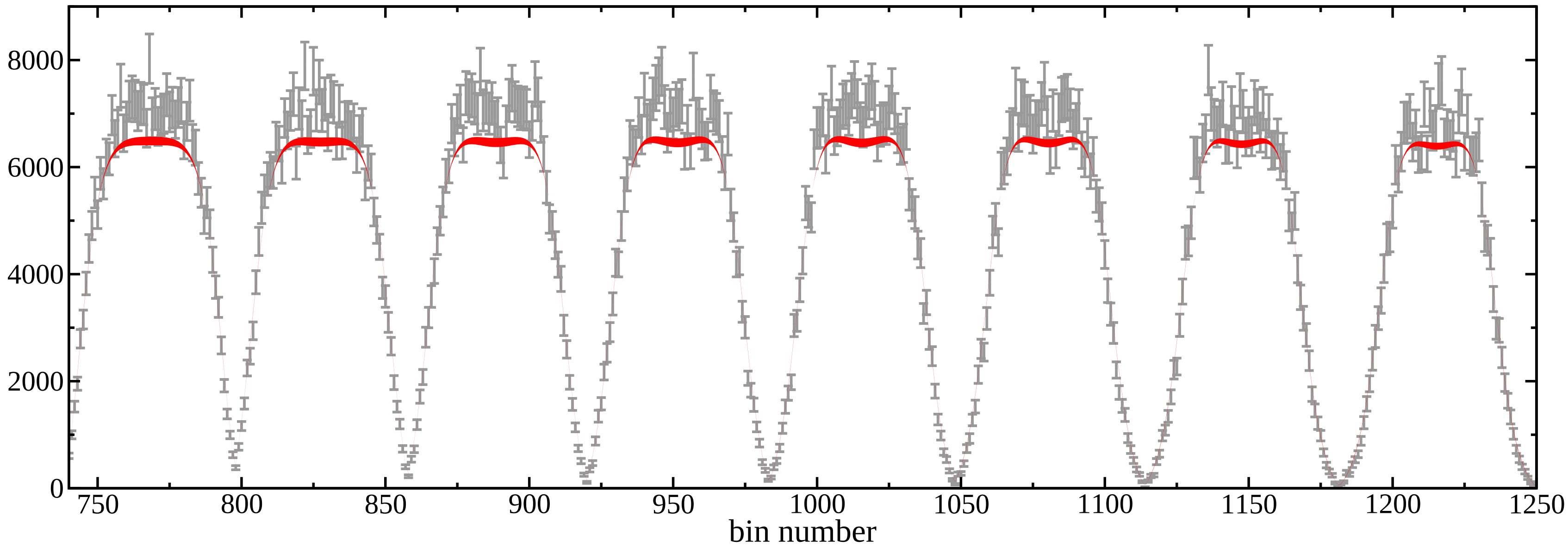

$\hat{\mathcal{F}} = 0$	
χ^2/ndof	$1.71 \dots 2.06$

$$\mathcal{F}(s) = a\,\Omega(s) = a\,\exp\left[\frac{s}{\pi}\int_{4M_\pi^2}^{\infty}\frac{ds'}{s'}\frac{\delta_1^1(s')}{s'-s}\right]$$

Experimental comparison to $\phi \to 3\pi$

KLOE Dalitz plot: $2 \cdot 10^6$ events, 1834 bins   Niecknig, BK, Schneider 2012

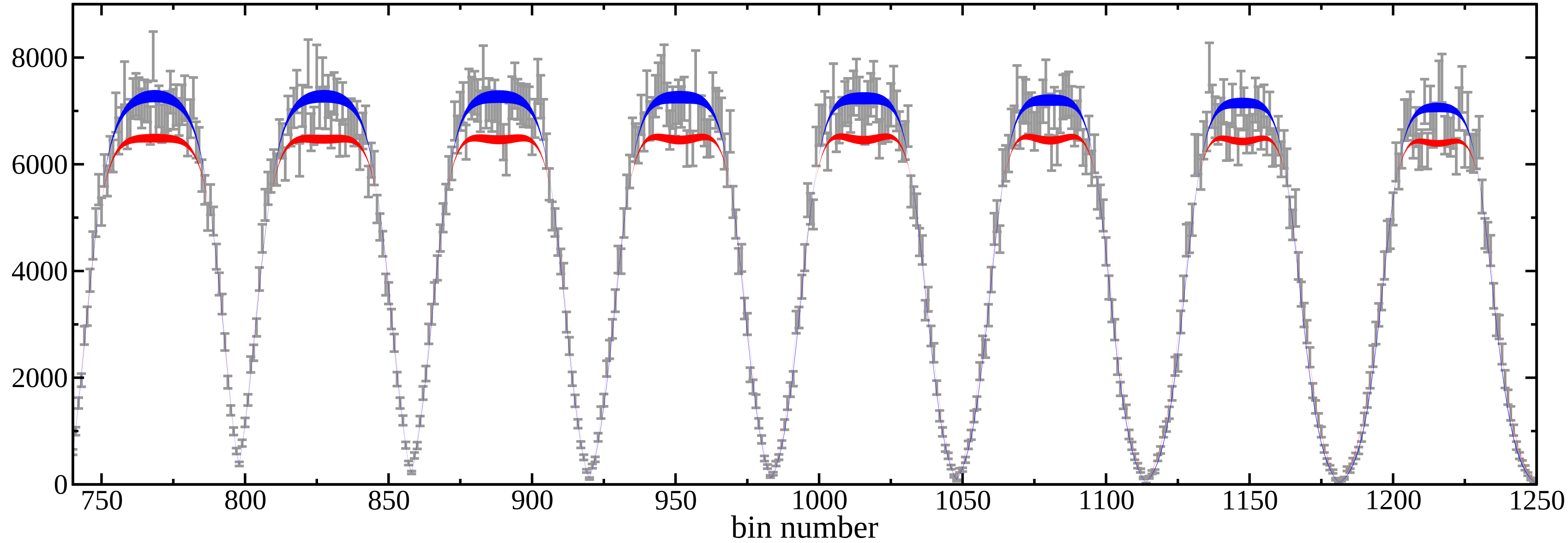

	$\hat{\mathcal{F}} = 0$	once-subtracted
χ^2/ndof	$1.71 \ldots 2.06$	$1.17 \ldots 1.50$

$$\mathcal{F}(s) = a\,\Omega(s)\left[1 + \frac{s}{\pi}\int_{4M_\pi^2}^{\infty}\frac{ds'}{s'}\frac{\hat{\mathcal{F}}(s')\sin\delta_1^1(s')}{|\Omega(s')|(s'-s)}\right]$$

Experimental comparison to $\phi \to 3\pi$

KLOE Dalitz plot: $2 \cdot 10^6$ events, 1834 bins   Niecknig, BK, Schneider 2012

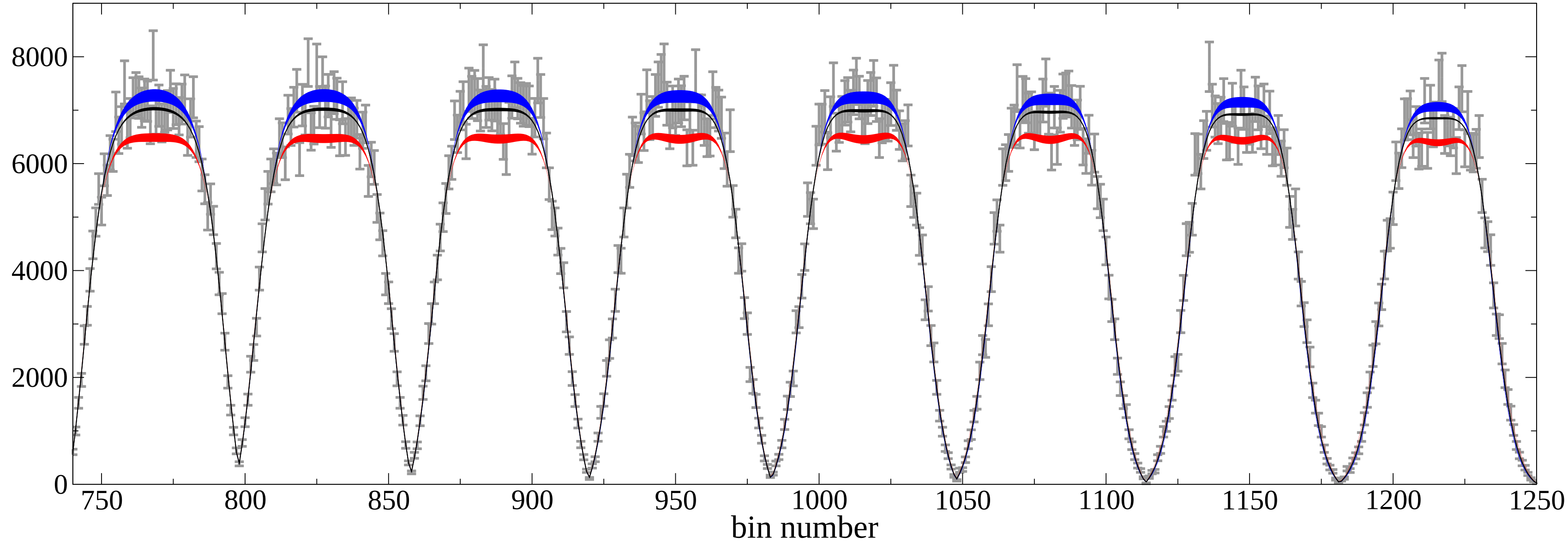

	$\hat{\mathcal{F}} = 0$	once-subtracted	twice-subtracted
χ^2/ndof	$1.71 \ldots 2.06$	$1.17 \ldots 1.50$	$1.02 \ldots 1.03$

$$\mathcal{F}(s) = a\,\Omega(s)\left[1 + b\,s + \frac{s^2}{\pi}\int_{4M_\pi^2}^{\infty}\frac{ds'}{s'^2}\frac{\hat{\mathcal{F}}(s')\sin\delta_1^1(s')}{|\Omega(s')|(s'-s)}\right]$$

Experimental comparison to $\phi \to 3\pi$

KLOE Dalitz plot: $2 \cdot 10^6$ events, 1834 bins   Niecknig, BK, Schneider 2012

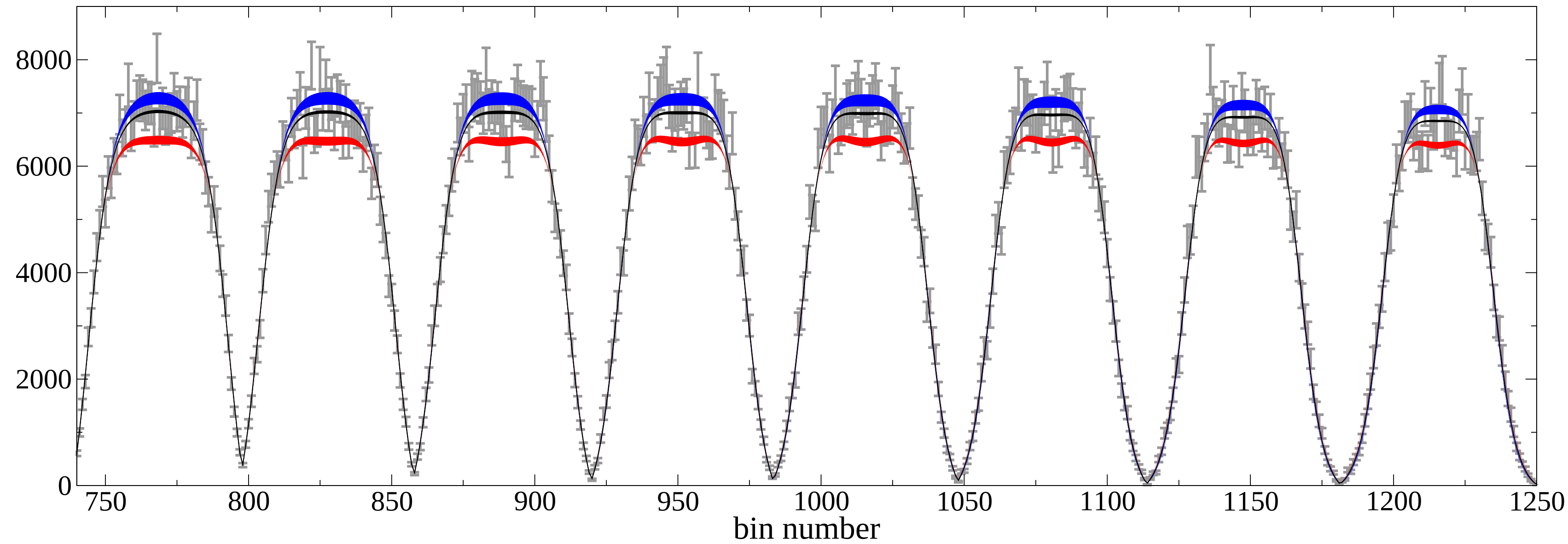

	$\hat{\mathcal{F}} = 0$	once-subtracted	twice-subtracted
χ^2/ndof	$1.71 \ldots 2.06$	$1.17 \ldots 1.50$	$1.02 \ldots 1.03$

- perfect fit respecting analyticity and unitarity possible
- contact term emulates neglected rescattering effects
- no need for "background" — inseparable from "resonance"

Transition form factor $\omega(\phi) \to \pi^0\ell^+\ell^-$

- $\pi^0 \to \gamma^*\gamma^*$ form factor linked to $\omega(\phi) \to \pi^0\gamma^*$ transition:

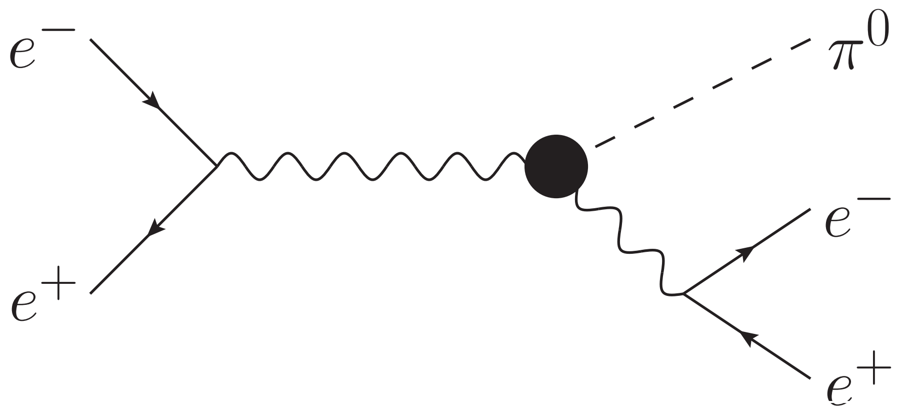

Transition form factor $\omega(\phi) \to \pi^0\ell^+\ell^-$

- $\pi^0 \to \gamma^*\gamma^*$ form factor linked to $\omega(\phi) \to \pi^0\gamma^*$ transition:

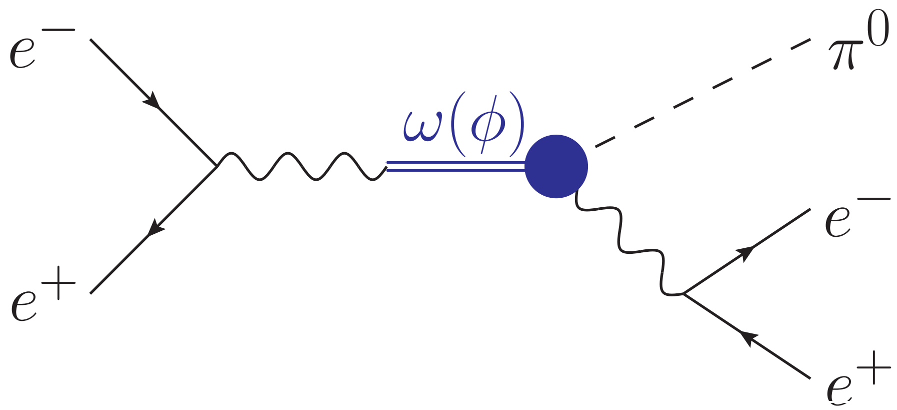

Transition form factor $\omega(\phi) \to \pi^0 \ell^+ \ell^-$

- $\pi^0 \to \gamma^* \gamma^*$ form factor linked to $\omega(\phi) \to \pi^0 \gamma^*$ transition:

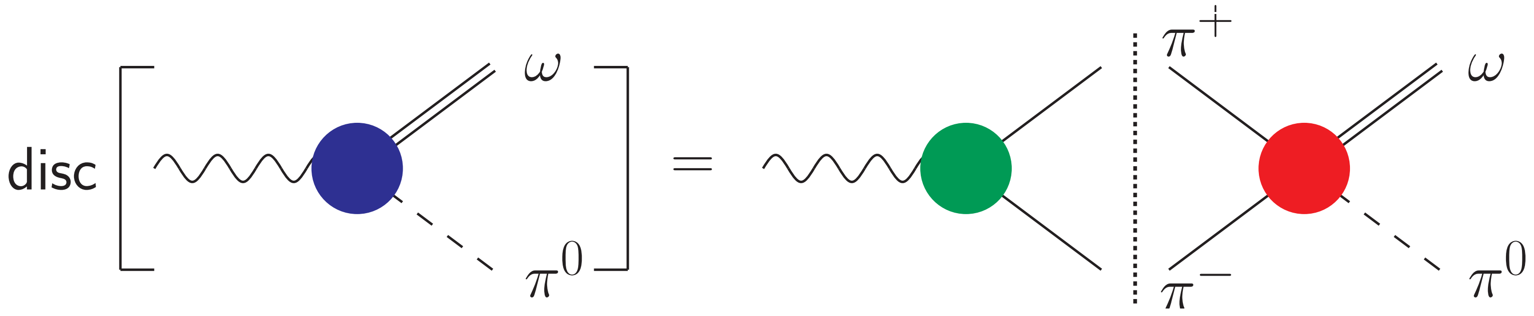

- ω transition form factor related to

pion vector form factor $\times$ $\omega \to 3\pi$ decay amplitude

Transition form factor $\omega(\phi) \to \pi^0\ell^+\ell^-$

- $\pi^0 \to \gamma^*\gamma^*$ form factor linked to $\omega(\phi) \to \pi^0\gamma^*$ transition:

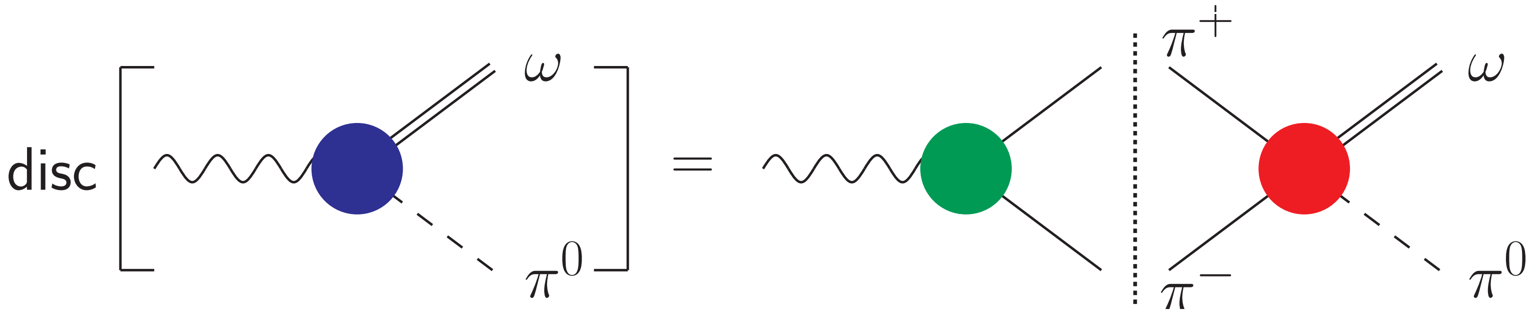

- ω transition form factor related to

  pion vector form factor $\times$ $\omega \to 3\pi$ decay amplitude

- form factor normalization yields rate $\Gamma(\omega \to \pi^0\gamma)$

  (2nd most important ω decay channel)

  $\longrightarrow$ works at 95% accuracy Schneider, BK, Niecknig 2012

Numerical results: $\omega \to \pi^0\mu^+\mu^-$

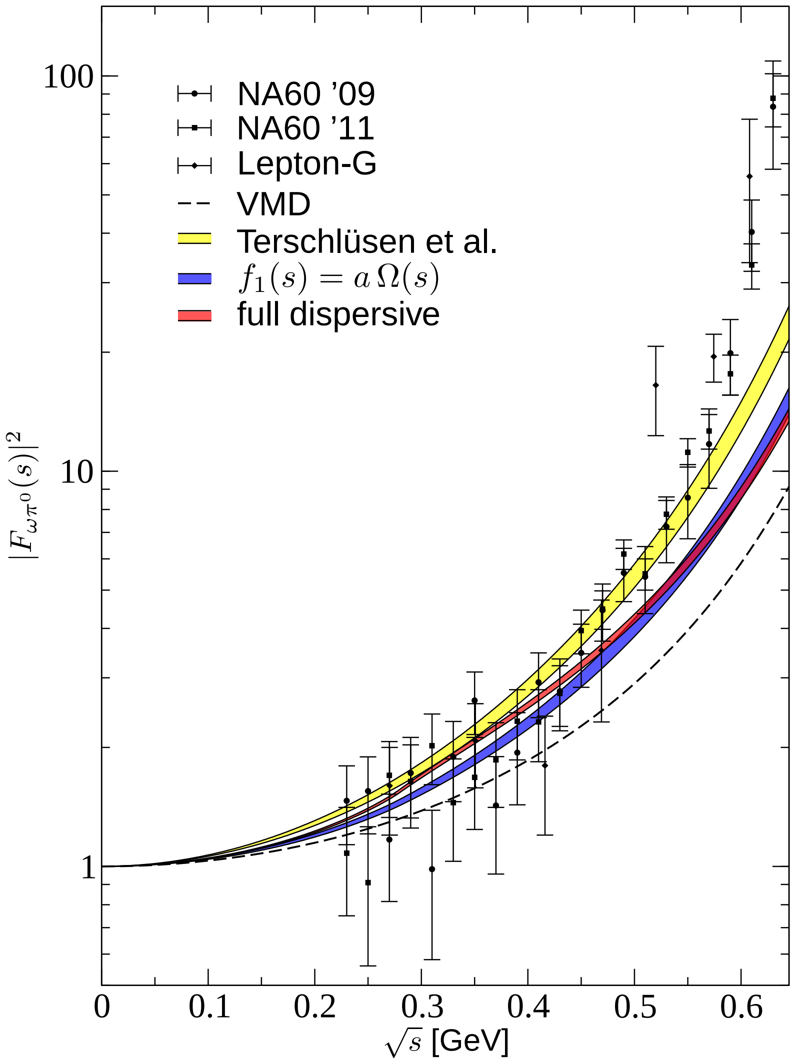

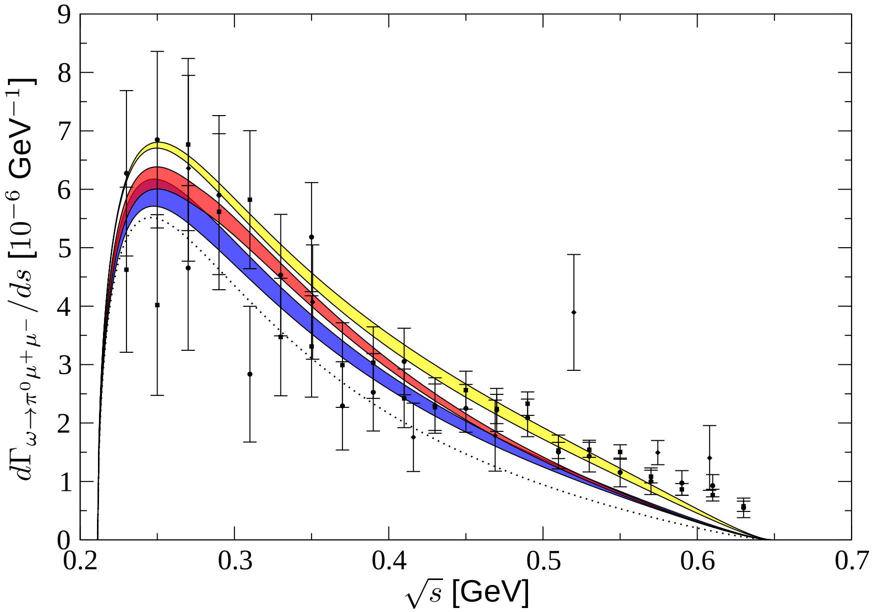

- clear enhancement vs. naive vector-meson dominance
- incompatible with data (from heavy-ion coll.) NA60 2009, 2011
- more "exclusive" data? CLAS

- NA60 data potentially in conflict with unitarity bounds

Ananthanarayan, Caprini, BK 2014

Naive extension to $e^+e^- \to \pi^0\omega$

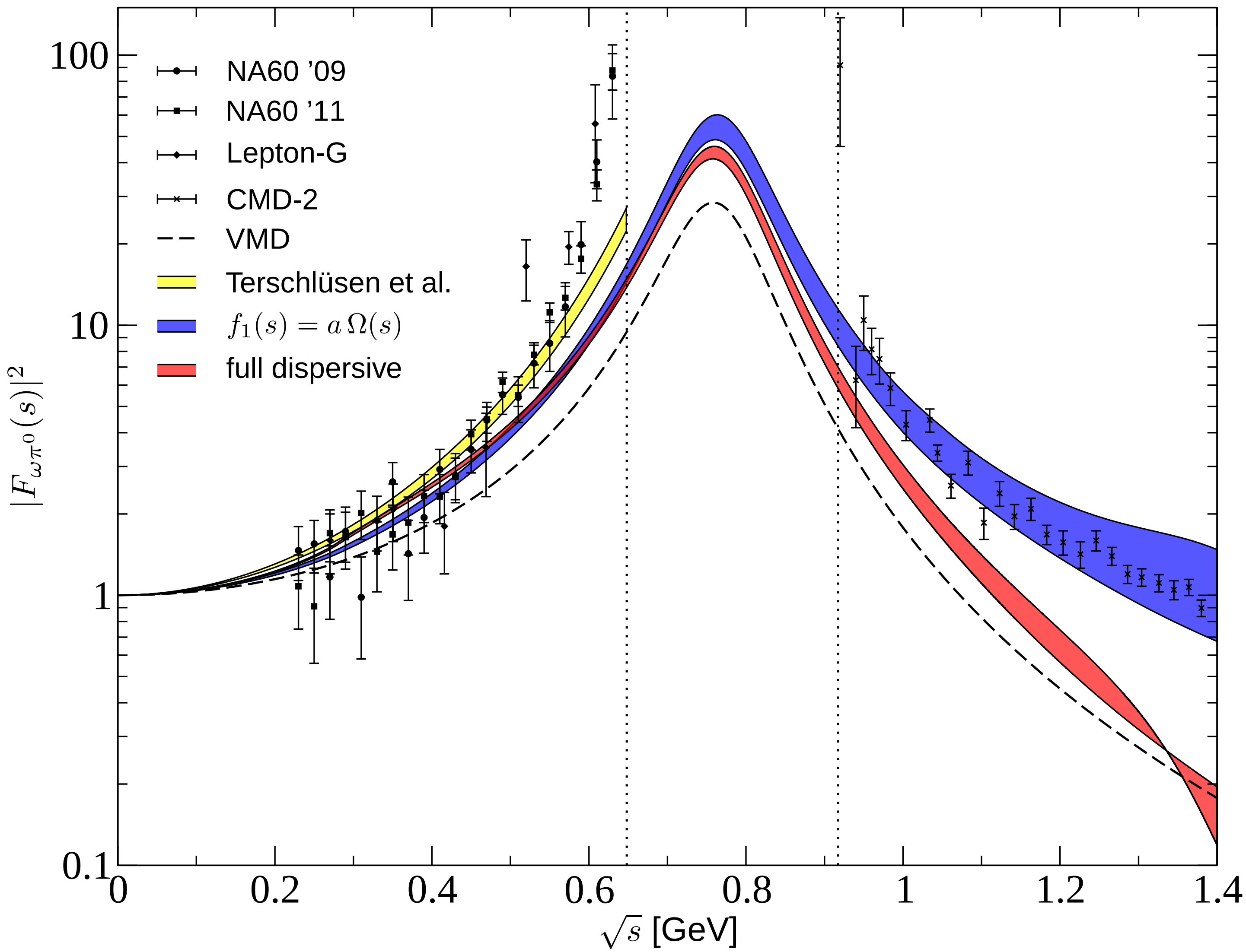

- full solution above naive VMD, but still too low
- higher intermediate states (4π / $\pi\omega$) more important?

One step further: $e^+e^- \to 3\pi$, $e^+e^- \to \pi^0\gamma^*$

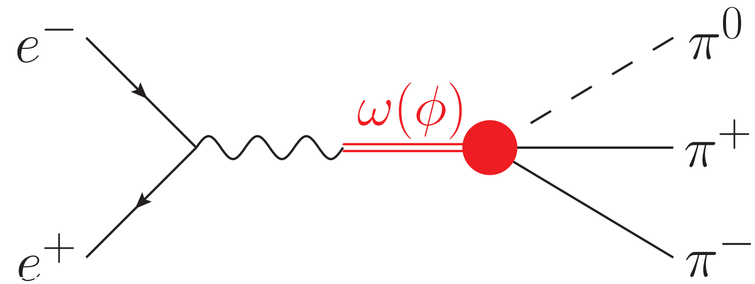

- decay amplitude for $\omega/\phi \to 3\pi$: $\mathcal{M}_{\omega/\phi} \propto \mathcal{F}(s) + \mathcal{F}(t) + \mathcal{F}(u)$

$$\mathcal{F}(s) = a_{\omega/\phi}\,\Omega(s)\left\{1 + \frac{s}{\pi}\int_{4M_\pi^2}^{\infty}\frac{ds'}{s'}\frac{\sin\delta_1^1(s')\hat{\mathcal{F}}(s')}{|\Omega(s')|(s'-s)}\right\}$$

$a_{\omega/\phi}$ adjusted to reproduce total width $\omega/\phi \to 3\pi$

One step further: $e^+e^- \to 3\pi$, $e^+e^- \to \pi^0\gamma^*$

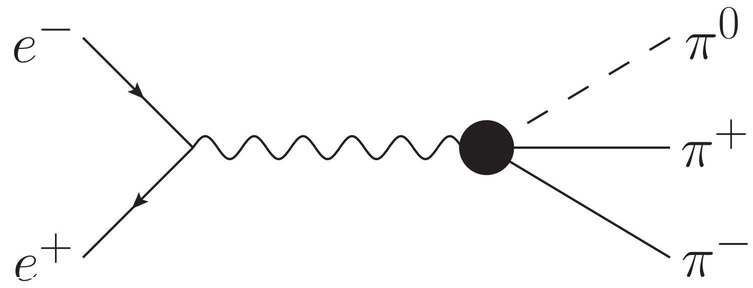

- decay amplitude for $e^+e^- \to 3\pi$: $\mathcal{M}_{e^+e^-} \propto \mathcal{F}(s) + \mathcal{F}(t) + \mathcal{F}(u)$

$$\mathcal{F}(s,q^2) = a_{e^+e^-}(q^2)\,\Omega(s)\left\{1 + \frac{s}{\pi}\int_{4M_\pi^2}^{\infty}\frac{ds'}{s'}\frac{\sin\delta_1^1(s')\hat{\mathcal{F}}(s',q^2)}{|\Omega(s')|(s'-s)}\right\}$$

$a_{e^+e^-}(q^2)$ adjusted to reproduce spectrum $e^+e^- \to 3\pi$

contains 3π resonances $\longrightarrow$ no dispersive prediction

One step further: $e^+e^- \to 3\pi$, $e^+e^- \to \pi^0\gamma^*$

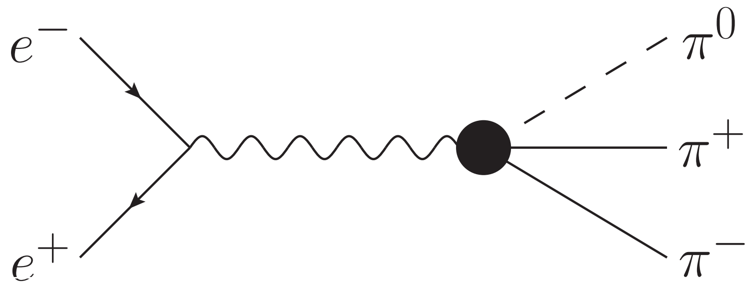

- decay amplitude for $e^+e^- \to 3\pi$: $\mathcal{M}_{e^+e^-} \propto \mathcal{F}(s) + \mathcal{F}(t) + \mathcal{F}(u)$

$$\mathcal{F}(s,q^2) = a_{e^+e^-}(q^2)\,\Omega(s)\left\{1 + \frac{s}{\pi}\int_{4M_\pi^2}^{\infty}\frac{ds'}{s'}\frac{\sin\delta_1^1(s')\hat{\mathcal{F}}(s',q^2)}{|\Omega(s')|(s'-s)}\right\}$$

$a_{e^+e^-}(q^2)$ adjusted to reproduce spectrum $e^+e^- \to 3\pi$

- parameterisation:

$$a_{e^+e^-}(q^2) = \frac{F_{3\pi}}{3} + \beta\, q^2 + \frac{q^4}{\pi}\int_{\text{thr}}^{\infty} ds' \frac{\text{Im}BW(s')}{s'^2(s'-q^2)}$$

$$BW(q^2) = \sum_{V=\omega,\phi}\frac{c_V}{M_V^2 - q^2 - i\sqrt{q^2}\,\Gamma_V(q^2)}$$

One step further: $e^+e^- \to 3\pi$, $e^+e^- \to \pi^0\gamma^*$

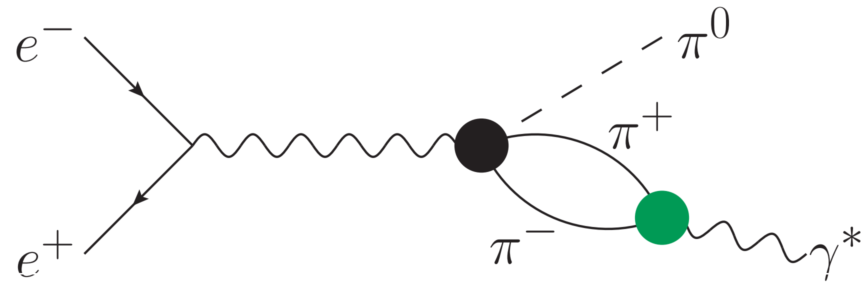

- decay amplitude for $e^+e^- \to 3\pi$: $\mathcal{M}_{e^+e^-} \propto \mathcal{F}(s) + \mathcal{F}(t) + \mathcal{F}(u)$

$$\mathcal{F}(s,q^2) = a_{e^+e^-}(q^2)\,\Omega(s)\left\{1 + \frac{s}{\pi}\int_{4M_\pi^2}^{\infty}\frac{ds'}{s'}\frac{\sin\delta_1^1(s')\hat{\mathcal{F}}(s',q^2)}{|\Omega(s')|(s'-s)}\right\}$$

$a_{e^+e^-}(q^2)$ adjusted to reproduce spectrum $e^+e^- \to 3\pi$

- parameterisation:

$$a_{e^+e^-}(q^2) = \frac{F_{3\pi}}{3} + \beta\, q^2 + \frac{q^4}{\pi}\int_{\text{thr}}^{\infty} ds' \frac{\text{Im}BW(s')}{s'^2(s'-q^2)}$$

$$BW(q^2) = \sum_{V=\omega,\phi} \frac{c_V}{M_V^2 - q^2 - i\sqrt{q^2}\,\Gamma_V(q^2)}$$

- fit to $e^+e^- \to 3\pi$ data $\longrightarrow$ prediction for $e^+e^- \to \pi^0\gamma^*$

Fit to $e^+e^- \to 3\pi$ data

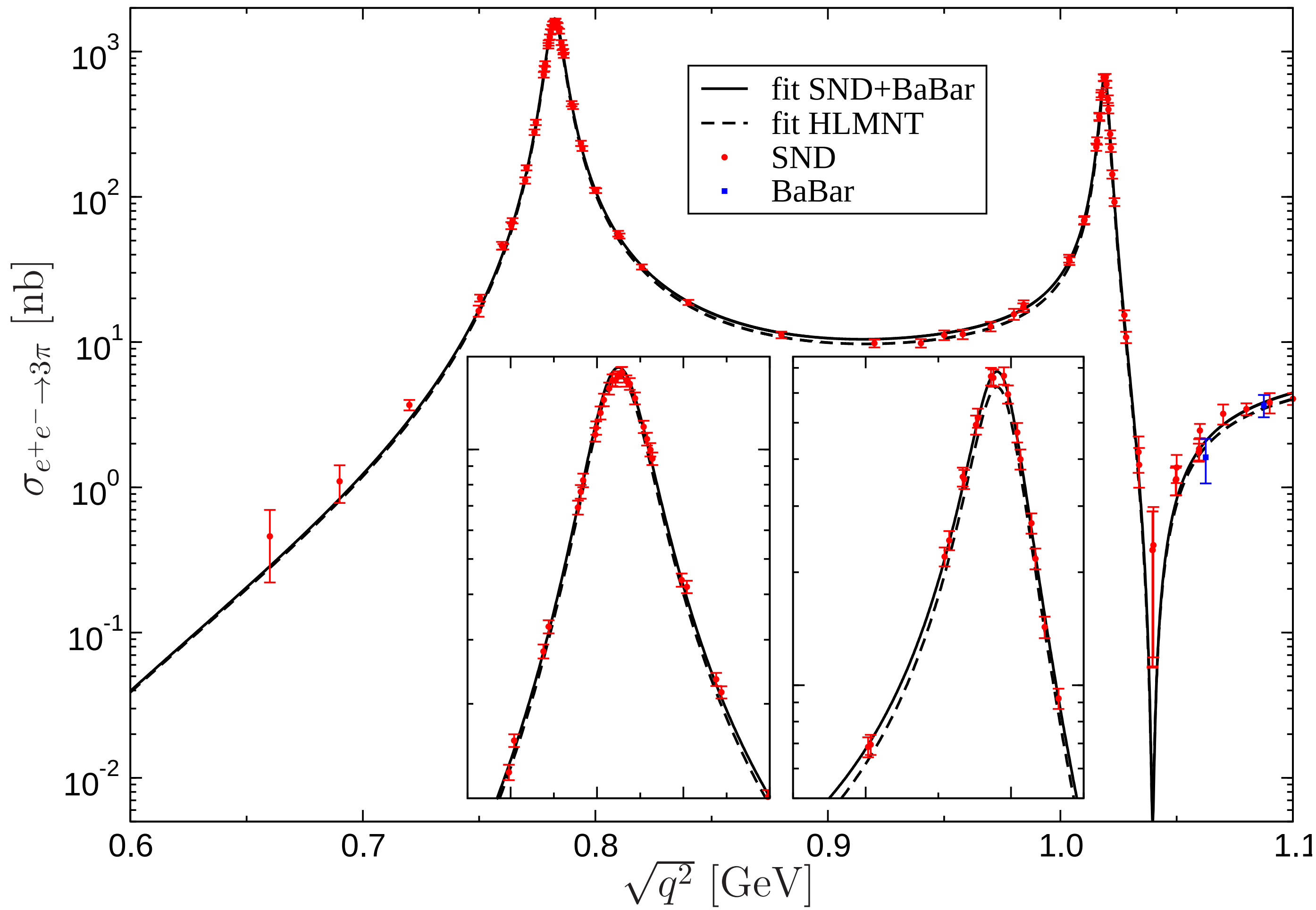

Hoferichter, BK, Leupold, Niecknig, Schneider 2014

- one subtraction/normalisation at $q^2 = 0$ fixed by $\gamma \to 3\pi$
- fitted: ω, ϕ residues, linear subtraction β

Comparison to $e^+e^- \to \pi^0\gamma$ data

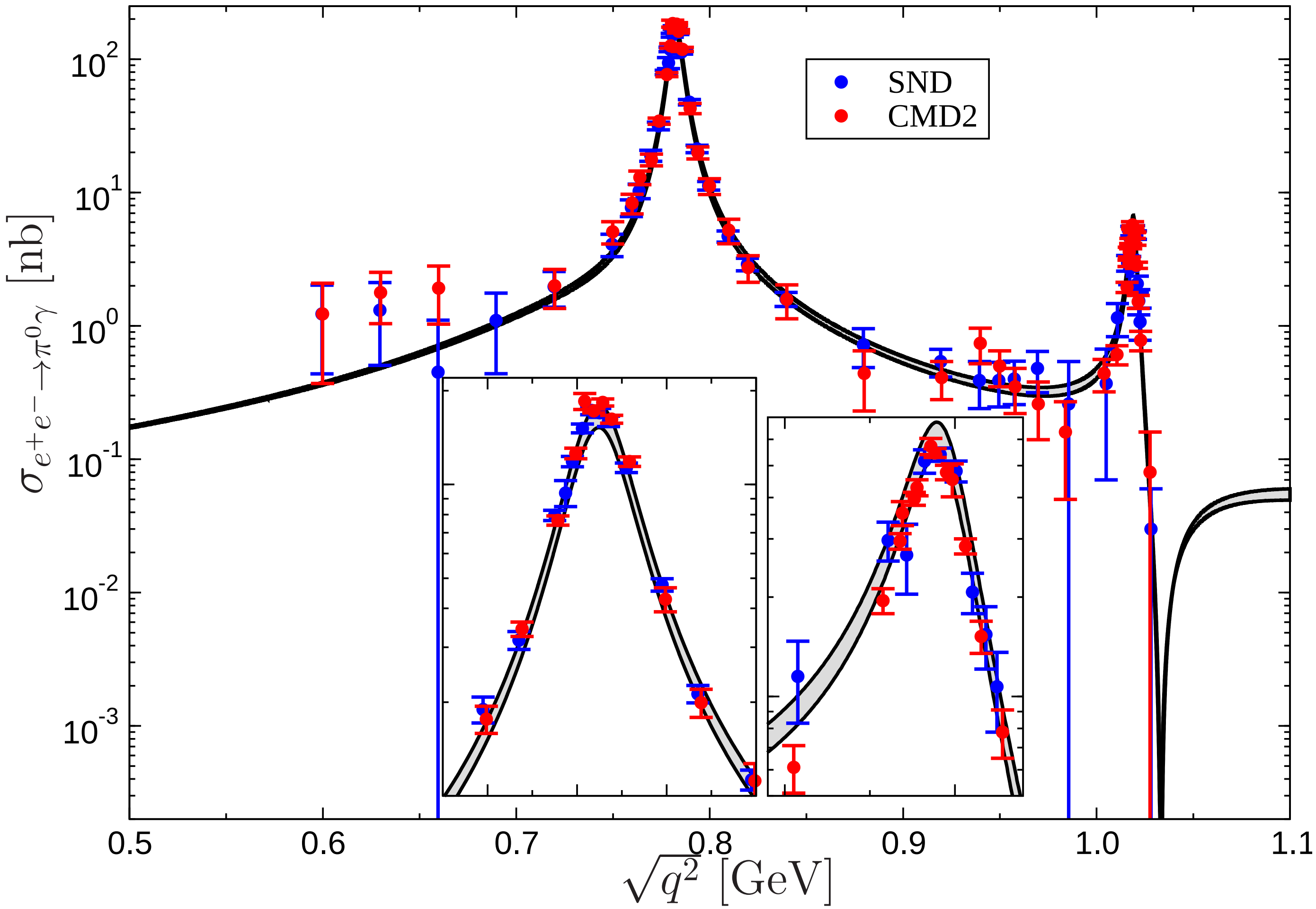

Hoferichter, BK, Leupold, Niecknig, Schneider 2014

- "prediction"—no further parameters adjusted
- data well reproduced

Extension to spacelike region; slope

- continuation to spacelike region: use another dispersion relation

$$F_{\pi^0\gamma^*\gamma}(q^2,0) = F_{\pi\gamma\gamma} + \frac{q^2}{\pi}\int_{4M_\pi^2}^{\infty} ds' \frac{\mathrm{Im}\, F_{\pi^0\gamma^*\gamma}(s',0)}{s'(s'-q^2)}$$

$\longrightarrow$ work in progress; high-energy completion of the integral? convergence/uncertainties?

- sum rule for slope $\quad F_{\pi^0\gamma^*\gamma}(q^2,0) = F_{\pi\gamma\gamma}\Big\{1 + a_\pi \frac{q^2}{M_{\pi^0}^2} + \mathcal{O}(q^4)\Big\}$

$$a_\pi = \frac{M_{\pi^0}^2}{F_{\pi\gamma\gamma}} \times \frac{1}{\pi}\int_{4M_\pi^2}^{\infty} \frac{ds'}{s'^2}\, \mathrm{Im}\, F_{\pi^0\gamma^*\gamma}(s',0)$$

$$= (30.7 \pm 0.6) \times 10^{-3}$$ Hoferichter et al. 2014

compare: $\quad a_\pi = (32 \pm 4) \times 10^{-3}$ PDG 2014

- theory error estimate: $\pi\pi$ phases and cutoff effects (in $\gamma^* \to 3\pi$ partial waves and $[\gamma^* \to 3\pi] \longrightarrow [\gamma^* \to \pi^0\gamma]$) only!

Summary / Outlook

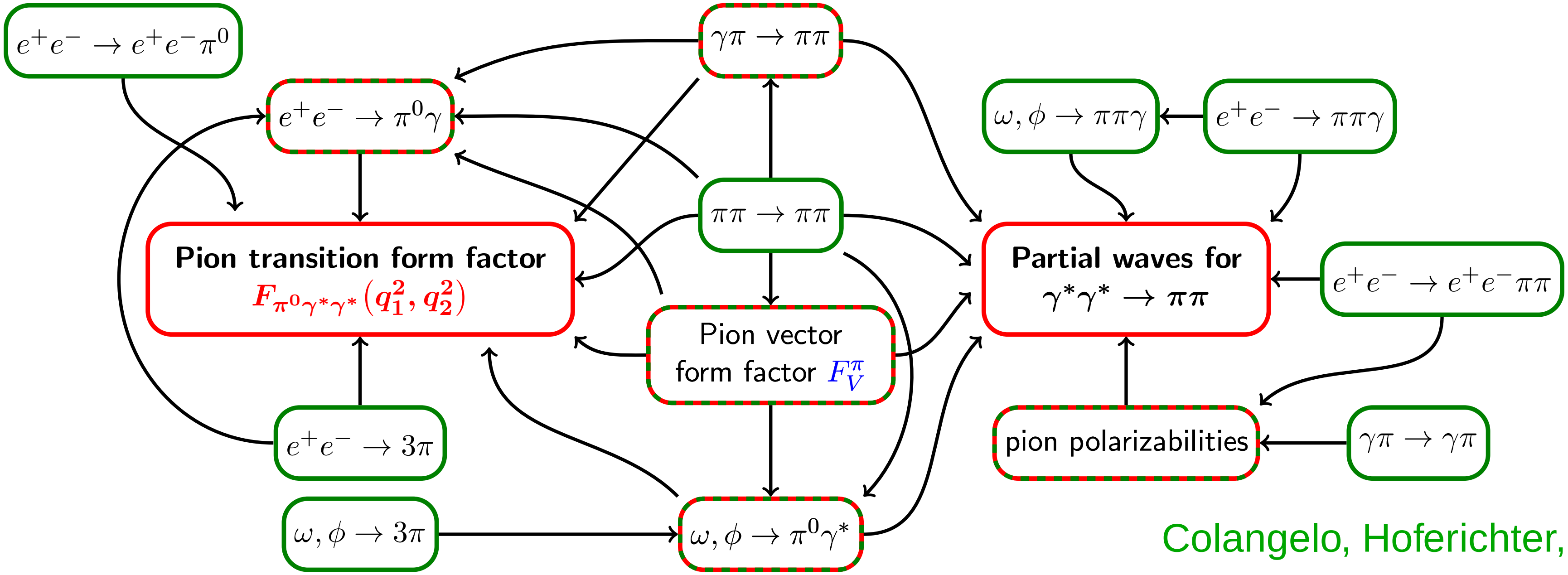

Colangelo, Hoferichter,
BK, Procura, Stoffer 2014

Summary / Outlook

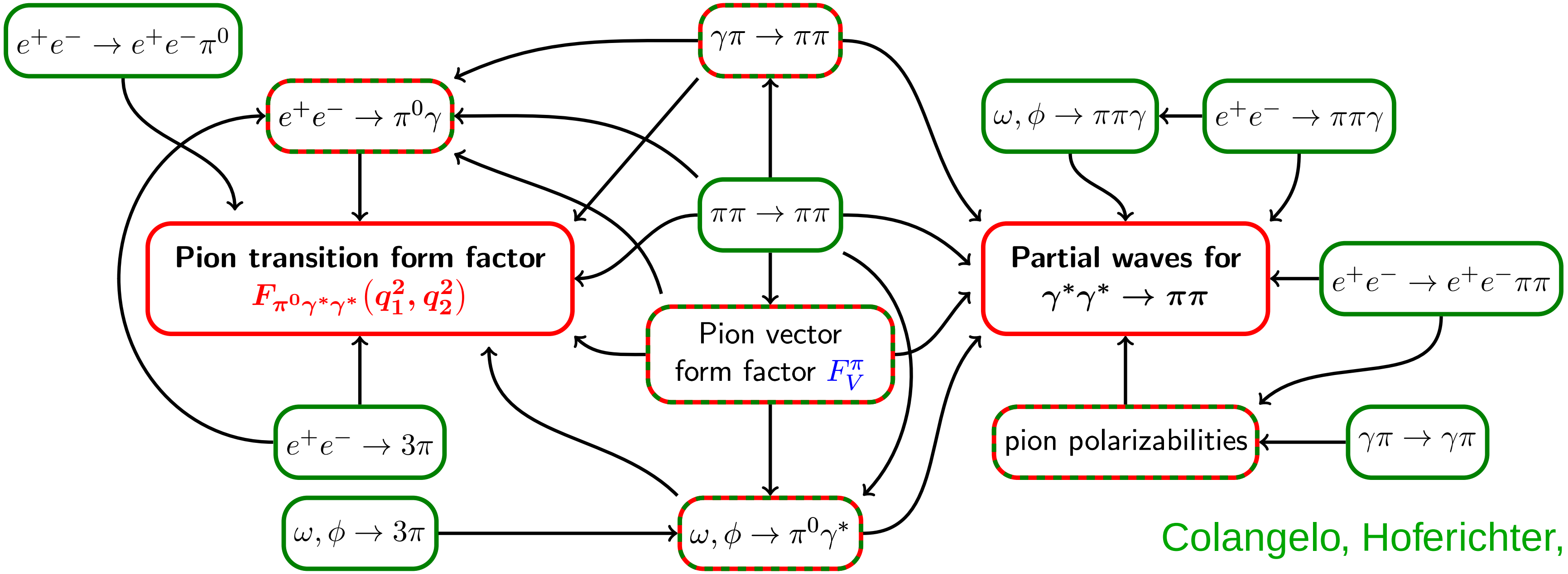

Colangelo, Hoferichter, BK, Procura, Stoffer 2014

Further experimental input for π^0 and η transition form factors:

- Primakoff reactions $\gamma\pi \to \pi\pi$, $\gamma\pi \to \pi\eta$ — COMPASS
- $\omega \to 3\pi$ precision Dalitz plot — CLAS
- $\omega/\phi \to \pi^0\gamma^*$ test doubly virtual $F_{\pi^0\gamma^*\gamma^*}$ with precision
- $e^+e^- \to \eta\pi^+\pi^-$ differential data — C.-W. Xiao et al.

$\longrightarrow$ determine $(g-2)_\mu$ contributions with controlled uncertainty

Spares

Total cross section $\gamma\pi \to \pi\eta$

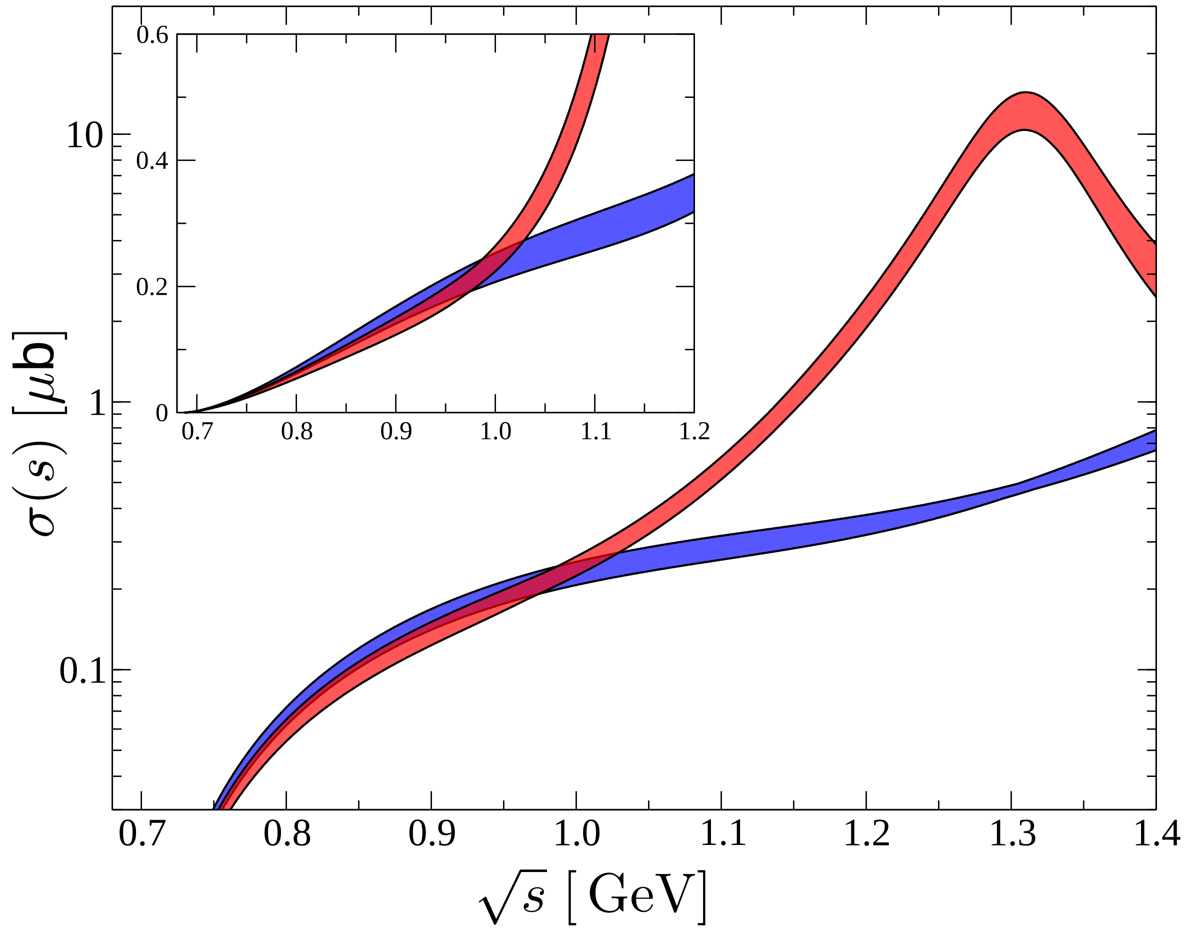

blue: t-channel dynamics / "ρ" only red: full amplitude

- t-channel dynamics dominate below $\sqrt{s} \approx 1\,\mathrm{GeV}$
- uncertainty bands: $\Gamma(\eta \to \pi^+\pi^-\gamma)$, α, a_2 couplings BK, Plenter 2015

Differential cross sections $\gamma\pi \to \pi\eta$

- amplitude zero visible in differential cross sections:

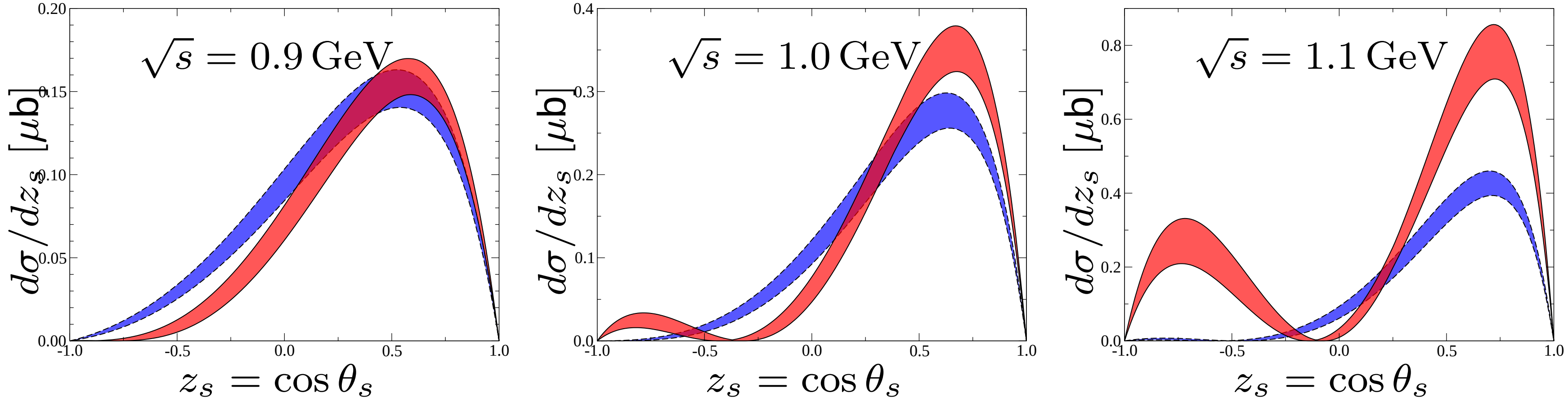

blue: t-channel dynamics / "ρ" only   red: full amplitude

Differential cross sections $\gamma\pi \to \pi\eta$

- amplitude zero visible in differential cross sections:

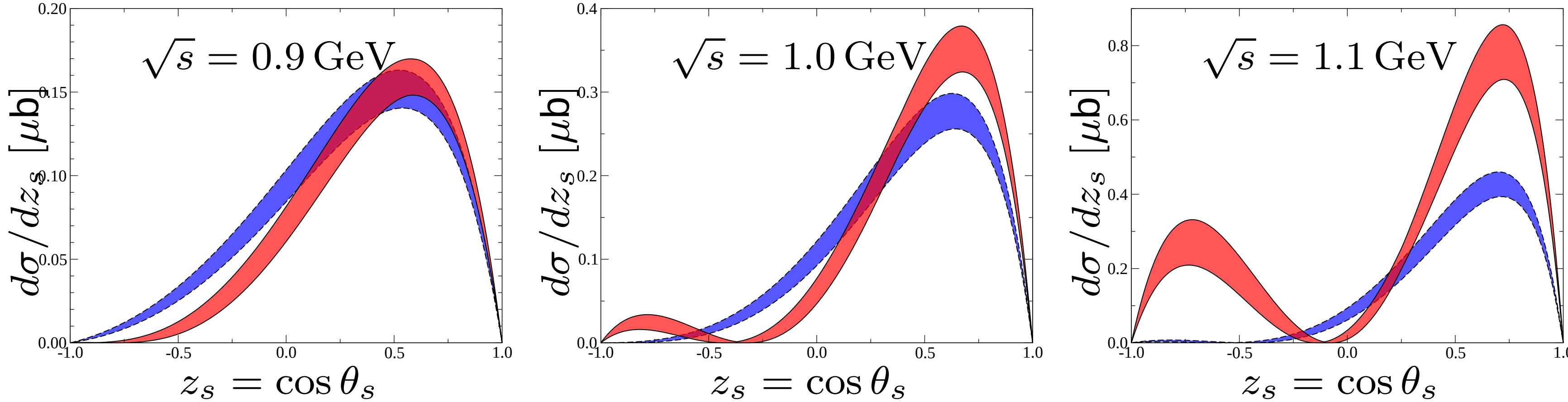

blue: t-channel dynamics / "ρ" only   red: full amplitude

- strong P-D-wave interference
- can be expressed as forward-backward asymmetry

$$A_{\rm FB} = \frac{\sigma(\cos\theta > 0) - \sigma(\cos\theta < 0)}{\sigma_{\rm total}}$$

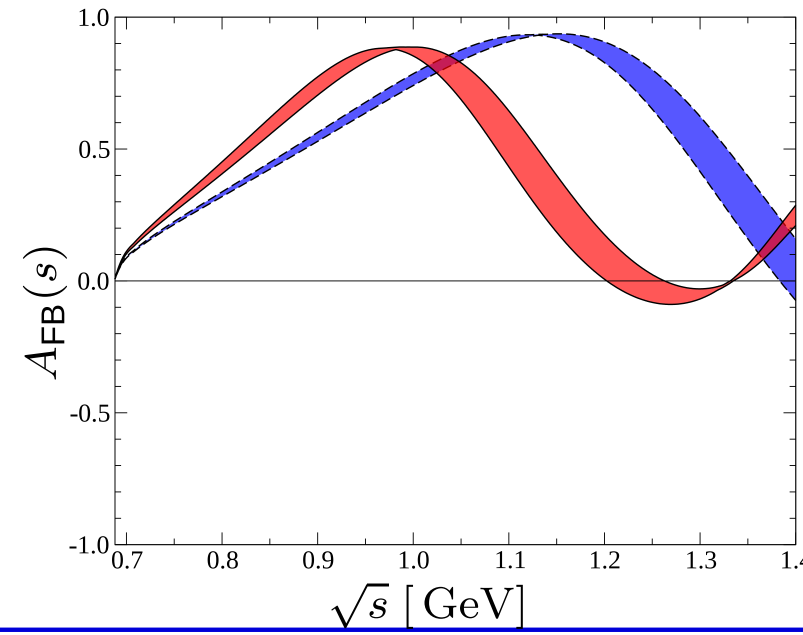

Summary: processes and unitarity relations for $\pi^0 \to \gamma^*\gamma^*$

process	unitarity relations	SC 1	SC 2
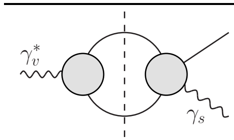	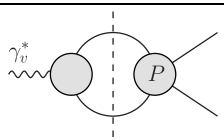		$F_{\pi^0\gamma\gamma}$
	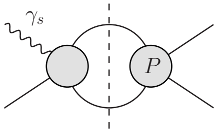	$F_{3\pi}$	$\sigma(\gamma\pi \to \pi\pi)$
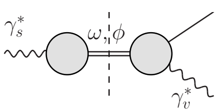	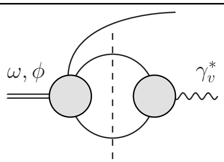		$\Gamma_{\pi^0\gamma}$
	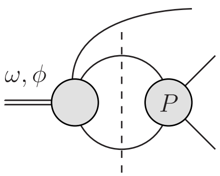	$\Gamma_{3\pi}$	$\frac{d^2\Gamma}{ds\,dt}(\omega,\phi \to 3\pi)$
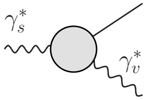	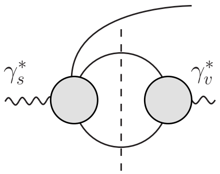		$\sigma(e^+e^- \to \pi^0\gamma)$
	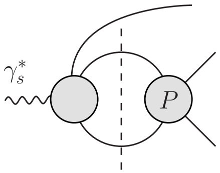	$\sigma(e^+e^- \to 3\pi)$	$\sigma(\gamma\pi \to \pi\pi)$ $\frac{d^2\Gamma}{ds\,dt}(\omega,\phi \to 3\pi)$
	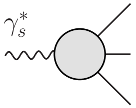	$F_{3\pi}$	$\sigma(e^+e^- \to 3\pi)$

Colangelo, Hoferichter, BK, Procura, Stoffer 2014

$\gamma\pi \to \pi\pi$

$\omega \to 3\pi$, $\phi \to 3\pi$

$\gamma^* \to 3\pi$

common theme:
resum $\pi\pi$ rescattering

Subtraction constants

$$\mathcal{F}(s) = \Omega(s)\left\{a + \frac{s}{\pi}\int_{4M_\pi^2}^{\infty}\frac{ds'}{s'}\frac{\sin\delta_1(s')\hat{\mathcal{F}}(s')}{|\Omega_1(s')|(s'-s)}\right\}$$

- one subtraction $a \longrightarrow$ fix to partial width, Dalitz plot prediction

Subtraction constants

$$\mathcal{F}(s) = \Omega(s)\left\{ a + \frac{s}{\pi}\int_{4M_\pi^2}^{\infty} \frac{ds'}{s'} \frac{\sin\delta_1(s')\hat{\mathcal{F}}(s')}{|\Omega_1(s')|(s'-s)} \right\}$$

- one subtraction $a \longrightarrow$ fix to partial width, Dalitz plot prediction
- $\omega \to 3\pi$ vs. $\phi \to 3\pi$: crossed-channel effects depend on decay mass!

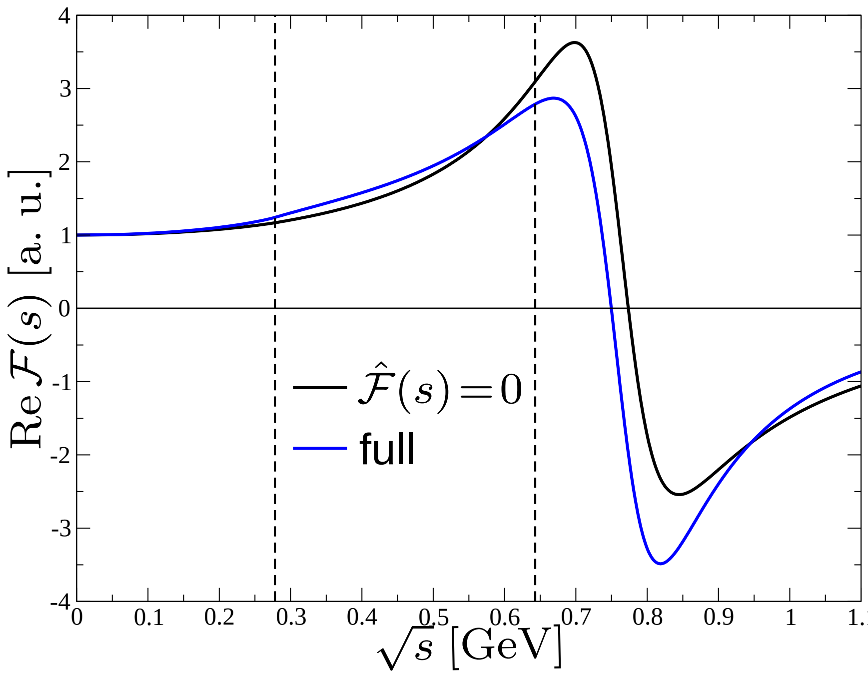

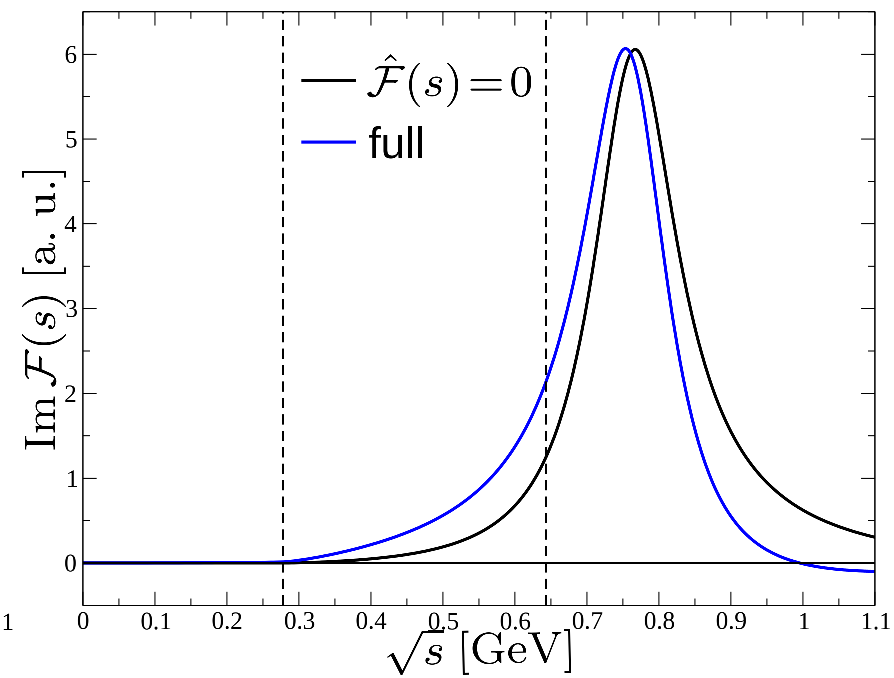

Niecknig, BK, Schneider 2012; cf. Danilkin et al. 2014

Subtraction constants

$$\mathcal{F}(s) = \Omega(s)\left\{a + \frac{s}{\pi}\int_{4M_\pi^2}^{\infty}\frac{ds'}{s'}\frac{\sin\delta_1(s')\hat{\mathcal{F}}(s')}{|\Omega_1(s')|(s'-s)}\right\}$$

- one subtraction a $\longrightarrow$ fix to partial width, Dalitz plot prediction
- $\omega \to 3\pi$ vs. $\phi \to 3\pi$: crossed-channel effects depend on decay mass!

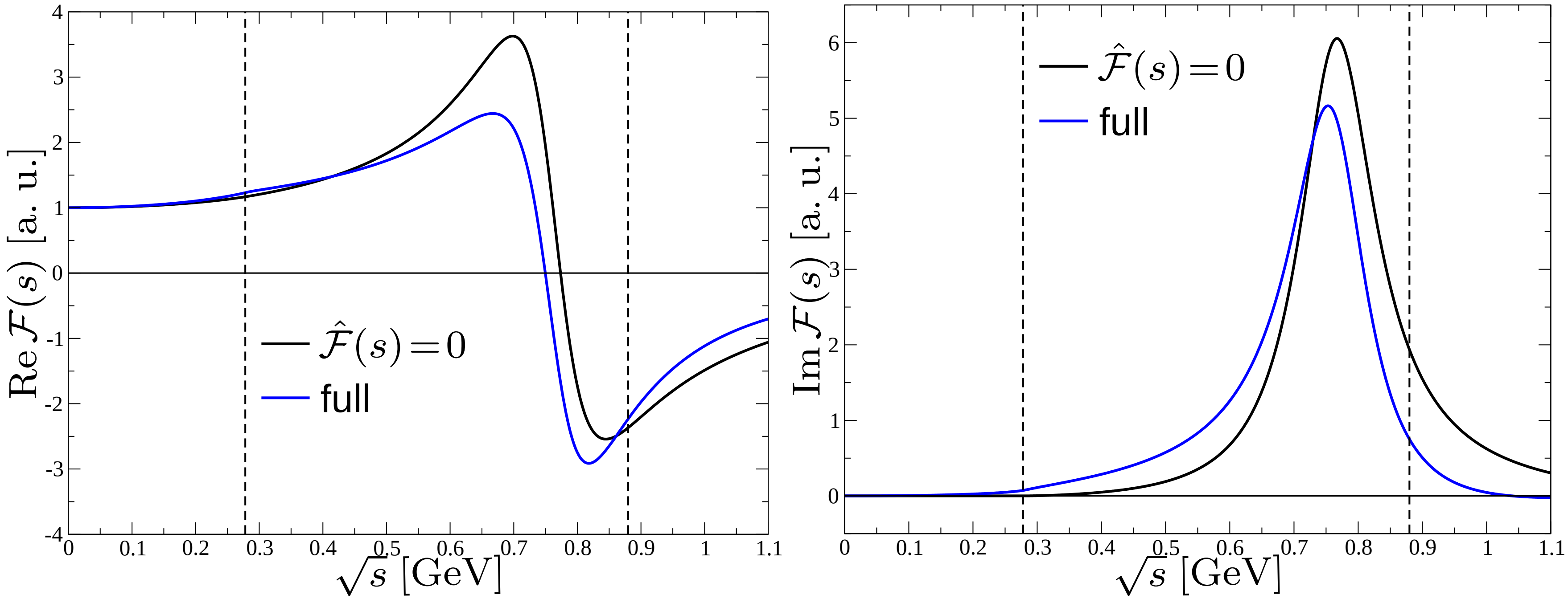

Niecknig, BK, Schneider 2012; cf. Danilkin et al. 2014

Numerical results: $\phi \to \pi^0 \ell^+ \ell^-$

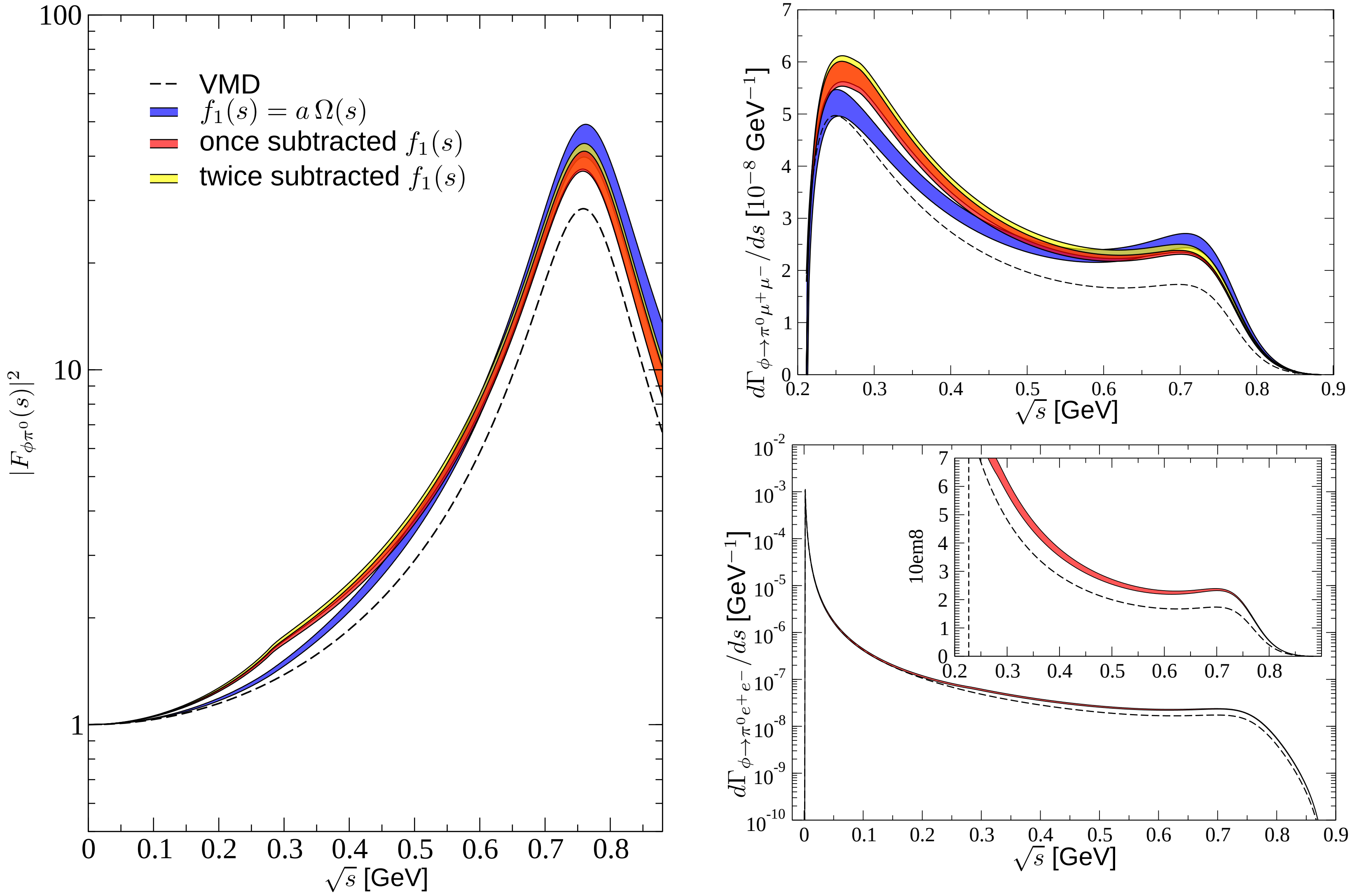

- measurement would be extremely helpful: ρ in physical region!
- partial-wave amplitude backed up by experiment

Improved Breit–Wigner resonances

Lomon, Pacetti 2012; Moussallam 2013

- "standard" Breit–Wigner function with energy-dependent width

$$B^\ell(q^2) = \frac{1}{M_{\rm res}^2 - q^2 - iM_{\rm res}\Gamma_{\rm res}^\ell(q^2)}$$

$$\Gamma_{\rm res}^\ell(q^2) = \theta(q^2-4M_\pi^2)\frac{M_{\rm res}}{\sqrt{q^2}}\left(\frac{q^2-4M_\pi^2}{M_{\rm res}^2-4M_\pi^2}\right)^\ell \Gamma_{\rm res}(M_{\rm res}^2)$$

  - ▷ no correct analytic continuation below threshold $q^2 < 4M_\pi^2$
  - ▷ wrong phase behaviour for $\ell \geq 1$:

$$\lim_{q^2\to\infty} \arg B^1(q^2) \approx \pi - \arctan\frac{\Gamma_{\rm res}}{M_{\rm res}} \qquad \lim_{q^2\to\infty} \arg B^{\ell\geq 2}(q^2) = \frac{\pi}{2} \;(!)$$

- remedy: reconstruct via dispersion integral

$$\tilde{B}^\ell(q^2) = \frac{1}{\pi}\int_{4M_\pi^2}^\infty \frac{{\rm Im}\,B^\ell(s')ds'}{s'-q^2} \quad\longrightarrow\quad \lim_{s\to\infty}\arg B^\ell(q^2) = \pi$$

On the approximation for the 3-pion cut

Compare:

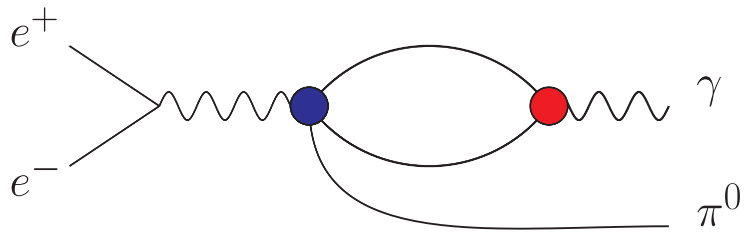

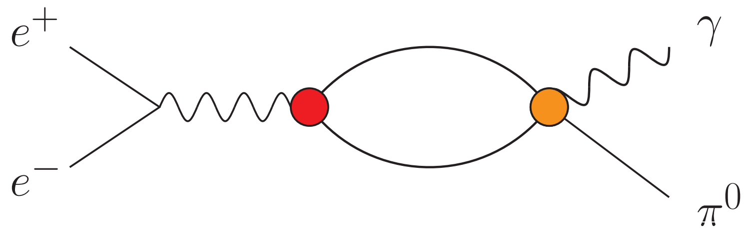

$\longrightarrow$ isoscalar contribution looks simplistic; why not instead

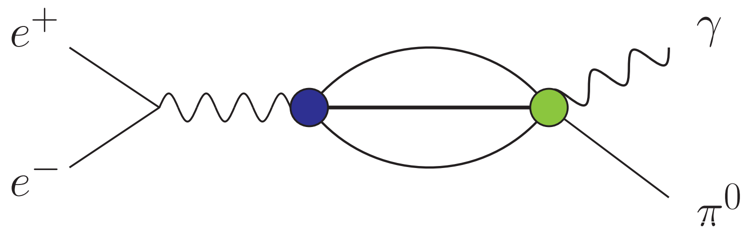

$\longrightarrow$ contains amplitude $3\pi \to \gamma\pi$

On the approximation for the 3-pion cut

Compare:

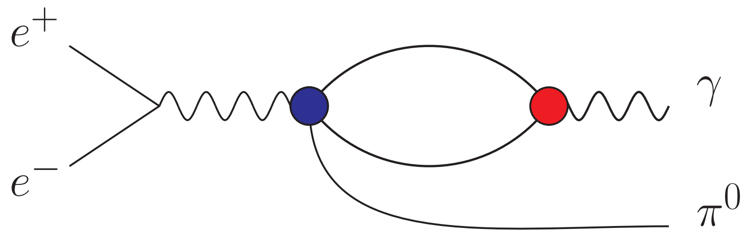

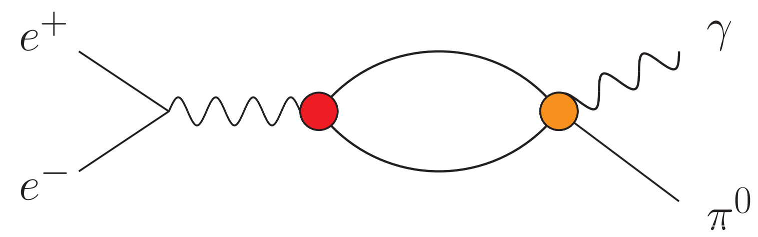

$\longrightarrow$ isoscalar contribution looks simplistic; why not instead

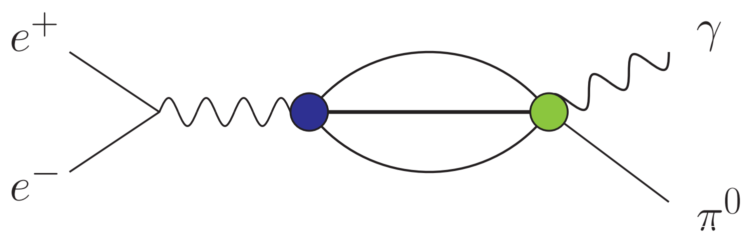

$\longrightarrow$ contains amplitude $3\pi \to \gamma\pi$

Our approximation:

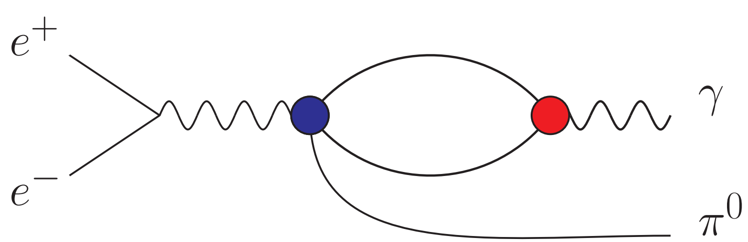

includes

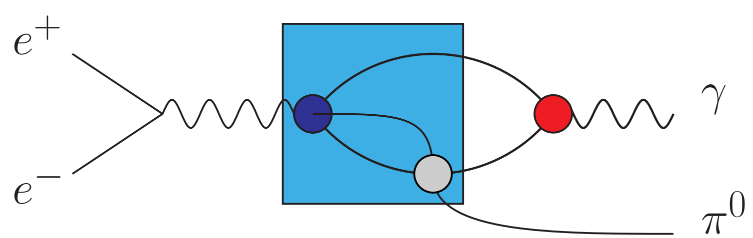

On the approximation for the 3-pion cut

Compare:

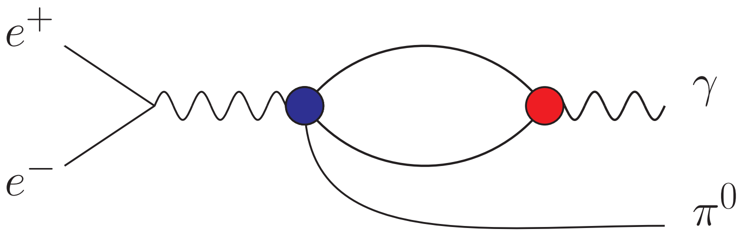

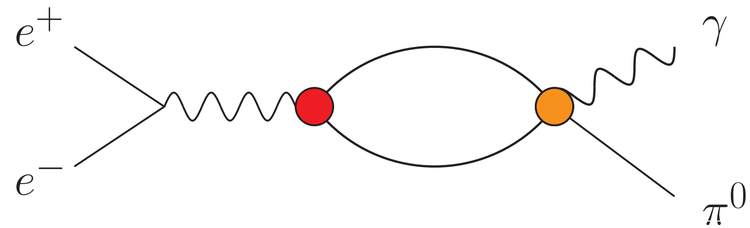

$\longrightarrow$ isoscalar contribution looks simplistic; why not instead

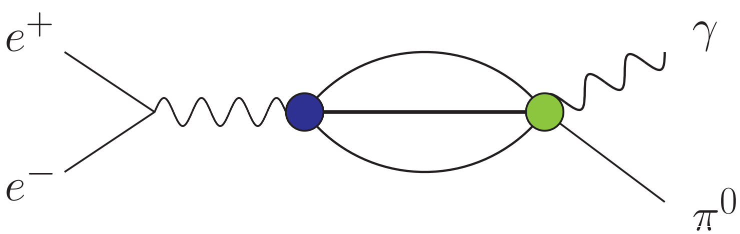

$\longrightarrow$ contains amplitude $3\pi \to \gamma\pi$

Our approximation:

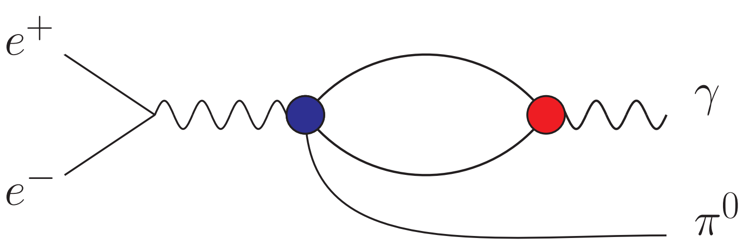

includes

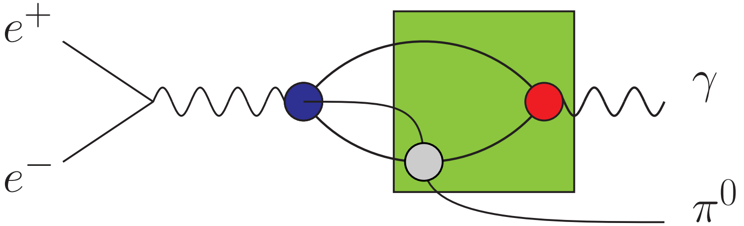

$\longrightarrow$ simplifies left-hand-cut structure in $3\pi \to \gamma\pi$ to pion pole terms

$\pi\pi$ scattering constrained by analyticity and unitarity

Roy equations = coupled system of partial-wave dispersion relations
+ crossing symmetry + unitarity

- twice-subtracted fixed-t dispersion relation:

$$T(s,t) = c(t) + \frac{1}{\pi}\int_{4M_\pi^2}^{\infty} ds' \left\{ \frac{s^2}{s'^2(s'-s)} + \frac{u^2}{s'^2(s'-u)} \right\} \mathrm{Im}T(s',t)$$

- subtraction function $c(t)$ determined from crossing symmetry

$\pi\pi$ scattering constrained by analyticity and unitarity

Roy equations = coupled system of partial-wave dispersion relations
+ crossing symmetry + unitarity

- twice-subtracted fixed-t dispersion relation:

$$T(s,t) = c(t) + \frac{1}{\pi}\int_{4M_\pi^2}^{\infty} ds' \left\{ \frac{s^2}{s'^2(s'-s)} + \frac{u^2}{s'^2(s'-u)} \right\} \mathrm{Im}T(s',t)$$

- subtraction function $c(t)$ determined from crossing symmetry
- project onto partial waves $t_J^I(s)$ (angular momentum J, isospin I)
$\longrightarrow$ coupled system of partial-wave integral equations

$$t_J^I(s) = k_J^I(s) + \sum_{I'=0}^{2}\sum_{J'=0}^{\infty}\int_{4M_\pi^2}^{\infty} ds' K_{JJ'}^{II'}(s,s')\mathrm{Im}t_{J'}^{I'}(s')$$

Roy 1971

- subtraction polynomial $k_J^I(s)$: $\pi\pi$ scattering lengths
can be matched to chiral perturbation theory   Colangelo et al. 2001
- kernel functions $K_{JJ'}^{II'}(s,s')$ known analytically

$\pi\pi$ scattering constrained by analyticity and unitarity

- elastic unitarity $\longrightarrow$ coupled integral equations for phase shifts
- modern precision analyses:
  - ▷ $\pi\pi$ scattering — Ananthanarayan et al. 2001, García-Martín et al. 2011
  - ▷ πK scattering — Büttiker et al. 2004
- example: $\pi\pi$ $I = 0$ S-wave phase shift & inelasticity

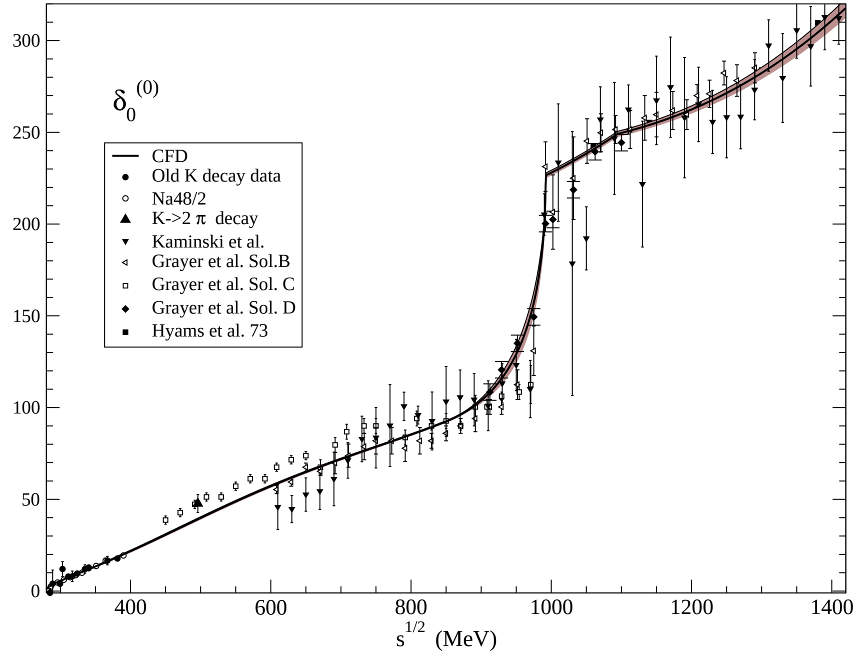

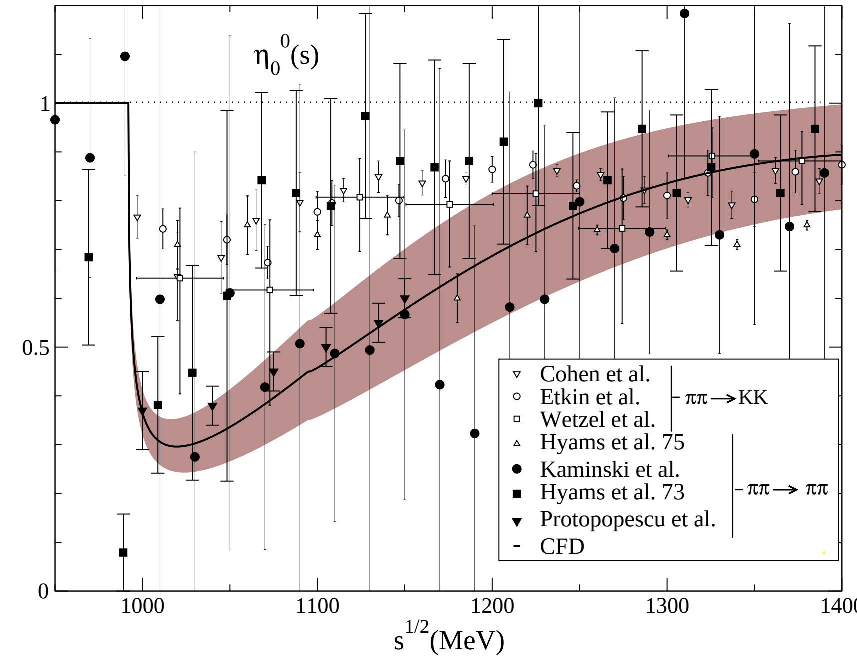

García-Martín et al. 2011

- strong constraints on data from analyticity and unitarity!